Influence of Fire Regimes on Subtropical Grasslands in Bardia National Park, Nepal

by

Femke Boyd - 4687159

A Master's Thesis

Submitted to Faculty of Geoscience, University of Utrecht

Msc Sustainable Development: Environmental Change and Ecosystems

Project: Save the tiger! Save the Grasslands! Save the Water!

Supervisor: Pita Verweij

Second reader: Jasper Griffioen

Mentor: Jitse Bijlmakers

Utrecht University

SAVE
THE TIGER
THE GRASSLANDS
THE WATER

Abstract

The open grasslands of Bardia National Park in Nepal are critical habitats for several endangered species, yet they are increasingly threatened by the encroachment of woody vegetation. This process reduces forage availability for large herbivores and compromises the prey base for species such as the Greater One-horned Rhinoceros, Asian Elephant, and Royal Bengal Tiger. These grasslands rely on disturbance to remain open, and fire has long served this role, but the effects of repeated burning on grassland structure and biodiversity remain understudied in the region.

This thesis investigates how fire regimes shape vegetation structure and species composition in Bardia's subtropical grasslands. A Sentinel-2 burn-detection model was developed for the years 2016 to 2025, achieving 92 percent accuracy and a Cohen's κ of 0.84 for early-season fires. Fifty 10 × 10 metre plots were sampled for vegetation data.

Fire mapping revealed clear spatial patterns. Fires were most frequent in accessible southern floodplain grasslands, where prescribed burns are regularly applied, and in drier northeastern Sal forest terraces, where fires tend to occur naturally later in the season. Moist riverine zones burned rarely. Vegetation structure showed consistent responses across the fire gradient: although canopy height and bulk density tended to decline with fire frequency, only NDVI increased significantly. Dried biomass remained stable, indicating that productivity recovers quickly after burning. Early-successional traits, particularly those of pioneer tall grasses, appeared to drive the increase in greenness. Species composition responded less strongly: Saccharum spontaneum was more common in frequently burned plots, while Narenga porphyrocoma dominated long-unburned areas. Shannon diversity increased linearly with fire frequency and recent burns, offering partial support for the Intermediate Disturbance Hypothesis.

The findings suggest that a fire regime with frequent and well-timed burns helps maintain the open structure of Bardia's disturbance-climax grasslands. An adaptive approach where small-scale burning, cutting, and managed grazing is combined is likely the best management option for reversing the encroachment of trees and supporting grassland-dependent wildlife. However, these results are impacted by several limitations such as severe under-detection of late-season fires, a single-season sampling window, and limited samples. Nevertheless, the results highlight the importance of research to inform sustainable fire management under increasingly variable climatic conditions.

Acknowledgements

This thesis is submitted in partial fulfilment of the requirements for the Master's programme Sustainable Development at Utrecht University. It represents the culmination of my research on grassland ecology and fire regimes in Bardia National Park, Nepal. I hope this thesis can contribute to a better understanding of grassland dynamics in Bardia and the Terai Arc Landscape.

I am grateful to my supervisor, Dr. Pita Verweij, for their guidance and feedback throughout the process. I would also like to sincerely thank Jitse Bijlmakers, whose insights into Bardia and remote sensing were crucial. To my travel companion Gijs whose company across Nepal's trails, safaris, and field sites made the chaos a whole lot more fun.

I also wish to thank the entire team at National Trust for Nature Conservation Bardia for their hospitality, assistance, and logistical support. Their local expertise and commitment to conservation made the fieldwork not only possible but deeply meaningful. Special thanks go to my guide Krisna, whose tireless energy, knowledge, and enthusiasm brought this project to life. His commitment to helping us spot a tiger was unmatched, though unfortunately, the tigers had other plans.

Table of Content

1. Introduction

Grasslands are an important terrestrial ecosystem, covering around 40% of the Earth's land area (Stevens, 2018). This ecosystem is found on every continent, except Antarctica, across a wide range of climates and soil types. These systems are often dominated by grasses (*Poaceae*) and other grass-like plants, with less than 10% of the vegetation cover being trees (Stevens, 2018). The grasslands support a rich diversity of plant and animal and contribute approximately one-third to global terrestrial net primary production (Vitousek, 2015). This ecosystem also provides essential ecosystem services such as carbon storage, soil stabilisation, and support for livestock-based livelihoods (Lamicchane et al., 2024; Stevens, 2018; Bhusal et al., 2024).

In Nepal, grasslands cover roughly 11.5% of the country's total land area, which equals 1.7 million hectares (Bhusal et al., 2024). This ecosystem is mainly found within four protected areas in the lower Terai Region, which is part of the larger Terai Arc Landscape (Peet et al., 1999). The Terai Arc Landscape (TAL) is a unique and biodiverse ecosystem located along the Nepalese-Indian border (**figure 1**). In Nepal alone, the TAL covers an area of 24710 square kilometres and contains a mix of wetland, agriculture, forest and grasslands (Ahrestani & Sankaran, 2016). This diversity of the different ecosystems provides important habitat for a wide variety of flora and fauna (Peet et al., 1999; Thapa et al., 2021). This includes some of the world's most endangered species such as the Royal Bengal Tiger (*Panthera tigris tigris*), Bengal Florican (*Houbaropsis bengalensis*), Greater One-horned Rhinoceros (*Rhinoceros unicornis*) and the Asian Elephant (*Elephas maximus*).

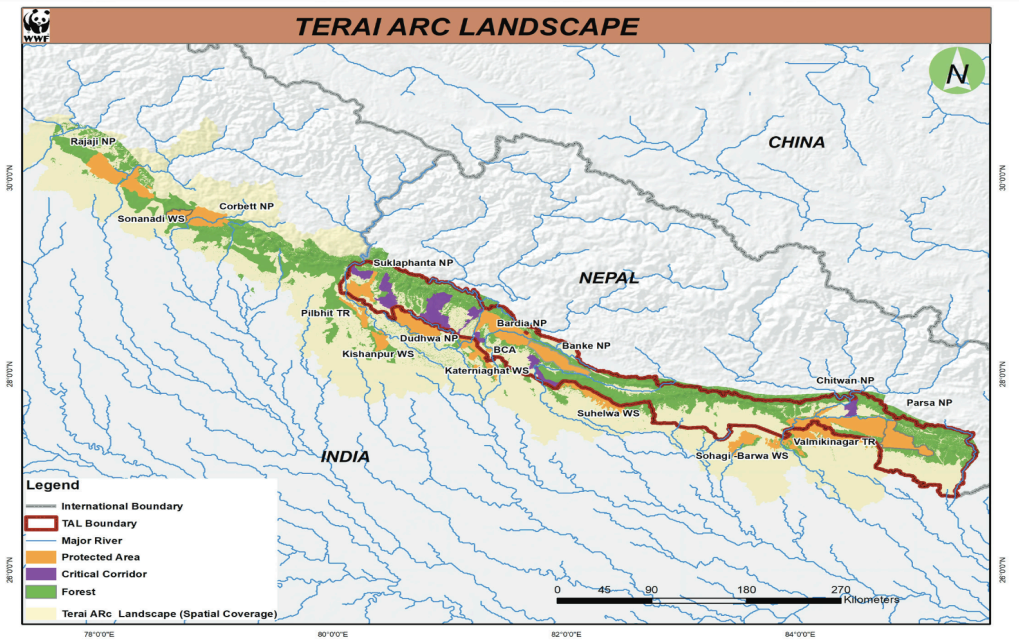

Figure 1: Overview of the Terai Arc Landscape (TAL), showing protected areas and national parks, including Bardia National Park in western Nepal (Bhandari, 2023)

One of the protected areas in the TAL is Bardia National Park (BNP), located in the western part of Nepal. It is the largest national park in Nepal with an area of 968 square kilometres, established in 1988. These subtropical grasslands are unique in their ability to sustain a wide array of herbivores. Compared to the African grasslands, Asian grasslands sustain a

variety of feeding strategies, accommodating grazers, browsers, and mixed feeders in a relatively smaller area (Ahrestani and Sankaran, 2016). Thapa (2023) points out the range of species in the grasslands from small species like the Hispid Hare (*Caprolagus hispidus*) to large megafauna such as the Asian Elephant. The grasslands in BNP serve as key habitats for many of the rare and endangered species by supporting complex food webs and ecological processes (Peet et al., 1999; Thapa et al., 2021). For instance the grasslands are essential for the Royal Bengal tiger, as the habitat supports its prey species which rely on open grasslands. Bardia now holds the highest tiger density in the world, with its population nearly tripping over the past 15 years thanks to targeted conservation efforts (DNPWC, 2023). This success is closely linked to the availability and health of grassland habitats (Bhattarai & Kindlmann, 2011).

However, these grasslands are under increasing pressure. In recent decades, they have been steadily declining due to the encroachment of forest and woody vegetation (Peet et al., 1999a**;** Odden et al., 2005**)**. If this shift continues, it risks destabilising the entire ecosystem, disrupting ecological processes and threatening the survival of species that depend on open habitats (Bhattarai & Kindlmann, 2011). To understand why this decline is happening, it is important to understand the ecological dynamics and disturbance processes that shape the grasslands. Peet et al. (1999) documented several distinct vegetation communities across the park, each characterised by differences in soil development, hydrology, and successional state. These communities reflect different stages of succession and highlight the ecological complexity of the system.

The structure and composition of these vegetation communities play a central role in shaping habitat availability for different species. The early-successional *Saccharum spontaneum* community offers habitat for the Wild Buffalo (*Bubalus bubalis*). The mid-successional, short grass *Imperata cylindrica* grasslands provide crucial habitat for endangered species like the Hispid Hare and Bengal Florican, while the later-successional *Narenga porphyrocoma* grasslands serve as grazing grounds for ungulates like the Swamp Deer (*Rucervus duvaucelii*). These plant communities reflect the ecological complexity of the landscape and contribute to its high biodiversity.

The grasslands of BNP are highly dynamic, constantly shaped by natural and anthropogenic pressures. Abiotic factors such as hydrology, soil type, fire regimes and grazing impact the composition and structure of grasslands (Peet et al., 1999**;** Lehmkuhl, 1989; Das et al., 2021). Those factors contribute to habitat fragmentation, biodiversity loss and shifts in vegetation composition (Peet et al., 1999**;** Lehmkuhl, 1989; Das et al., 2021). Fire especially has an extensive impact on the grasslands (Das et al., 2021). Both natural and anthropogenic fires play a crucial role in preventing forest encroachment, maintaining open grasslands and stimulating young grass shoots which are preferred by grazers. The fire regimes are especially critical during the dry winter season, when fires counterbalance the woody vegetation which is driven by the monsoon rains (Das et al., 2021). Fire also helps reset succession and maintain early-stage vegetation communities. Historically, such disturbance was shaped by local land-use practices. Rotational grazing and seasonal burning by communities helped maintain the grassland landscape and prevent succession toward forest. Thapa (2023) describes present-day grasslands as a legacy of these historic practices. Today, modern conservation management continues to apply controlled burns to

replicate these traditional disturbance regimes and preserve the ecological function of the grasslands (CNP, 2016)

Hydrology is another important driver of grasslands dynamics in Bardia NP. The western part of the park lies within the Karnali floodplain, where the landscape is shaped by seasonal river systems, wetlands, and groundwater reserves. Seasonal flooding during the monsoon deposits nutrient-rich sediments and helps maintain open grasslands, especially in low-lying areas (Dinerstein, 1979; Peet et al., 1999). In contrast, the dry winter season introduces hydrological stress as water levels drop, leaving grasslands dependent on remaining soil moisture for regeneration (Dinerstein, 1979; Peet et al. 1999). Changes in river flow, sedimentation, or water retention can shift species composition and alter the long-term stability of grassland ecosystems (Bijlmakers et al., 2023).

Given the importance of recurring disturbance, the grassland ecosystems within the Terai Arc Landscape can be characterised as a disturbance climax (Peet et al., 1999; Lehmkuhl, 1989). A disturbance climax refers to a relatively stable ecological state that is maintained with periodic disruptions, such as fire, grazing, or anthropogenic activity (Turner & Seidl, 2023; Peet et al., 1999). In the absence of such disturbances, these grasslands will most likely transition toward Sal (Shorea robusta) forest, which is the climax vegetation of the region (Gautam & Devoe, 2005). Another useful theory here is the Intermediate Disturbance Hypothesis (Connell, 1978), which suggests that biodiversity tends to peak under intermediate levels of disturbance. When disturbance is too infrequent, dominant species may outcompete others, while excessive disturbance can limit the establishment of slower-growing or less resilient species (Moi et al., 2020; Connell, 1978). Both theories can help make sense of how Bardia grasslands function. One points to the role of disturbance in keeping the system structurally stable, the other showing how diversity patterns might be shaped in the process. Together, they front the basis for this research into how disturbance regimes influence vegetation structure and species composition.

1.1 Relevance and Objectives

Although fire is widely used in grassland management, there is still limited understanding of how it shapes vegetation structure and species composition in Bardia. Earlier studies have raised questions about the long-term effects of fire suppression (Lehmkuhl, 1989; Bijlmakers, 2023). While fire is thought to help maintain open grasslands, there is little clarity on what frequencies or timings are most effective for supporting biodiversity and ecosystem function (Dinerstein, 1979; Lehmkuhl, 1989). More recently, Lamichhane et al. (2024) pointed to the lack of research on how fire affects plant communities and their structural traits in Nepal's subtropical grasslands. While some comparisons have been made between burning and cutting, fewer studies look specifically at how fire regimes across time influence vegetation within and between different grassland communities. This research builds on these gaps by examining how fire frequency over the past decade has shaped biomass, vegetation structure, and species dominance in Bardia's grasslands.

Research Questions

The research is structured around the following main and sub-questions:

How do fire regimes shape grassland structure and biodiversity in Bardia national park in Nepal?

1. *How accurately does the fire detection model capture the spatial and temporal occurrence of fire?*

2. *What are the spatial and temporal patterns of fire regimes in Bardia's subtropical grasslands over the past decade, and how do they vary across hydrological gradients and grassland types?*

3. *How does fire affect the vegetation structure and biomass of Bardia's subtropical grasslands?*

4. *How does fire influence the species composition and the associated functional traits in Bardia's subtropical grasslands?*

Hypothesis

Frequent fire is expected to reduce vegetation height and biomass, as repeated burning limits the growth of taller grasses and woody species. In areas that haven't burned for a while, vegetation is likely to be taller and denser. These differences in fire history are also expected to affect which grass species dominate. Sites with high fire frequency may be dominated by early-successional species, while less frequently burned areas are more likely to support later-successional species. Following the Intermediate Disturbance Hypothesis, species diversity is expected to peak at moderate fire frequencies, where disturbance is enough to create variation but not too frequent to exclude slower-growing species.

2. Conceptual Framework

2.1 Fire and Vegetation

In Bardia's grasslands, vegetation communities are defined mainly as the dominant grass species present. These species do not reflect just successional stages but also disturbance patterns and site conditions. A vegetation community refers to a group of plant species that occur under similar environmental conditions and disturbance regimes, with a few species often dominating the vegetative cover (Peet et al., 1999). Following the classification of Peet et al. (1999), the main vegetation communities for this research are *Saccharum spontaneum, Imperata cylindrica, Narenga porphyrocoma* and *Themeda arundinacea*.

The successional development of vegetation communities in Bardias grasslands is shaped by a complex interaction between disturbance regimes, site conditions and species-specific traits **(**Dinerstein 1979a; Peet et alk, 1999; Lehmnkuhl, 1989). *Saccharum spontaneum* (SS) often establishes itself on newly deposited riverine alluvium as a pioneer species (Lehmkuhl, 1989; Peet et al., 1999). It forms a thick and compact growth and due to an extensive rhizomatous root network can regrow within a short period after a disturbance such as fire. The early-stage grasslands are typically found along rivers, where bare sediment provides ideal conditions for colonisation. It is also known to shift in tandem with the changing course of the rivers (Lehmkuhl, 1989; Bijlmakers et al., 2023). As the substrate begins to stabilise and becomes more compact, the *Saccharum Bengalense* (SB) can appear alongside or take over in the slightly older and drier riverbank areas (Peet et al., 1999; Lehmkuhl, 1989). Although this species is commonly found through the grasslands, it is classified as part of the *Saccharum spontaneum* vegetation community due to its co-dominance alongside *SS* and a clear, direct successional relationship (Peet et al., 1999).

Further along the successive gradient, *Imperate cylindrica* (IC) tends to dominate grasslands on abandoned agricultural sites or older terraces, where soil development is more developed and established (Dinerstein, 1979a; Lehmkuhl 1989; Peet et al., 1999). This short grass has an extensive root system with more than 60% of its total biomass found under the ground (Flory et al., 2018). These traits make IC a rapid coloniser that is highly competitive under disturbance regimes like frequent fires and heavy grazing. (Lehmkuhl, 1989). It is often the only grass to flower shortly after a fire event due to quick resprouting (Lehmkuhl, 1989). This allows the IC to recover quickly and maintain its dominance in an ecosystem shaped by frequent fire. Fire also improved the nutritional quality of fresh shoots, which is preferred by herbivores (Lehmkuhl, 1989). However, in the absence of disturbance, it is gradually replaced by later successional species such as *Narenga porphyrocoma* (NP) and *Themeda arundinacea* (TA). Tall grasses such as NP are typically found on more stable, well-drained alluvial soils (Lehmankuhl, 1994). *Themeda arundinacea* can be found on even more established sites and often marks the transition into late-stage grasslands which, without disturbance, both are eventually replaced by Sal (*Shorea robusta*) forest as the climax community (Peet et al., 1999).

Fire plays a central role in shaping grassland succession in Bardia, not only influencing which species dominate but also affecting the physical structure and function of these ecosystems. Frequent burning tends to favour earlier-successional, fire-tolerant species

such as *Saccharum spontaneum* and *Imperata cylindrica*, while long-unburned areas accumulate more biomass and gradually shift toward later-successional species like *Narenga porphyrocoma* (Dinerstein, 1979; Lehmkuhl, 1989; Peet et al., 1999). These successional patterns and fire responses suggest that different fire regimes support different stages of grassland development. In this context, the Intermediate Disturbance Hypothesis (Connell, 1978) offers a useful framework to understand species diversity patterns. It proposes that species richness is highest when disturbance occurs at intermediate levels, as this allows both colonising and later-successional species to coexist. In systems where disturbance is too frequent, only a few disturbance-tolerant species are able to survive, while in the absence of disturbance, dominant competitors can exclude others. The relationship between disturbance and diversity is visualised in **figure 2.1**. Applied to Bardia, this framework suggests that moderate fire frequencies could help maintain a shifting patchwork of successional stages and support higher plant diversity. It could help connect fire regimes to vegetation composition and support an analysis of how species respond under different disturbance conditions.

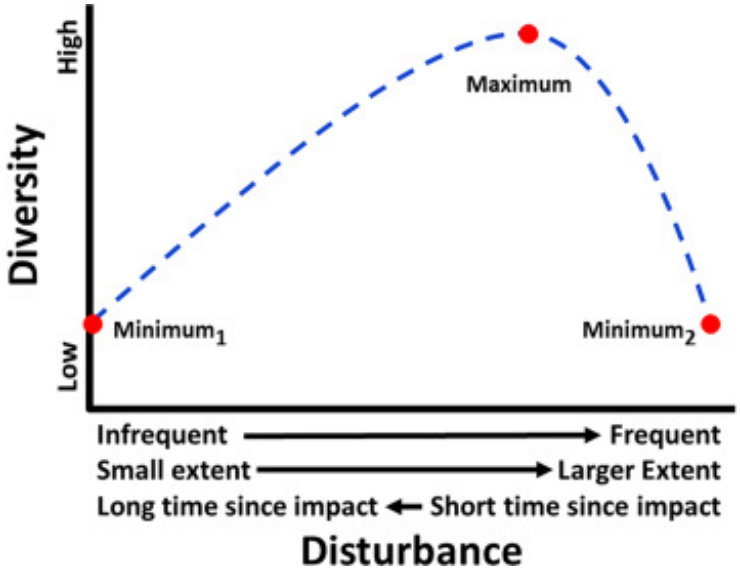

Figure 2.1 Simplified illustration of the Intermediate Disturbance Hypothesis, illustrating how species diversity is expected to be lowest at both low and high disturbance levels, and highest at intermediate levels. Adapted from Connell (1978)

While fire is a natural part of the grassland ecosystem, it is also increasingly driven by human activity. **Figure 2.2** shows that the TAL has a very high fire vulnerability compared to the rest of Nepal. About 58% of the occurring forest fires in Nepal are caused by the deliberate burning of the forest by hunters, grazers, foragers and poachers (Pandey et al., 2022). Fire is widely used as a land management tool to manage grassland structure, reduce biomass, and stimulate the growth of fresh, palatable shoots for livestock and wild herbivores (Lamichhane, 2024). Early season burns can also help reduce the accumulation of fuel load and reduce the risk of uncontrolled wildfires later in the season. However, not all fires are intentional. Accidental fire spreading is a significant issue, with winds or human negligence causing fires to escape control and spread to surrounding areas. This can result in the unintentional destruction of forests and wildlife habitats. Pandey et al. (2022) point out that the lack of forest management practices in Nepal have a direct link to the increase of

forest fire risk. Currently, 29.5% of Nepalese forest is likely to catch fire every single year (Reddy et al., 2019).

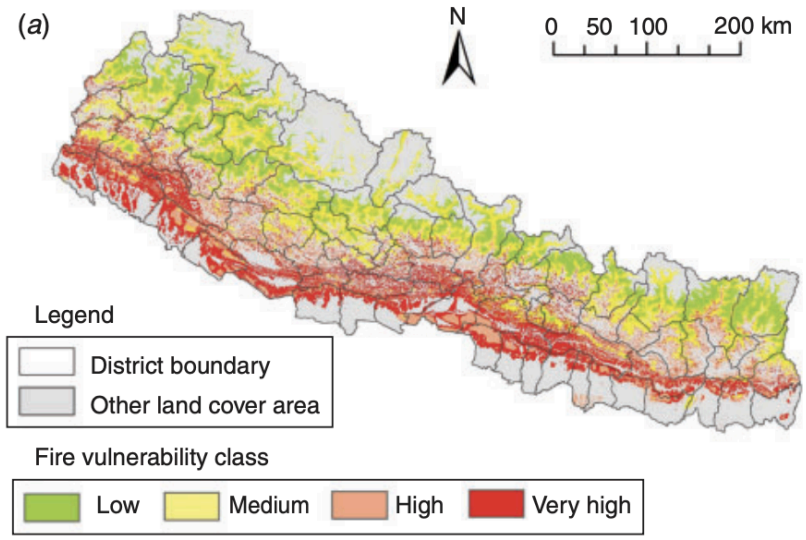

***Figure 2.2**: Forest fire risk map of Nepal highlighting the very high vulnerability of the Terrai Arc Landscape region (Matin et al., 2017)*

2.2 Other factors shaping the grassland dynamics

While fire plays a key role in shaping the composition and structure of Bardia's grasslands, it is not the only factor influencing grassland dynamics. Climatic variability, hydrological processes, local land management practices, and broader conservation policies all contribute to the changing vegetation patterns across the landscape.

Climatic conditions play a big role in how these grasslands are shaped. BNP has a monsoon-influenced humid subtropical Cwa climate and experiences distinct climatic seasons. The monsoon season, from June to September, accounts for 90% of the annual discharge of the Karnali River system and recharges the groundwater (Bijlmakers et al., 2023). This is counterbalanced by a dry season lasting from October to May, during which the fire risk increases. At the end of the dry season in April and May, approximately 80% of Nepal's annual fires take place (Mathema, 2013). These seasonal extremes do not only affect vegetation growth and water availability, but also determine the timing and intensity of disturbance events, which are essential for maintaining open grasslands (Das et al., 2022).

Hydrological dynamics also play a crucial role in vegetation structure and succession. Peak discharges of the Karnali river have caused major fluvial disturbance which have led to successional resets of grasslands where flooding causes erosion and sediment deposition (Bijlmakers et al. 2023). These processes promote the growth of pioneer grass species in the newly reset areas. However changes in Karnali river course have reduced flooding in certain areas which has led to the disturbance-dependent grasslands slowly transitioning into taller grass communities or even forest (Bijlmakers et al., 2023). It shows the impact river dynamics can have with its cascading effects on vegetation patterns and, as a result, the fauna that depend on them. While maybe not as significant as fluvial disturbances, extreme precipitation events can trigger localised flooding and erosion, particularly along

ephemeral streams outside the floodplain. These events contribute to the maintenance of grasslands in those areas (Bijlmakers et al., 2023).

Beyond climatic and hydrological influences, land management practices such as mowing and grazing are important in shaping grasslands composition. The mowing is carried out approximately two or three times a year and has helped maintain the grasslands (CNP, 2016). The local community also manually cut grass for construction of traditional local houses and as feed for livestock (CNP, 2016). While the cutting was initially banned after the establishment of the national park, permits were introduced to regulate the cutting and reduce illegal harvesting. However, the community demand often exceeds what the grass cutting programs allow, leading to continued illegal grass cutting which can disrupt ecological balance (CNP, 2016). Historically, domestic livestock grazed alongside wild herbivores within the areas which currently are the national parks (Dinerstein, 1979). In 1975, the biomass of livestock in these parks was estimated to be roughly 15 times higher than that of wild ungulates. Thapa (2021) suggests that this combined grazing pressure, along with grass cutting by local communities, may have contributed to the creation of the mosaic of tall and short grassland patches in the subtropical grasslands of Bardia National Park.

Finally, conservation policy and the socio-political landscape also shape grassland dynamics. Since the mid-20th century, Nepal has made significant conservation efforts to protect and conserve its unique biodiversity. Currently in 2025, there are 12 national parks in Nepal (DNPWC, 2023). While these efforts are often celebrated as conservation success stories, they also have profound socio-economic consequences for local communities. The creation of the national parks imposed strict restrictions on traditional activities such as grazing, farming and forest use, displacing many local communities to buffer zones without compensation (Thapa, 2023). The loss of access to vital resources for food, shelter, land and medicine disproportionately affected already marginalised groups (Amnesty International Nepal, 2021). Today, rising wildlife populations increasingly cause crop damage, livestock loss and even human injury, intensifying tensions between conservation goals and local livelihoods (Amnesty International Nepal, 2021).

2.3 Indicators

To systematically analyse how Bardia's grasslands respond to disturbances, this study uses a set of ecological indicators and functional classifications that reflect vegetation structure, species composition, and underlying environmental conditions. The grouping of the dominant grass species was sorted into functional groups, based on their growth form and position along the successional gradient. A functional group refers to a set of species that share similar ecological roles or responses to environmental drivers, regardless of their taxonomic relatedness (Blondel, 2003). In this case, the grouping follows the dominant vegetation communities identified by Peet et al. (1999) and reflects how these grasses interact with disturbance and landscape position. In **table 2.3** below the functional groups are shown. The pioneer tall grasses are typically found in recently disturbed or dynamic environments such as floodplains and are quick to establish after fire or sediment deposition. Short grasses form dense mid-successional stands and are especially important for herbivore forage, while late-successional tall grasses tend to occur in more stable areas with lower disturbance pressure. This functional classification helps to link species composition to

disturbance regimes and provides a framework for understanding how different grassland types respond to changing fire frequencies and moisture conditions.

Table 2.3 *Functional groups, Vegetation Community (Peet et al., 1999) and the included grass species in Bardia National Park*

Functional Group	Vegetation Community	Included Species
Pioneers Tall Grasses	*Saccharum spontaneum*	*Saccharum bengalense*, *Saccharum spontaneum*
Short Grasses	*Imperata cylindrica*	*Imperata cylindrica*
Late-Successional Tall Grasses	*Narenga porphorycoma*	*Narenga porphorycoma*

In addition to the functional groups, several indicators were selected to capture specific aspects of vegetation structure, composition, and response to disturbance. These indicators reflect different ecological processes relevant to fire and water dynamics in Bardia's grasslands and help to link field patterns to broader ecosystem functioning. **Table 2.4** below gives an overview of the indicators used and their interpretation.

Table 2.4 *Overview of ecological indicators used to assess vegetation responses to fire and hydrological conditions in Bardia National Park.*

Indicator	Description	Interpretation of values
Normalised Difference Vegetation Index	Reflects vegetation greenness based on red and near-infrared reflectance.	*Higher values indicate dense, photosynthetically active vegetation; lower values suggest sparse, stressed, or dry cover.*
Differenced Normalised Burn Ratio	Measures fire occurrence and severity by comparing pre- and post-fire reflectance.	*Positive values indicate fire-induced vegetation loss; values near zero suggest little change; negative values may signal post-fire regrowth.*
Soil Bulk Density	Indicates soil compaction and structure, influencing root growth and water infiltration.	*High values reflect compacted soils that may limit root development and reduce water availability; lower values suggest looser, more porous soils.*
Plant Water Content	Measures plant hydration by comparing fresh and dry biomass weights.	*High values reflect well-hydrated plants, often with higher fire resistance; low values suggest drought stress or dry conditions.*
Leaf Size	Represents species morphology and adaptation to environmental stress.	*Smaller leaves often indicate adaptation to repeated fire or drought; larger leaves are common in wetter, less disturbed areas.*
Shannon Diversity Index	Captures both species richness and evenness within a plant community.	*Higher values indicate a more diverse and balanced community; lower values reflect species dominance or reduced richness.*
Specific Leaf Area	Refers to the ratio of leaf area to dry mass, indicating resource-use strategy.	*High values are typical of fast-growing species in moist or disturbed environments; low values suggest conservative strategies in dry or fire-prone conditions.*

3. Methodology

3.1 Study Area

The research was conducted in January and February 2025 in Bardia National Park (28°15'–28°35.5'N, 80°10'–81°45'E). The park is located in the southwestern part of Nepal as seen **in figure 3.1** and covers an area of 968 km² with a surrounding buffer zone of 507 km² (DNWPC, 2023). The research focused on south-western corner of Bardia National Park, where the Karnali floodplain lies, because it contains a wide range of habitat types within a relatively small area. This part of the park includes floodplain grasslands, riverine forests, and patches of sal-dominated woodland, making it one of the most floristically diverse sections of the park (Dinerstein, 1979). This ecological variation made it a suitable area for studying how different grassland types respond to fire and other environmental conditions

In this study, field data collection was combined with remote sensing and satellite imagery. By collecting field observations, ground truth sampling was used to attempt to validate the satellite datasets. A total of twelve grasslands were selected for fieldwork across BNP. **Figure 3.1** displays a map of the sampling location. These grasslands differ in disturbance history and hydrological conditions, offering a gradient from riverine to more established habitats. Important as the stratification is based on vegetation, the goal was to sample at least 10 plots of each grassland type. In practice however, the numbers were determined by field accessibility, feasibility and ecological variation. In the end, the final plot numbers are visible in the **table 3.2** below.

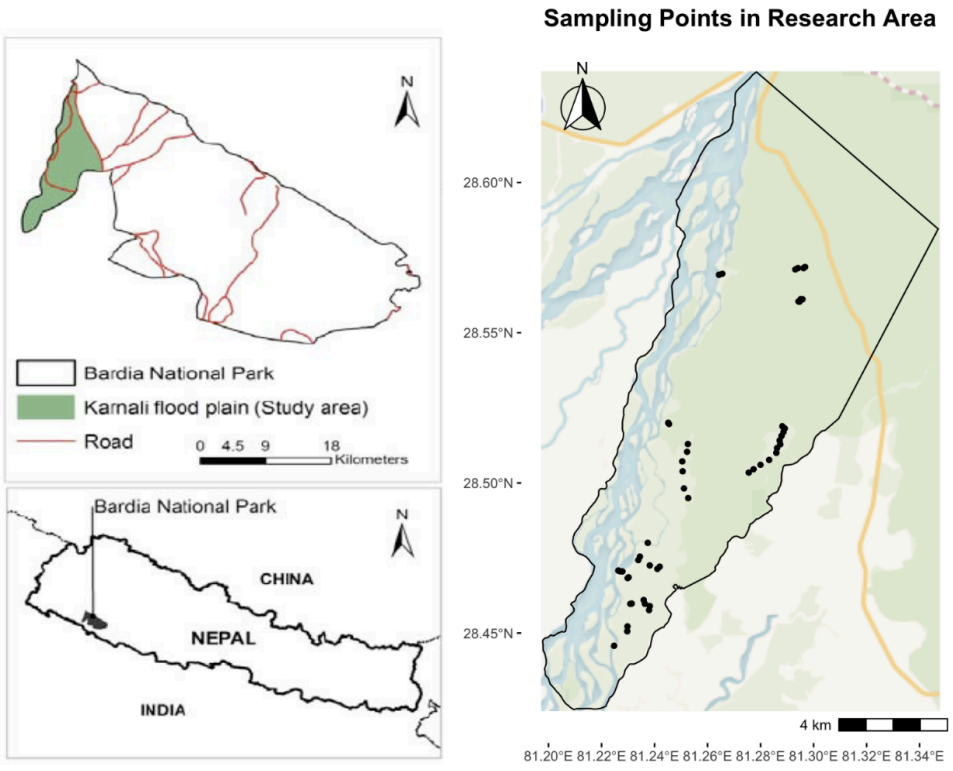

Figure 3.1 *Study area in Bardia National Park, Nepal. The bottom left shows the park's national location and the top left marks the location of the Karnali floodplain where the study was conducted (adapted from Gautam, 2013). The right panel shows the vegetation sampling points within the study area.*

Table 3.2 *Number of vegetation plots sampled per dominant grass species during fieldwork in Bardia National Park*

Dominant Species	**Amount of plots**
Sb: *Saccharum bengalense*	11
Ic: *Imperata cylindrica*	16
Np: *Narenga porphorycoma*	10
Ss: *Saccharum spontaneum*	11
Ta: *Themeda arundinacea*	2
In total	**50**

3.2 Field Collection

In the field, each vegetation plot was located in a grassland and was demarcated as a 10×10 metre square. Within each plot, data was collected to assess vegetation structure, soil properties, species composition and disturbance indicators.

1. Soil Sampling

Soil Bulk Density (BD)

A 100 ml soil core was extracted using a soil ring (5 cm height, 5 cm diameter; volume of 98.17cm³). Samples were stored in labelled bags and weighed fresh upon return from the field.Samples were then oven-dried for 24 hours at ~100°C to determine the dry weight. Bulk density was calculated using formula (1) from Zhang (2011).

$$Bulk\ density\ (g/cm^3) = Dry\ soil\ weight\ (g) / Soil\ volume\ (cm^3) \quad (1)$$

Soil Nutrients

Composite soil samples were collected using a hand auger. Two subsamples were mixed, and half the material was discarded. These samples were stored in cool conditions before being sent off for lab analysis by a partner lab. However, this data was excluded from the analysis as the laboratory was unable to provide the results within the required timeframe

2. Vegetation Sampling

Biomass Collection:

Within each 10×10 m plot, a 40×40 cm quadrat was used for biomass collection. All vegetation within the quadrat was clipped to ~5 cm above ground level. The samples were sorted into green and brown leaves and stems and weighed fresh and dried. The drying was done by placing the vegetation in the sun for a minimum of 5 days.

Structural measurements:

From each quadrat, five stems were randomly selected to measure structural parameters, including stem diameter, length (total and stem), width, and amount of leaves. For three of the five stems, five leaves were randomly selected to have their length and width also noted.

Plant Functional traits

With the vegetation data collected, the following plant functional traits were calculated:

Leaf size (LS) is calculated as the product of leaf length, width and a leaf shape-specific correction factor (Schrader et al., 2021) as seen in formula (2).

$$Leaf\ Size\ (cm^2) = leaf\ length\ (cm) * leaf\ width\ (cm) * 0.75 \quad (2)$$

The *Specific Leaf Area* (SLA) was calculated by multiplying the average leaf size with the average leaf amount (Garnier et al., 2001). This was then divided by the amount of dried leaf weight by summing the dry weight of all the leaves (here noted as green and brown leafs) as seen in (3).

$$Specific\ Leaf\ Area\ (cm^2/g) = \frac{Average\ leaf\ size\ (cm^2) * Average\ leaf\ amount}{Dry\ weight\ green\ leafs\ (g) + Dry\ weight\ brown\ leafs\ (g)} \quad (3)$$

3. Vegetation Survey

A structured survey form was completed in ‘Fieldmaps’. Variables recorded included date, time, GPS location, management type, vegetation community, dominant species, canopy cover, tree/clump counts, and understory condition (green/brown biomass, herbivore damage). In addition, a full Braun-Blanquet survey was conducted per plot, recording all species, their cover and abundance estimates.

3.3 Data Analysis

Moisture Calculations

Gravimetric Moisture content (GMC) gives the percentage of water in the soil relative to the dry weight. It was calculated using formula (4).

$$Gravic\ Moisture\ Content\ (\%)\ =\ \frac{Fresh\ weight\ of\ soil\ (g) - Dry\ weight\ of\ soil\ (g)}{Dry\ weight\ of\ soil\ (g)} * 100\% \quad (4)$$

Volumetric moisture content (VMC) indicates how much of a given soil volume is actually water. VMC refers to the amount of water held within the soil while focussing on volume, while GMC focusses on mass. VMC was calculated using formula (5).

$$Volumetric\ Moisture\ Content\ (\%)\ =\ Gravic\ Moisture\ Content\ (\%)\ *\ Bulk\ density\ (g/cm^3) \quad (5)$$

Water Content (WC) expresses the amount of water in plant tissue relative to its dry weight, indicating how many grams of water are present per gram of dry plant tissue. WC was calculated using formula (6).

$$Water\ Content\ (g/g)\ =\ \frac{Fresh\ Weight\ (g) - Dry\ Weight(g)}{Dry\ Weight(g)} \quad (6)$$

Species Diversity

Species diversity was calculated using the Shannon Diversity Index (H'). The Shannon Diversity Index was calculated in R-studio using the '*diversity'* function from the vegan package. The cover and abundance values of each species were originally recorded in Braun-Blanquet classes which are categorical and not usable in quantitative analysis. This led to the Braun-Blanquest cover class being converted into a more usable numeric format. A midpoint value was selected for each class for further analysis, the conversion can be found in the **appendix table A1.**

3.3 Remote Sensing Analysis

Burn frequency mapping

In Google Earth Engine (GEE), burn frequency maps were generated using Sentinel-2 imagery. Burn detection was based on changes in vegetation indices (dNBR and NDVI) before and after three seasonal fire periods: early (Jan-Feb), middle (Mar-Apr) and late (May) fires for the years (2016-2025). For 2025 the late fire was not able to be generated due to satellite imagery not being available. Same goes for the years before 2016 as Sentinel-2 data is only available from June 2015 onwards.

Burn frequency was defined as how many times a specific area or pixel was burned between 2016 and may 2025. The pixels were stacked on top of each other in R (Version 2024.12.1+563) and are assigned values based on the amount of burns. If there was no fire, the value of 0 was assigned. By summing the pixels in all the layers, the total burn frequency per pixel was created.

Fire Map Validation

The early 2025 burn frequency map was validated using the collected field data. The burned areas detected via satellite were compared to the actual ground-truth fire presence in the field. A confusion matrix showed how many pixels were correctly or incorrectly classified into the fire and no fire categories. The number of true positives, true negatives, false positives and false negatives were computed. Additionally, accuracy metrics such as overall accuracy, the kappa coefficient and class-specific accuracy, precision, recall and f1 scores were calculated to identify how the burn frequency map was performing. Finally, the false positives and false negatives were visualised to show where and why errors occurred to help improve the fire visualisation model. An overview of the key accuracy metrics can be found in **table 3.3**.

Table 3.3 *Accuracy metrics used in the analysis of the fire model validation with definition & formula.*

Term	Definition	Formula
True Positives (TP)	Ground Truth said fire, prediction said fire	-
True Negatives (TN)	Ground truth say no fire, prediction say no fire	-
False Positives (FP)	Ground truth said no fire, prediction say fire	-
False Negatives (FN)	Ground truth said fire, prediction said no fire	-
Cohen's Kappa (κ)	It compares the observed accuracy (Po) with the expected accuracy (Pe)	κ = (Po - Pe) / (1 - Pe)
Precision	Of the pixels which were predicted as fire, how many were actually fire	TP/ (TP+FP)
Recall	Of the actual fire pixels, how many were correctly detected	TP/(TP+FN)

Digital Elevation Model (DEM) Mapping

For the Digital Elevation Model (DEM) map, the SRTM30-tiles were acquired via the 'elevatr' R package. These tiles combine data from the Shuttle Radar Topography Mission and the U.S. Geological Survey's GTOPO30 data set, provides a 30 metre resolution raster. The DEM raster was projected to match the Sentinel-2 data and combined with the burn frequency data. This data was plotted against the total number of burns in a scatter plot and statically checked with spearman correlation. A stratification of the election values into bands of 50 metres helps to interpret the data.

Time Since Last Fire Mapping

The 'Time Since Last Fire' (TSLF) map was calculated by stacking the burn frequency maps on top of each other in R. The most recent burn year for each pixel was identified and subtracted from 2025 (most recent reference year). This gave the time since the last fire. If a pixel never burned in the selected time period then a value of 0 was assigned. This resulted in a map which showed for each location how many years have passed since it last burned.

Statistical Analysis

Vegetation structure, biomass, and species composition were assessed using statistical tests in R. Non-parametric tests such as the Wilcoxon rank-sum and Kruskal-Wallis tests were applied where assumptions of normality were violated, while ANOVA and Welch's t-tests were used for normally distributed data. Homogeneity of variance was checked using Levene's test, and normality assessed using the Shapiro-Wilk test. Shannon diversity was calculated using the diversity() function from the vegan package, based on Braun-Blanquet abundance values converted into numeric midpoint values.

4. Results

4.1 Fire model validation and Accuracy Assessment

In order to answer the first subquestion about the validation and accuracy of the fire model, an accuracy assessment was done with the help of a ground truth dataset which had 50 points collected in January and February of 2025. The results of the key accuracy metrics were calculated in Google Earth Engine. The confusion matrix **(Table 4.4.1)** showed that out of 50 ground-truth points, there were only 4 pixels that were classified incorrectly. One pixel was a false negative which is where the model said there was no fire, but in reality there was fire. And three pixels were false positives where the model stated fire, but in real life there was no fire. This confusion matrix shows 92% of the pixels checked with ground truth were correct which is the overall accuracy of the model. When split up per class, the accuracy for class No Fire is 0.8696% and Class Fire was 0.9630%. The Kappa coefficient was calculated at 0.8379%. Additionally for the fire class (as its a fire detection mode) the Precision was 0.897, Recall was 0.963 and F2 score was 0.929. Additionally, a map of all the positives and negatives (True & False) was created to visualise the misclassifications on a spatial level (***Figure 4.1.2***).

Table 4.1.1 Confusion matrix results of the fire detection model.

Confusion Metrix	
True positives	26
False positives	3
False negatives	1
True negatives	20

The spatial distribution of the classification results is shown in **Appendix Figure B1**, where all the ground-truth points are compared with the model predictions. The yellow and orange points are especially important as they represent the areas where the model made incorrect predictions. The false negatives (area where a fire occurred but was not detected by the model) are located near the edge of phantas. This suggests that the model may struggle with accurately delineating fire boundaries , especially in transitional zones. Interestingly there is a correctly predicted fire point just below this area, indicating that the model recognised the fire nearby, but failed to capture its full extent. The false positives (where the model predicted a fire but no fire was observed) are generally located close to actual fire

events. When comparing these points with high-resolution satellite imagery from Planet, it becomes clear that they are situated very close to burned areas, suggesting that the model may have picked up residual burn signals or misclassified pixels influenced by nearby fires. This highlights some of the spatial limitations of the model when detecting mall or edge fires.

4.2 Spatio-Temporal patterns of fire regimes

Burn Frequency Mapping

The fire frequency map (**Image 4.2.1)** shows the total number of years in which each pixel was classified as burned across the study area of Bardia National Park between 2016 and 2025. Spatial patterns are visible on this map. Most pixels fall within unburned class (visualised in grey) and 1-6 burns (shades as green). The highest fire frequencies with more than 15 burns (coloured orange/red) are located in the northeastern part of the map. This area overlaps with forested zones, a combination of mostly Sal but some riverine forest aswell. On the western side of the study area, the Karanli river runs and is indicated by the grey, unburned areas on the map. Adjacent to the river, grasslands are evident represented by the isolated pockets of 7-10 burns. A full land cover map can be referred to in the **appendix B2**. The grasslands are bordered by unburned areas which most likely correspond to the riverine forest. Variation in fire frequency within the grassland is most likely explained by the difference in species present.

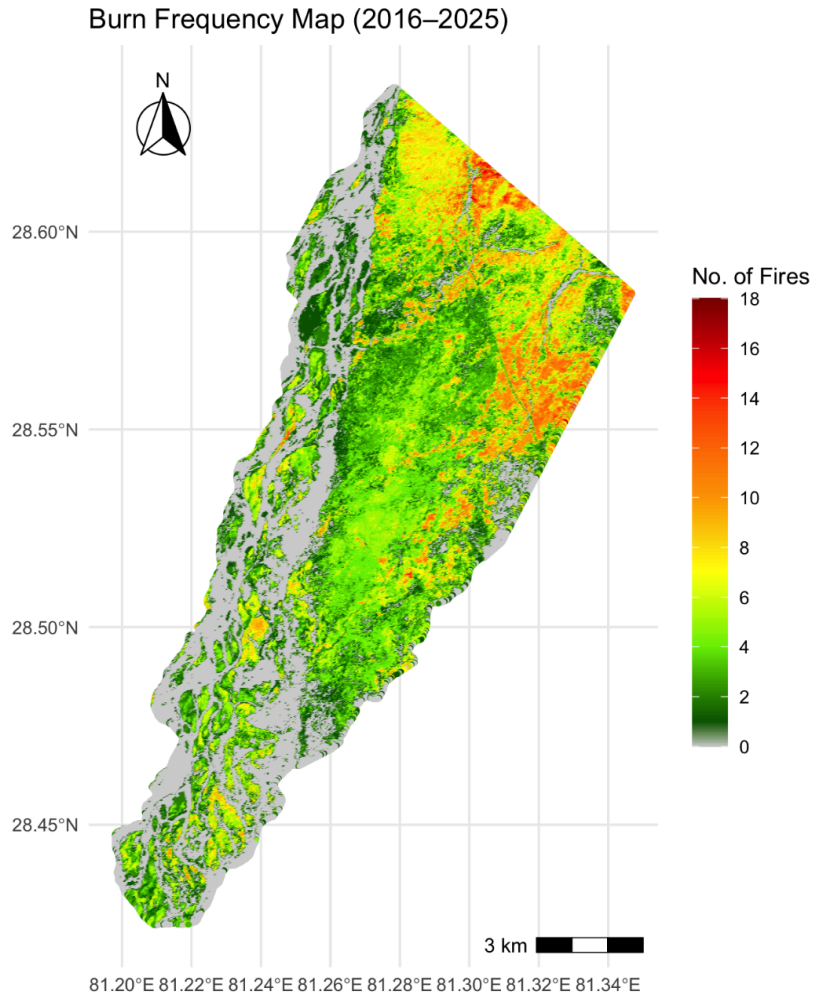

Figure 4.2.1 *Burn frequency map (2016–2025) in Bardia National Park, Nepal. Colours indicate the number of years each pixel was classified as burned, based on dNBR thresholding of Sentinel-2 imagery. Coordinate system: UTM Zone 44N (EPSG:32644). Data: Copernicus Sentinel-2 (harmonised)*

When focusing solely on the grasslands (**figure 4.2.3**) it becomes evident that the majority of the grassland pixels have experienced fire at least six times. Areas with the highest fire frequency, ranging between eight and twelve burns, are concentrated within certain sections of the grassland belt. These higher frequency zones are spatially clustered and generally occur within the larger grasslands which are also more easily accessible from the surrounding villages.

The map was clipped based on a land cover classification by Bijlmakers et al. (2023), using the following categories to define grasslands: bare soil, dry tall grasslands, wet tall grasslands, and short grasslands. The grey patches on the map likely correspond to the bare soil category although changes in the ecosystem since 2019 may have altered some classification. In particular, the river system is highly dynamic and subject to temporal shifts, which can create discrepancies between the current satellite imagery one on which the fire frequency was based and the static 2019 land use map. Consequently, areas currently appearing as riverbed may have been categorised differently in the original classification, potentially affecting the spatial delineation of grassland areas.

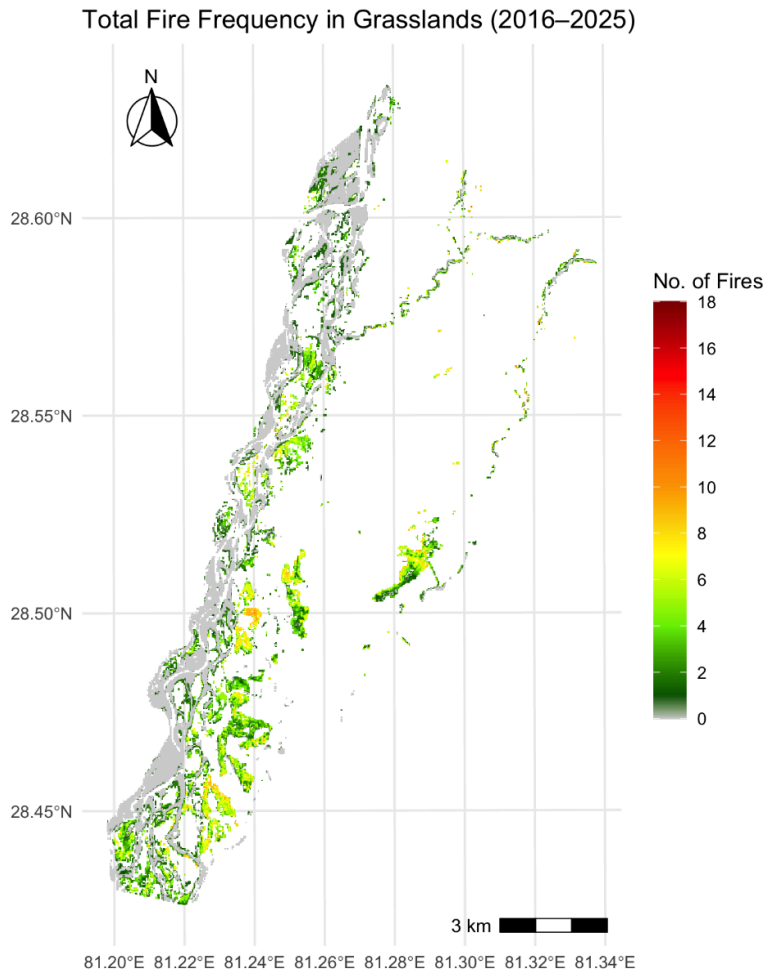

Figure 4.2.2 *Burn frequency map clipped to only the grasslands (Bijlmakers et al., 2023) in Bardia National Park, Nepal (2016–2025). Colours indicate the number of years each pixel was classified as burned, based on dNBR thresholding of Sentinel-2 imagery. Coordinate system: UTM Zone 44N (EPSG:32644). Data: Copernicus Sentinel-2 (harmonised)*

Hydrological Gradient

The burn frequency data was compared to a Digital Elevation Model (SRTM 30m; see **appendix B3**) which serves as a proxy for hydrological conditions. In floodplain systems like Bardia, lower elevations tend to be closer to rivers or flooding areas, where soils usually have higher soil moisture and better access to groundwater. Higher elevations on the other hand, are typically further away from water and drain more quickly, creating drier conditions. These patterns mean elevation could be a useful indicator of landscape-level water availability.

A spearman's rank correlation shows a moderate, positive relationship between elevation and burn frequency (ρ= 0.537; figure 4.2.3) in **figure 4.2.3**. This suggests that fire occurs more often in the higher, drier areas and less in the lower wetter zones. In general, there appears to be a west-to-east gradient across the research area. A transition from the more moist soil conditions in the west next to the river where there are less fires to the more drier conditions found on a higher elevation in the east where more frequent burns can be found. When comparing this to the burn frequency (**Figure 4.2.1**) a similar gradient is visible with

the most frequent burns happening on the higher altitudes. In **Appendix B4**, a scatterplot can be found of the relationship between burn frequency and elevation.

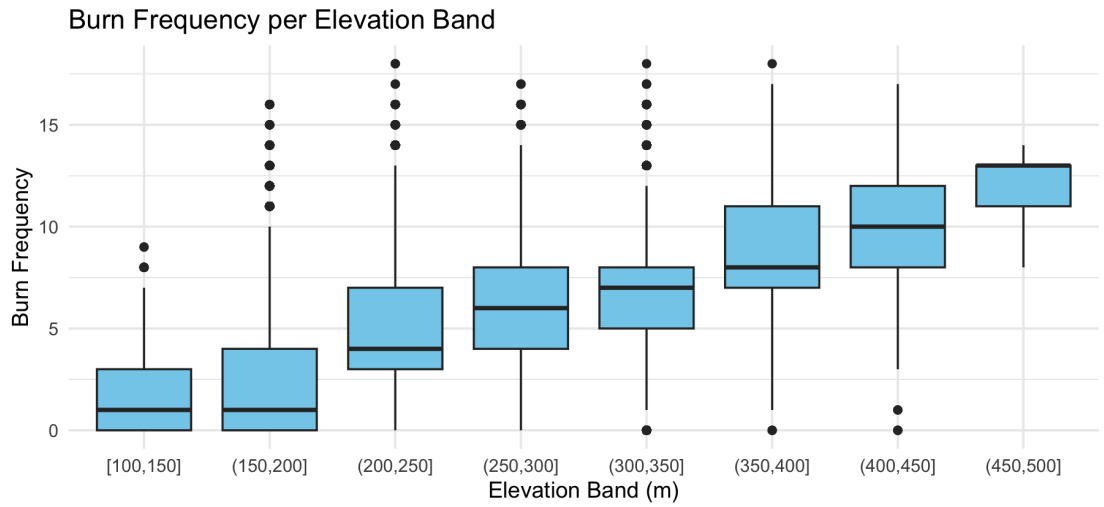

Figure 4.2.3 *Relationship between burn frequency and elevation bands (n = 406352). A Spearman correlation (ρ = 0.537) shows a moderate positive association between elevation and fire frequency.*

Temporal mapping

The frequency burn map has been split up into different time periods. The early fire period refers to the months of January and February.The middle part of the fire period are the months April and May. By then, the park is getting drier and the natural wildfires tend to increase. The last ‘late’ period is May which is the driest month with the most wildfire. When breaking the burn frequency map up into the different time periods different patterns emerge.

Early Fire Map

The early fire frequency map covers a period of January and February across nine years, beginning in 2016. This map as shown in **figure 4.2.4**, was validated using ground truth data collected during the 2025 early fire period. Early-season fires are concentrated alongside the Karnali river, located on the western edge of the study area. Here a distinct band of yellow, orange and red pixels of high fire frequency (6-9 fires) indicate near-annual burning. In contrast, the central region which is dominated by Sal forest, remains largely unburned (grey: 0 fires). The highest burn frequency indicating annual burning is mainly reserved for the specific grassland patches, such as grasslands in the southern tip with the two biggest being Laumkali and Baghaura. This maximum frequency however accounts for less than 2% of the park. About 80% of the high-frequency burns (>6 fires) lie within 2 km of the main flood plain. However in the northern part of the study area, some non-grassland also have fire activity, in particular the areas which are classified as riverine forest, with Sal forest surrounding this. This region is also among the highest elevation of the study area, indicating that possible a drier environment can increase fire frequency during these earlier fire months.

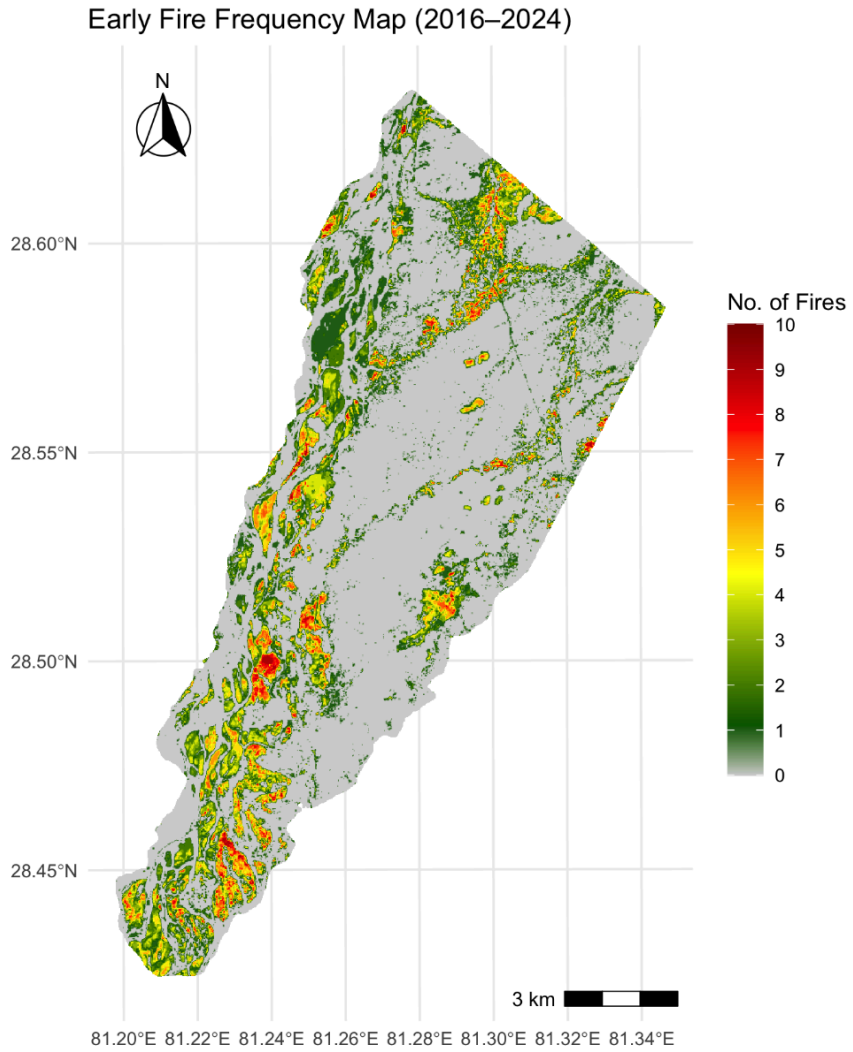

Figure 4.2.4 *Early fire season (January and February) Burn frequency map (2016–2025) in Bardia National Park, Nepal. Colours indicate the number of years each pixel was classified as burned, based on dNBR thresholding of Sentinel-2 imagery. Coordinate system: UTM Zone 44N (EPSG:32644). Data: Copernicus Sentinel-2 (harmonised)*

When clipped to just the grasslands as can be seen in ***figure 4.2.5***, the hotspots become more clear. The majority of the unburned land is part of the bare soil class. The maximum burn class (annual burns; 9) seems to be concentrated more downsouth, with the bigger grasslands such as Lamkauli and Baghaura being highlighted in the middle of the map. The grasslands along the river in the southern tip is also part of this high frequency zone. About 68% of the grassland pixels burned less than 2 times and 9% of the pixels burned more than 9%.

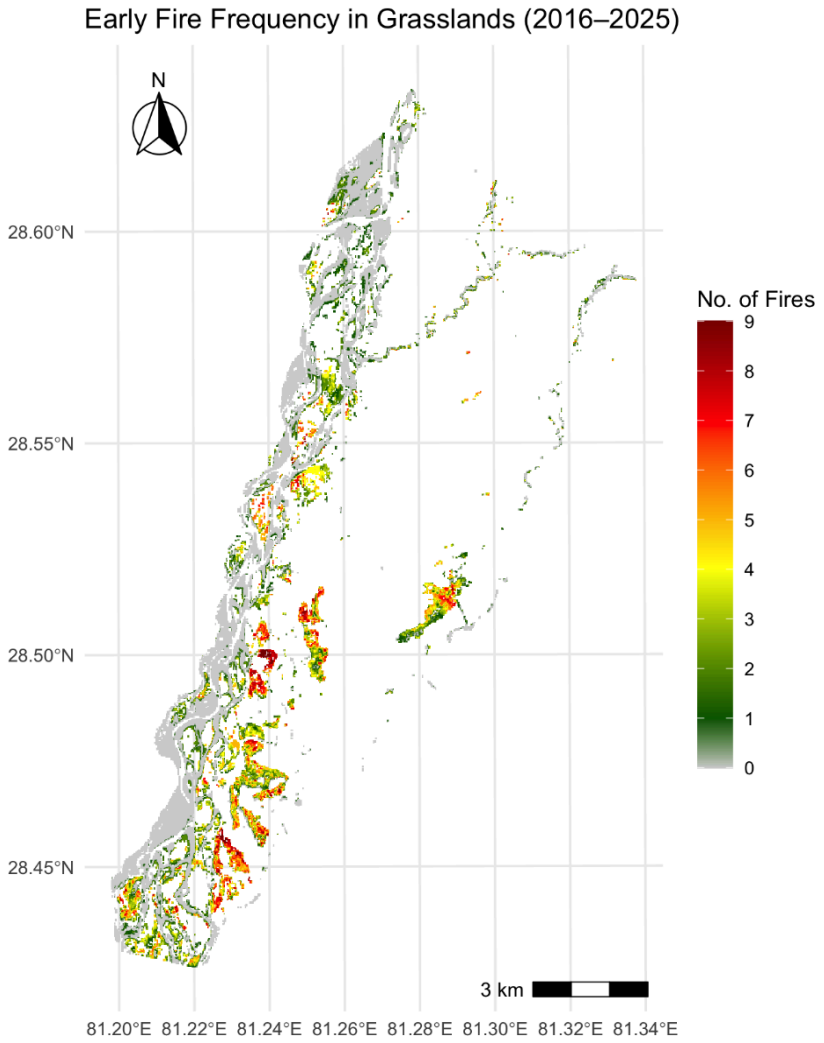

Figure 4.2.5 *Early fire season (January and February), burn frequency of grasslands (Bijlmakers et al., 2023) map in Bardia National Park, Nepal (2016–2025) . Colours indicate the number of years each pixel was classified as burned, based on dNBR thresholding of Sentinel-2 imagery. Coordinate system: UTM Zone 44N (EPSG:32644). Data: Copernicus Sentinel-2 (harmonised)*

Middle Fire maps

The middle fire period covers the months March and April. In **figure 4.2.6** a fire frequency map can be found of that middle fire period. The map shows that the majority of the fire detected by the model is in the north-eastern part of the park which overlaps with the Sal forest zone. There seems to be a very straight line from north to south with on the western (left) side of the area no to very little fire is found and on the eastern side (right) the fire is more common (3-9). This is very different from the 'early'-fire period where the almost exact opposite was seen. A figure where just the grasslands are shown can be found in **appendix C1**.

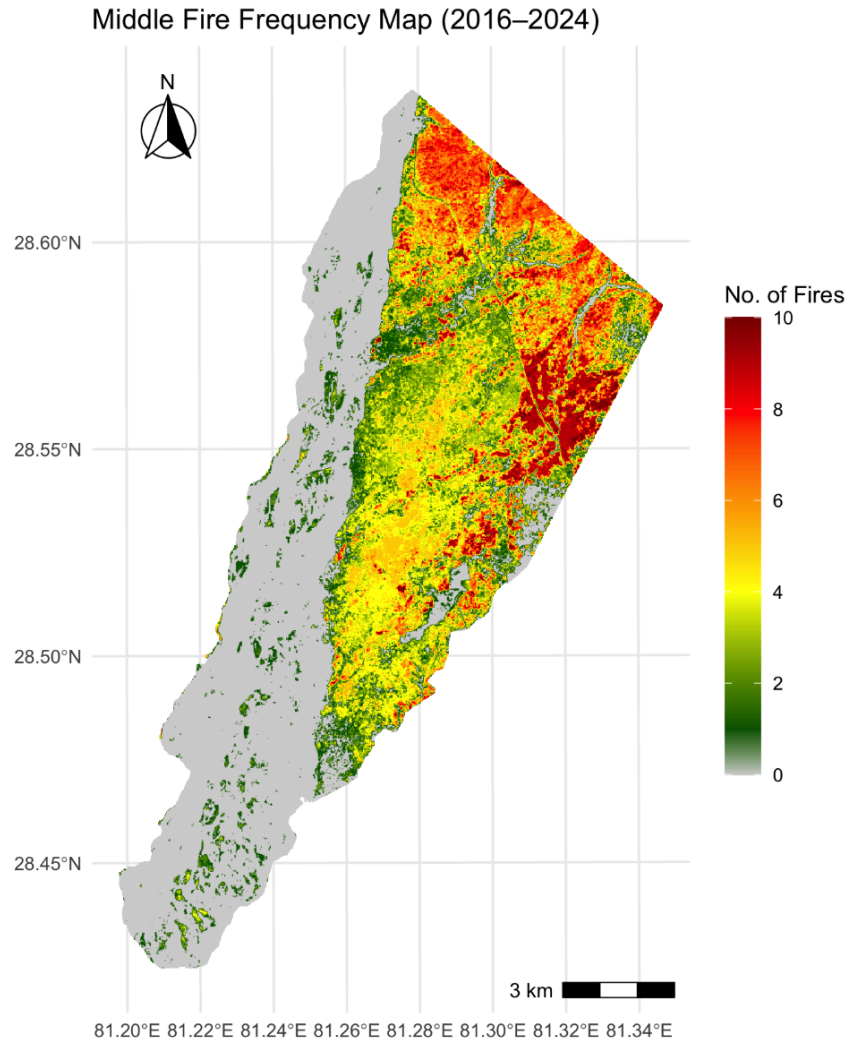

Figure 4.2.6 *Middle seasonal (March and April) burn frequency map (2016–2025) in Bardia National Park, Nepal. Colours indicate the number of years each pixel was classified as burned, based on dNBR thresholding of Sentinel-2 imagery. Coordinate system: UTM Zone 44N (EPSG:32644). Data: Copernicus Sentinel-2 (harmonised)*

In order to understand what actually burned during this period, the burn frequency was split up by land cover type. In **Appendix C3**, it can be seen that mainly Sal forest and riverine forest catch fire during March and April, with very little of the grasslands burning (between 1-3 times, but very low percentage of total grass land that burns). The shape of the largest grassland Lamkauli is clearly visible on the map due to the absence of fire across this area during the entire study period.

Late fire Maps

The late fire period, as seen in **figure 4.2.7**, corresponds to the month of May, which marks the end of the dry season and is characterised by extremely dry conditions. Typically, monsoon-induced rainfall begins in June which suppresses any remaining fire activity. The late fire frequency map shows very low fires occurrence during this period, with a maximum of five fires recorded in any location. The majority of the study area remained unburned, although some patches of Sal forest had fire activity up to two fires. Similarly the grasslands showed very limited fire activity in this period, as shown in **Appendix C2.**

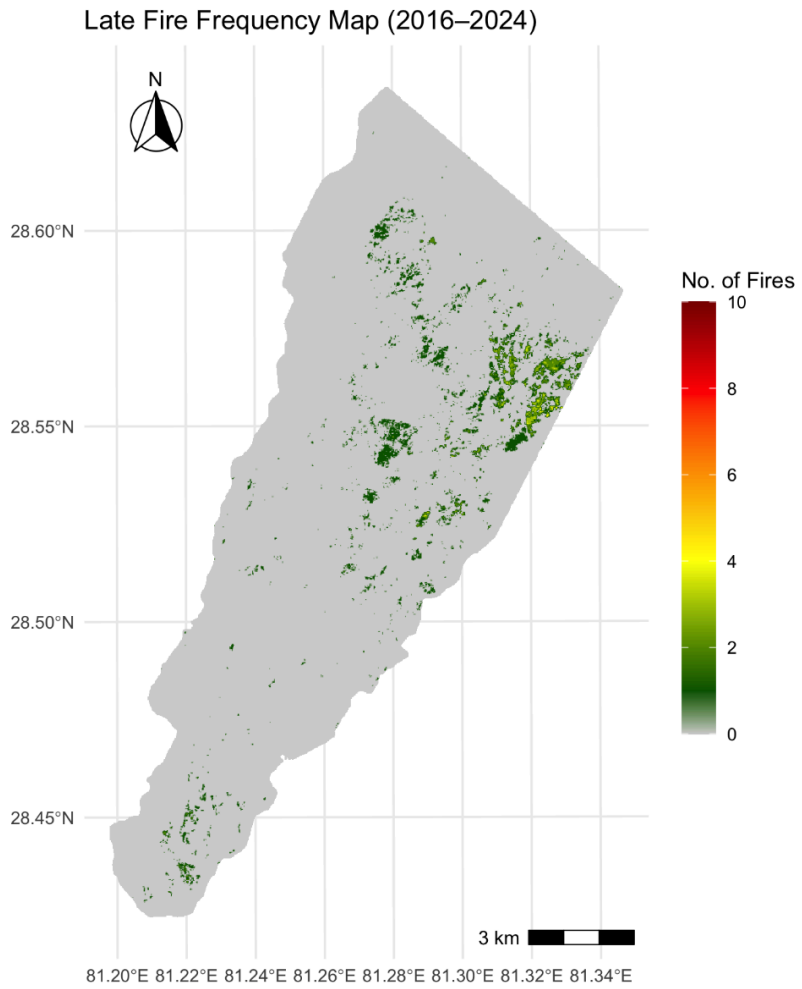

Figure 4.2.7 *Late season (May) burn frequency map (2016–2025) in Bardia National Park, Nepal. Colours indicate the number of years each pixel was classified as burned, based on dNBR thresholding of Sentinel-2 imagery. Coordinate system: UTM Zone 44N (EPSG:32644). Data: Copernicus Sentinel-2 (harmonised),*

Time Since Last Fire Mapping

Using the fire frequency data, the time-since-last-fire map was generated. **Figure 4.2.8** shows per pixel the last time it was caught on fire. The results show that the grasslands along the river have burned recently with fire occurring within the past 0-1 years. In contrast, the riverine forest position between the grasslands barely burns. As expected, the river itself is also clearly distinguishable and does not burn. Notably, recent fire activity is also observed in the sal forest. Notably, recent fire activity is also observed in the sal forest, particularly in areas situated at higher elevation (north eastern part of study region), which is also further away from the river.

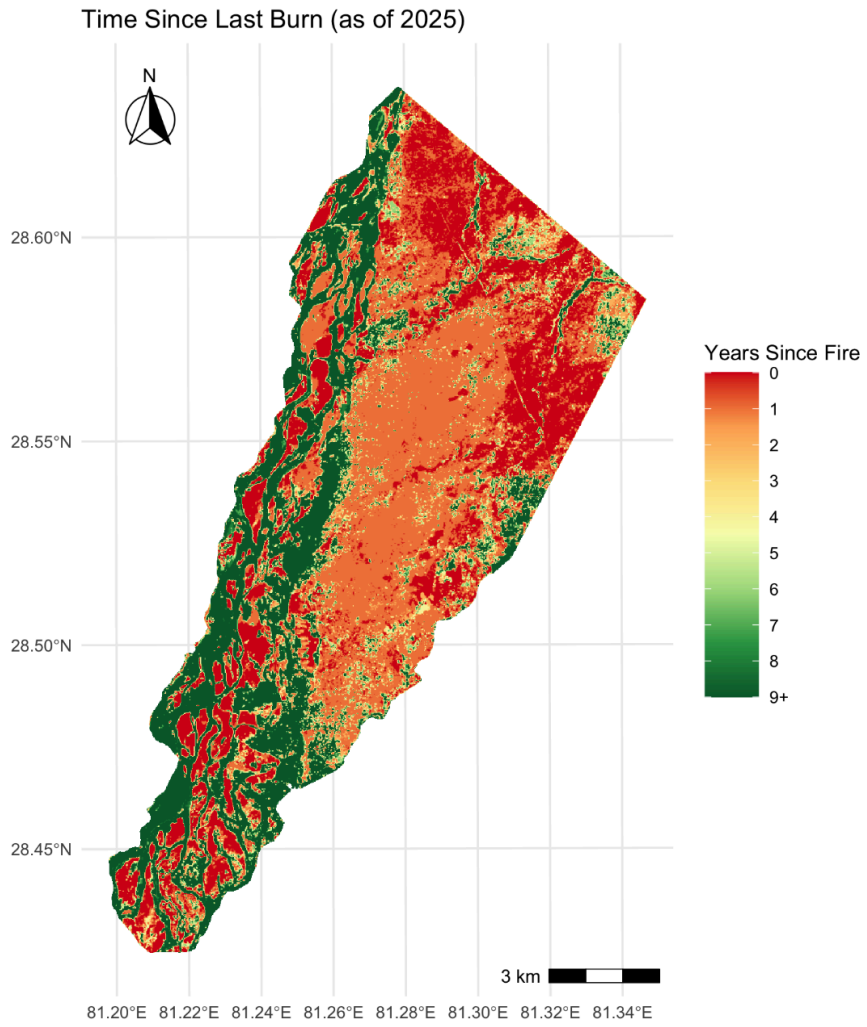

Figure 4.2.8 *A map showing the 'time since last fire' across the Bardia national park. Recently burned areas occur mainly in grasslands near rivers and sal forests at higher elevations.*

4.3 Effect of Fire on Vegetation Structure

This section presents the results related to Research Question 3 which focuses on vegetation structure and is supported by statistical analysis. Full output of the statistical test associated with each figure is provided in the appendix. Plots that were not critical for addressing the research question but provide additional context are presented in the appendix

Biomass

Biomass in Burned vs Unburned sites

To research the effect of recent fire on the grassland biomass, dried biomass was compared between sites which were burned within the last year and sites which remained unburned in that same period. The data is made up out of two independent groups burned and unburned. The plot is shown below in ***Figure 4.3.1.*** The Shapiro-Wilk test indicated that dried biomass values were not normally distributed in both groups with Burned (W = 0.66608, p = 9.784e-07, n = 28) and unburned (W = 0.73622, p-value = 5.867e-05, n = 22). Levene's test showed that there was no significant difference in variance between the groups (F(1,48) = 0.458, p = 0.502). The Wilcoxon rank-sum test showed that the difference between burned and unburned were not statistically significant (W = 343, p-value = 0.5001). This means there is no strong evidence for a difference in biomass based on fire occurrence.

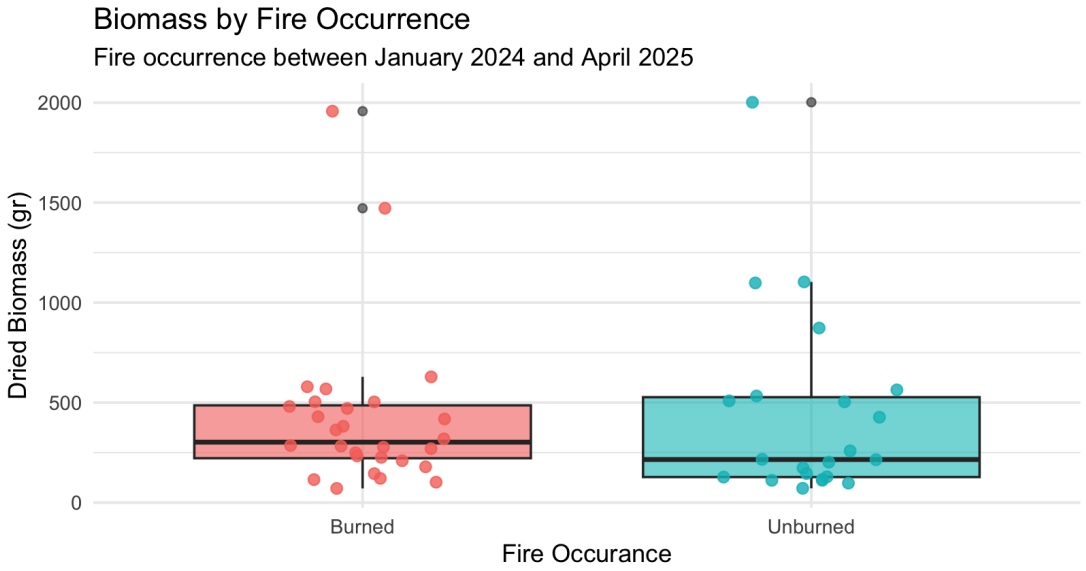

Figure 4.3.1 *Dried biomass in recently burned (n = 28) vs unburned sites (n = 22). Wilcoxon rank-sum test found no significant difference (W = 343, p = 0.5001). Full statistical analysis in Appendix D1*

To explore whether functional group identity affected the relationship between fire and biomass, biomass differences were further analysed within three dominant grass functional groups. No significant differences were found in any of the groups. Pioneering tall grasses showed unequal variance, but Welch's t-test indicated no significant difference (t(10.38) = –1.43, p = 0.182). For short grasses and late-successional tall grasses, Wilcoxon tests also

found no significant differences (both p = 0.2345). The figure and associated analysis can be found in **Appendix D2.**

Biomass across Fire Frequencies

The ***Figure 4.3.3*** displays the dried biomass in relation to the burn frequencies which have been measured since 2016. The data used violated normality assumption as tested with the Shapiro-Wilk Test (W = 0.8343, p-value = 5.968e-06) and homoscedasticity was met with the Levene's test (F(11,38) = 1.224, p = 0.305). As a result, the Kruskal-Wallis test was used to assess differences in biomass across the fire frequency levels. The test revealed no statistically significant difference ($\chi^2(11) = 7.77$, p = 0.734).

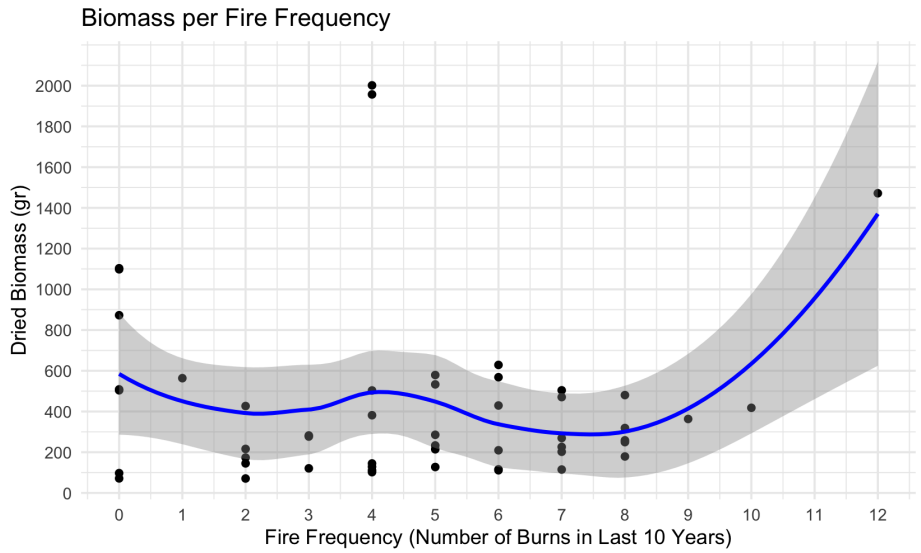

Figure 4.3.3 *Dried biomass across fire frequency classes (0–12 burns; total n = 50). Kruskal–Wallis test showed no significant effect ($\chi^2 = 7.77$, p = 0.734). Full statistical analysis in Appendix D3*

Fresh Green Biomass across Fire Frequency

In **Figure 4.3.4** the fresh weight of green leaves is plotted against the fire frequency of the sampled plot with a loess regression applied to the data. A Kruskal–Wallis rank sum test was used to assess whether fire frequency significantly influenced the fresh weight of green leaves. This non-parametric test was selected due to the violation of the normality assumption (Shapiro–Wilk W = 0.950, p = 0.033) despite homoscedasticity being confirmed (Levene's test: F = 1.071, p = 0.409, n = 50). The test revealed no statistically significant differences in fresh green biomass across fire frequency levels ($\chi^2(11) = 7.87$, p = 0.725, n = 50), with no clear pattern observed between biomass and fire frequency.

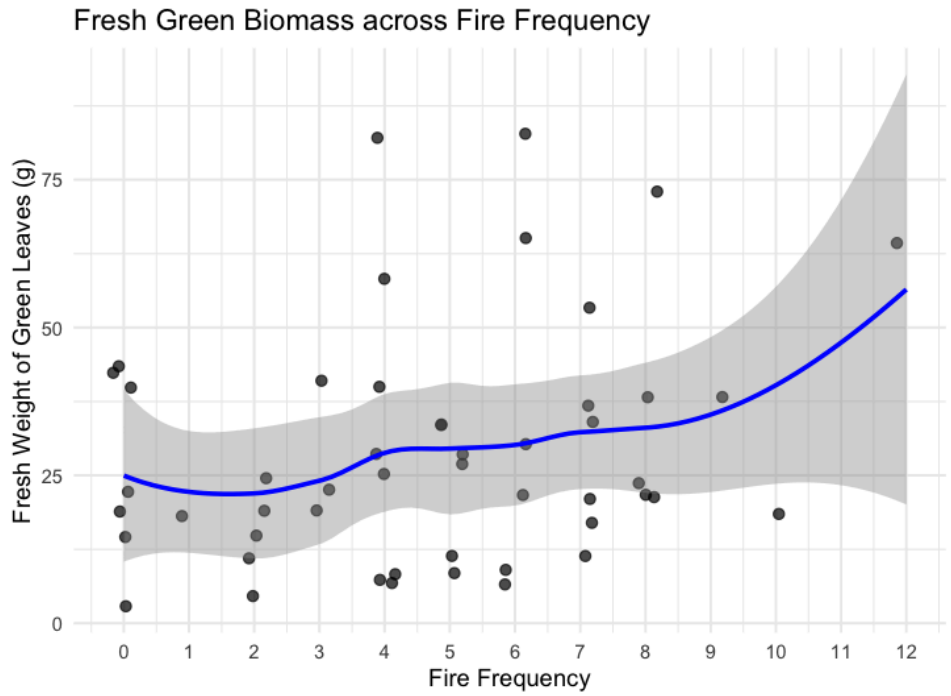

Figure 4.3.4 Fresh green biomass (living biomass) vs fire frequency with LOESS curve. Kruskal–Wallis test found no significant differences ($\chi^2 = 7.87$, $p = 0.725$, n = 50*). Full statistical analysis in Appendix D4*

NDVI

NDVI across Fire Frequencies

To compare with the field data (previously shown in figure 4.3.4), NDVI was generated with satellite data and plotted against fire frequency over the last 10 years in **figure 4.3.5.** A linear model was applied. The assumptions of the model were met with a normal distribution of the residuals (Shapiro–Wilk W = 0.978, p = 0.453, n = 50) and no significant heteroskedasticity was detected (Breusch–Pagan test: BP = 10.36, df = 11, p = 0.499, n = 50). The model was statistically significant in general (F(11, 38) = 7.204, p < 0.001) with roughly 68% of the variation in NDVI was explained ($R^2 = 0.676$, adjusted $R^2 = 0.582$). These results suggest a positive relationship between fire frequency and NDVI, indicating that areas with more frequent fires exposure tend to show higher vegetation greenness.

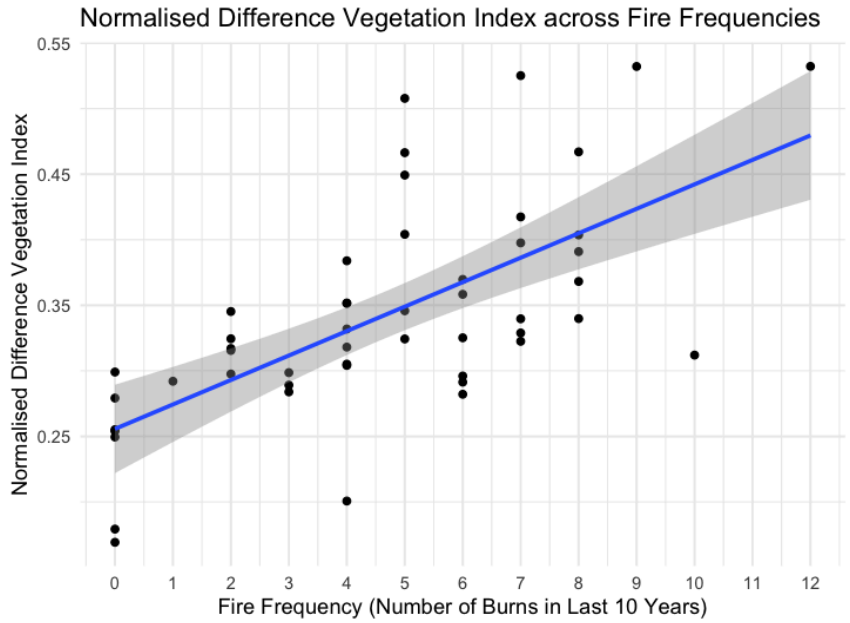

Figure 4.3.5 *NDVI across fire frequencies. Linear regression model was significant (F(11, 38) = 7.204, p < 0.001, R² = 0.676, n = 50), indicating a positive relationship between fire frequency and vegetation greenness. Full statistical analysis in Appendix D5.*

To explore the data further on a finer scale, NDVI was analysed per functional group using linear regressions as shown in **figure 4.3.6**. A significant positive relationship was found for *Pioneers Tall Grasses* (adjusted R² = 0.546, p < 0.001, n = 22), although the residuals slightly violated the assumption of normality (Shapiro–Wilk W = 0.906, p = 0.040). For *Short Grasses*, the model was also significant (adjusted R² = 0.286, p = 0.019, n = 16), with assumptions of normality met but variance homogeneity violated (Levene's test p = 0.004). However, *Late-Successional Tall Grasses* showed no significant trend (adjusted R² = 0.030, p = 0.275, n = 12), despite meeting all assumptions.

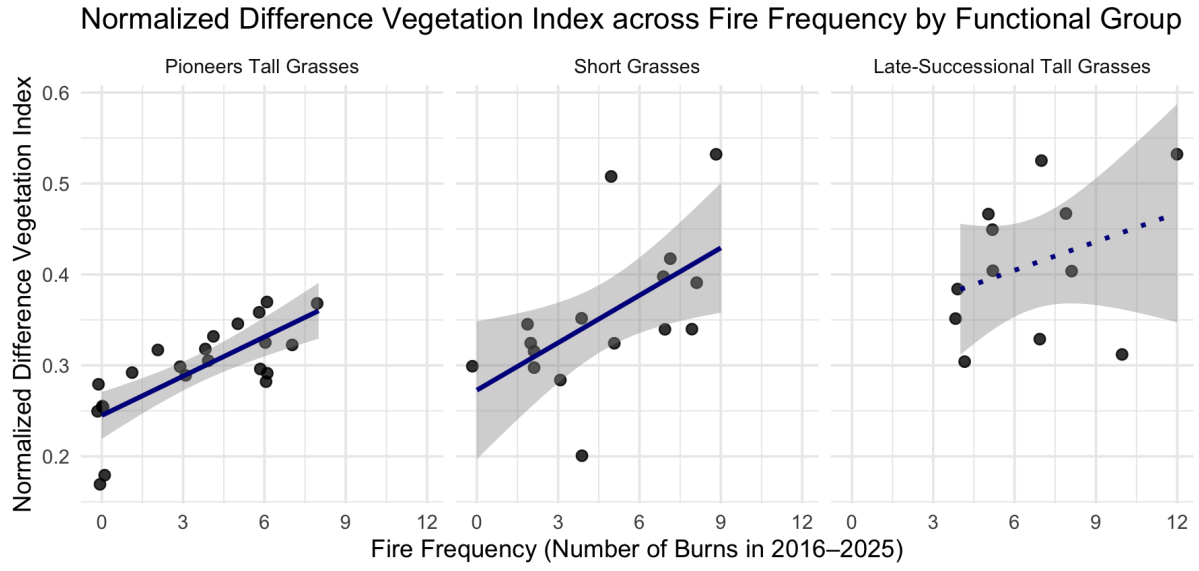

Figure 4.3.6 *NDVI vs fire frequency per functional group. Significant positive relationships were found for Pioneers Tall Grasses (R² = 0.546, p < 0.001*, n = 22*) and Short Grasses (R² = 0.286, p = 0.019, n*

= 16); no effect for Late-Successional Tall Grasses (R^2 = 0.030, p = 0.275, n = 12). Full statistical analysis in Appendix D6

NDVI and Time since Last Fire

A Kruskal–Wallis rank sum test was performed to evaluate differences in NDVI across three fire recency categories: recent burn (0 years), moderate time since burn (1–4 years), and long unburned (9+ years). This non-parametric test was selected due to a violation of the normality assumption (Shapiro–Wilk W = 0.919, p = 0.0021, n = 50), while homogeneity of variances was met (Levene's test: F = 0.832, p = 0.442, n = 50). The test indicated a statistically significant difference in NDVI across the fire recency categories ($\chi^2(2) = 14.78$, p = 0.0006, n = 50), as visualised in **Figure 4.3.7**.

Following the significant Kruskal–Wallis test, a Dunn's post hoc test with Bonferroni correction was applied. It showed that plots in the long unburned category had significantly lower NDVI compared to both the moderate (Z = –3.40, p = 0.0020, n = 50) and recent burn groups (Z = –3.72, p < 0.001, n = 50). No significant difference was found between the recent and moderate burn groups (Z = –0.05, p = 1.00).

Figure 4.3.7 *NDVI across time since last fire. Kruskal–Wallis test indicated a significant effect (χ^2 = 14.78, p = 0.0006,* n = 50*). Dunn's post hoc test showed significantly lower NDVI in long-unburned plots compared to moderate plots*(Z = –3.40, p = 0.0020, n = 50)*. Full statistical analysis in Appendix D7.*

Plant Structure and Physiological Traits

As none of the assessed structure or physiological variables showed statistically significant or consistent relationship with recent fire, they have been moved to the appendix.

- **Plant water content, which** was measured as the ratio of dried to fresh biomass, did not vary significantly with fire frequency ($\chi^2(11) = 10.83$, p = 0.457, n = 50). Similarly, no significant variation was found across vegetation communities ($\chi^2 = 3.04$, df = 3, p = 0.385). See **Appendices D8 & D9** for figures and full analysis
- For **stem diameter**, no significant differences were found between burned and unburned plots across species: *S.spontaneum* (t(9) = –0.86, p = 0.412, n = 11), *I. cylindrica* (t(14) = –1.06, p = 0.307, n = 16), *N. porphyrocoma* (t(8) = –0.35, p =

0.737, n = 10), and *S. bengalense* (Wilcoxon W = 2, p = 0.429, n = 11). **See appendix D10** for the graph with full statistical analysis.

- Similarly, **average leaf size** showed no significant differences: *S. spontaneum* (Wilcoxon W = 19, p = 0.185, n = 11), *S. bengalense* (Wilcoxon W = 8, p = 0.429, n = 11), *I. cylindrica* (Wilcoxon W = 39, p = 0.495, n = 16), and *N. porphyrocoma* (t(8) = –1.13, p = 0.292, n = 10). **See appendix D11** for the graph with full statistical analysis.
- **Grass height** also showed no significant difference between burned and unburned plots (Wilcoxon W = 353, p = 0.152, n = 48), and species-level regression models revealed no consistent effects: *S. spontaneum* (adjusted R^2 = 0.38, p = 0.149), *S. bengalense* (adjusted R^2 = 0.48, p = 0.194), *I. cylindrica* (adjusted R^2 = –0.15, p = 0.663), and *N. porphyrocoma* (adjusted R^2 = 0.66, p = 0.087). **See appendix D12 & D13** for the graphs with full statistical analysis.

Soil and Moisture

As no statistically significant relationships were found between fire frequency and soil variables, the corresponding graphs and analyses have been moved to the appendix.

- **Bulk density** did not vary significantly across fire frequency classes (ANOVA: F(11,38) = 1.42, p = 0.206, n = 50), with assumptions of normality and homogeneity of variance confirmed (Shapiro–Wilk W = 0.975, p = 0.354; Levene's test p = 0.368). **See appendix D14** for the graph with full statistical analysis.
- Similarly, **volumetric moisture content** showed no significant differences across fire frequencies (ANOVA: F(11,38) = 0.31, p = 0.979, n = 50), and assumptions were again met (Shapiro–Wilk W = 0.972, p = 0.226; Levene's test F = 1.20, p = 0.323). While visual trends such as a mid-range dip in volumetric moisture were noted, these patterns were not statistically supported, suggesting that fire frequency does not significantly influence soil moisture in the sampled grasslands. **See Appendix D15** for the graph with full statistical analysis.

4.4 Effect of Fire on species composition

This section presents the results for Research Question 4, which focuses on the effect of fire on species composition. The results are supported by statistical testing. Full outputs of the statistical tests for each figure are included in the appendix. Additional plots that were not essential for answering the main research question are also provided there for reference.

Fire Frequencies across Plot=Dominant Species

To investigate how the fire influenced the plot-dominant species, the fire frequency across different species was researched and visualised in figure **4.4.1**. For the burn frequency across the different plant species the following testing was done. Assumptions were met with normally disturbed residuals (Shapiro–Wilk W = 0.954, p = 0.058), and homogenous variance (Levene's test F(3,44) = 0.54, p = 0.657). The one-way ANOVA test showed that there was a significant difference in burn frequency between species (F(3,44) = 4.73, p = 0.006). A Tukey HSD post hoc test followed and shows that the difference is mainly due to the Narenga p.(n = 10) which is linked to the higher burn frequency compared to the Saccharum s. (p = 0.0028, n = 11;). No other pair has some statistical significance.

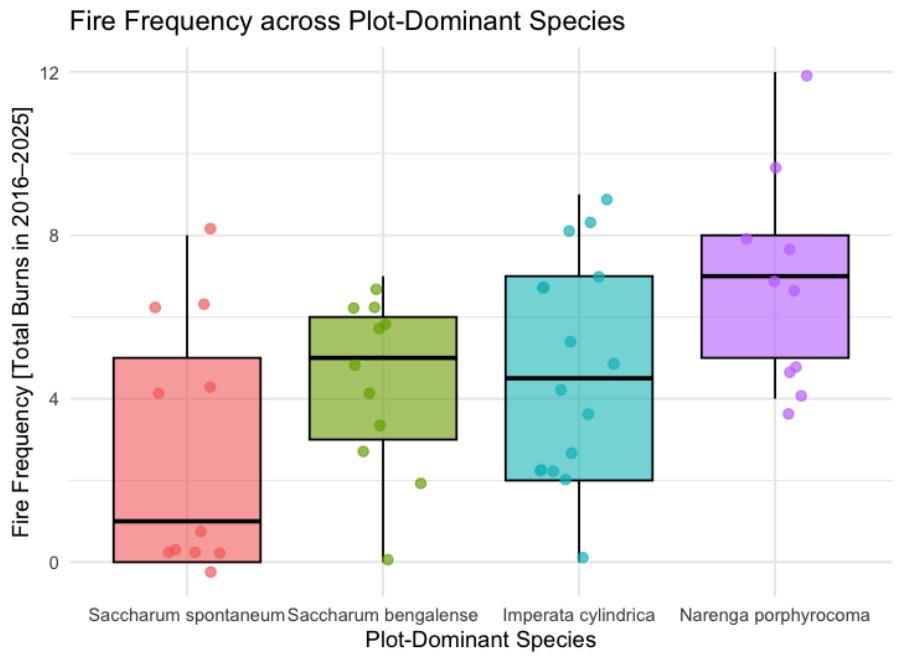

Figure 4.4.1 *Fire frequency across Plot-Dominant Species(n = 48). One-way ANOVA showed significant species differences (F(3,44) = 4.73, p = 0.006); post hoc test revealed higher fire frequencies for N. porphyrocoma compared to S. spontaneum. Full statistical analysis in Appendix E1*

Relative dominance vegetation across fire frequencies

To research how the vegetation communities are represented across the different fire frequencies, the relative dominance of each vegetation community in each fire frequency is shown in **figure 4.4.2.** This figure shows the relative dominance of vegetation communities across the fire frequency classes over the past 10 years. While formal statistical testing was not done due to small sample sizes in several burn frequency categories (classes 1, 9, 10, and 12), the dominant vegetation communities visibly changed along the fire frequency gradient. *S. spontaneum* is dominating the plots with no or few burns whereas *N. porphyrocoma* becomes increasingly more dominant in high-fire fire frequencies. Intermediate fires were more mixed, with *S. bengalense* and *I. cylindrica* co-dominating that part of the fire frequency.

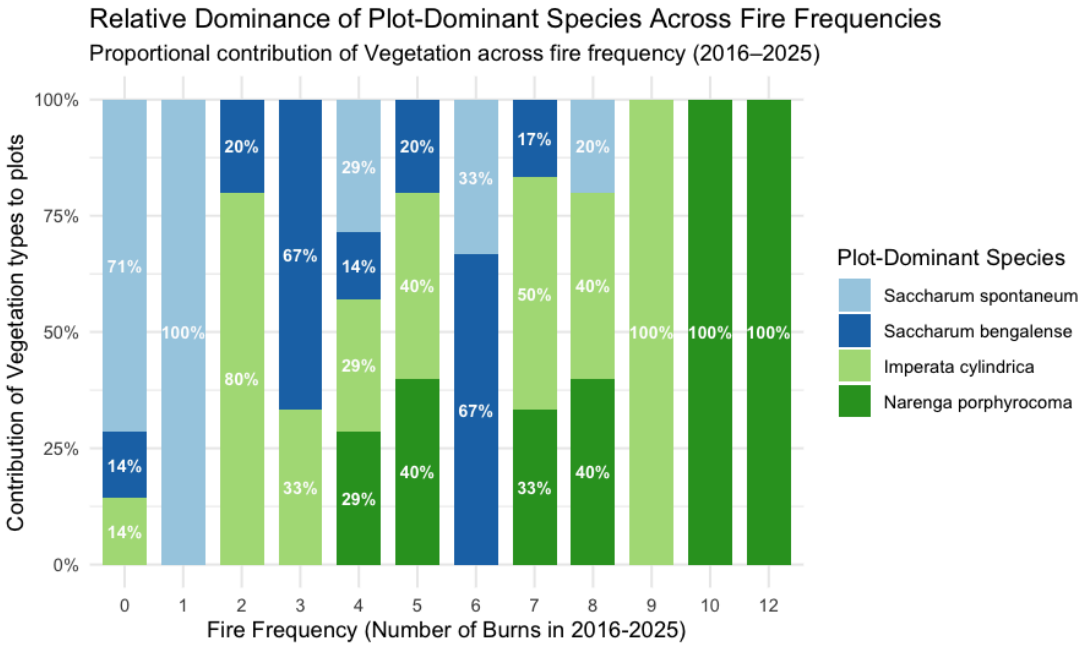

Figure 4.4.2 *Relative dominance of vegetation communities per fire frequency class. Visual trends suggest species turnover, with Saccharum s. dominating low-fire plots and Narenga p. in high-fire plots.*

Average Leaf Size

As no statistically significant relationships were found between fire frequency and **average leaf size**, the results have been moved to the appendix **E2**. Regression models showed no meaningful trends for *S. bengalense* (adjusted R^2 = –0.047, p = 0.476, n = 11), *I. cylindrica* (adjusted R^2 = 0.007, p = 0.312, n = 16), *N. porphyrocoma* (adjusted R^2 = –0.115, p = 0.793, n = 10), and *S. spontaneum* (adjusted R^2 = –0.098, p = 0.755, n = 11), with assumption checks confirming no consistent violations.

Amount of Leaves

In the **figure 4.4.3,** the relationship between the average amount of leaves and fire frequency is explored. The additional statistical testing was done. The assumptions for normality (Shapiro-Wilk test: W = 0.846, p < 0.001) and homogeneity of variance (Levene's test: F(11,38) = 2.21, p = 0.035) were both not met. These violations lead to the Kruskal-Wallis rank sum test being applied. The Krukal-Wallis test indicated a statistically significant difference in the average number of leaves across different fire frequency categories ($\chi^2(11)$ = 22.14, p = 0.023). However, the Dunn post hoc test with Bonferroni correction did not identify any pairwise comparisons as statistically significant after correction (all adjusted p-values > 0.05).

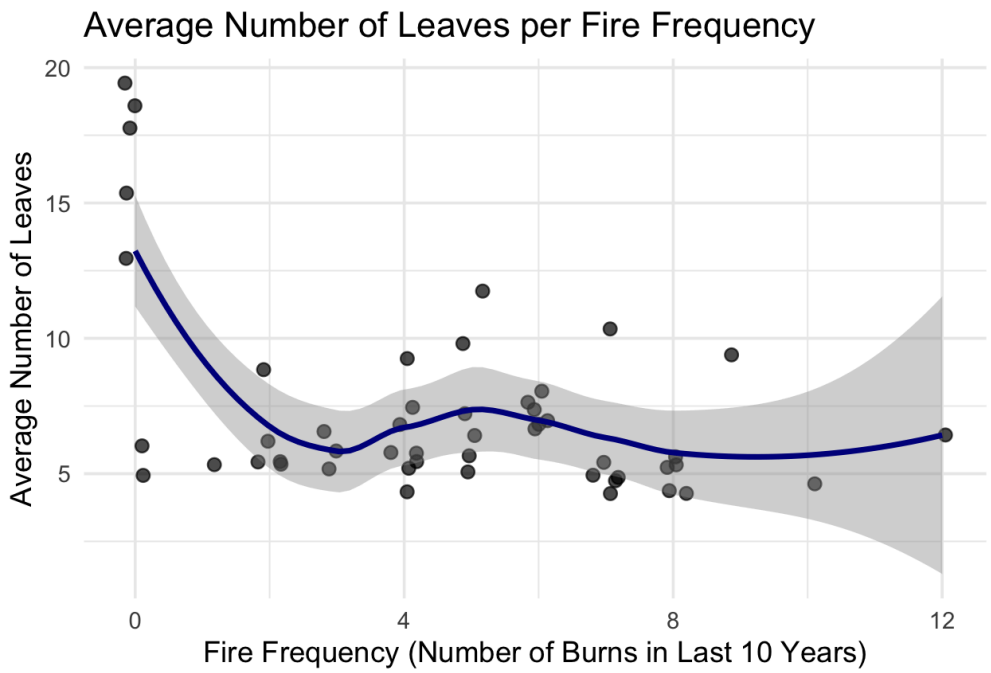

Figure 4.4.3 *Average number of leaves per fire frequency class. Kruskal–Wallis test indicated significant differences (χ^2 = 22.14, p = 0.023), but Dunn post hoc test showed no pairwise significance. Full statistical analysis in Appendix E3*

Specific Leaf Area

As no statistically significant differences in specific leaf area (SLA) were found between burned and unburned plots, the results have been moved to the **appendix E4**. Wilcoxon rank-sum tests showed no significant effect of recent fire for *S. spontaneum* (p = 1.000, n = 11), *S. bengalense* (p = 0.635, n = 11), *I. cylindrica* (p = 0.431, n = 16), and *N. porphyrocoma* (p = 0.110, n = 10). While *N. porphyrocoma* showed a visual trend toward higher SLA in unburned sites, this difference was not statistically supported.

Shannon Diversity Index

Shannon across Fire Frequency

A simple linear regression was done to evaluate the relationship between fire frequency and Shannon Diversity Index. The results **in figure 4.4.4** showed a significant positive relationship (p = 0.0025), indicating that higher fire frequency is associated with increased diversity. The regression model explained approximately 17.5% of the variance in Shannon Index ($R^2 = 0.1755$).

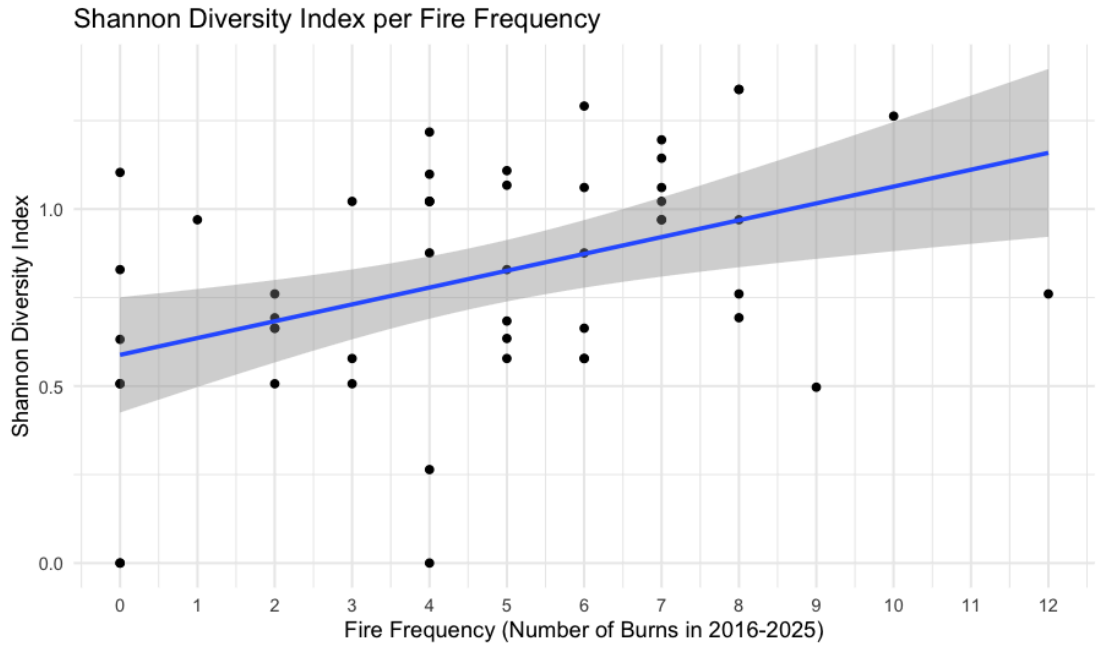

Figure 4.4.4 *Shannon Diversity Index vs fire frequency. Linear regression showed a significant positive relationship (R^2 = 0.1755, p = 0.0025, n = 50), suggesting increased diversity with higher fire exposure. Full statistical analysis in Appendix E5*

Shannon across Time Since Last Fire

The relationship between fire recency and Shannon diversity index was assessed using one-way ANOVA. Assumptions of normality (W = 0.970, p = 0.233, n = 50) and homogeneity of variances (F(2,47) = 1.05, p = 0.357) were met. ANOVA indicated a statistically significant effect of fire recency on Shannon diversity (F(2,47) = 5.43, p = 0.008). Post hoc comparisons using Tukey's HSD test showed that recently burned sites had significantly higher Shannon diversity than long unburned sites (mean difference = 0.405, p = 0.008). No significant differences were found between moderately burned and long unburned sites (mean difference = 0.234, p = 0.222), nor between recently and moderately burned plots (mean difference = 0.171, p = 0.195).

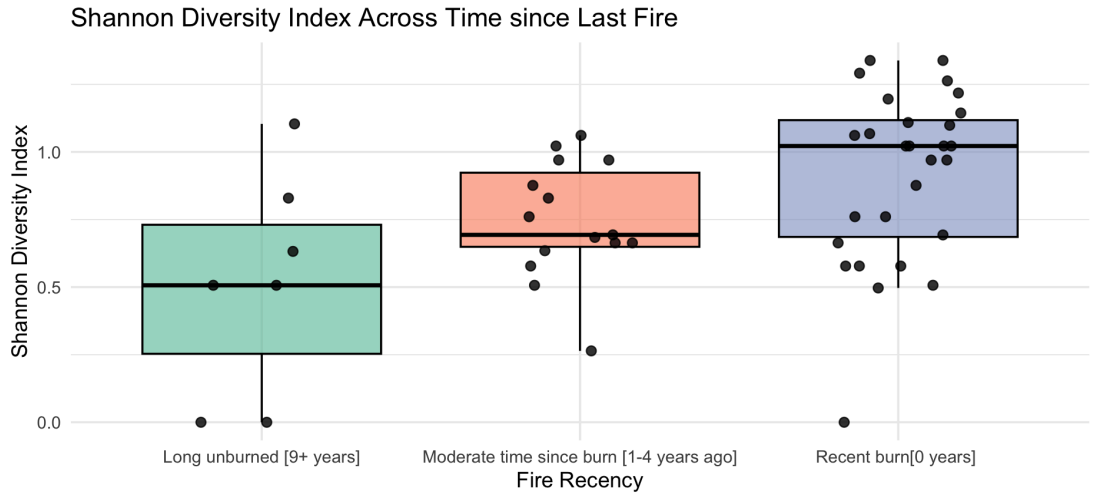

Figure 4.4.5 *Shannon Diversity Index across time since last fire. ANOVA showed significant differences (F(2,47) = 5.43, p = 0.008); Tukey's HSD found higher diversity in recently burned plots. Full statistical analysis in Appendix E 6*

Shannon Diversity Index per Plot-Dominant Species

The relationship between Shannon Diversity Index across plant species was investigated and **visualised in figure 4.4.6.** The assumptions of normality (p between 0.194 and 0.726) and homogeneity of variance (p = 0.2512) were met. But further testing with the one-way ANOVA showed that Shannon Diversity Index did not significantly differ across the four different grass species (ANOVA: F(3, 44) = 1.267, p = 0.297). But due to assumptions being met, minor differences in Shannon Index are visually present. However these are not statistically meaningful.

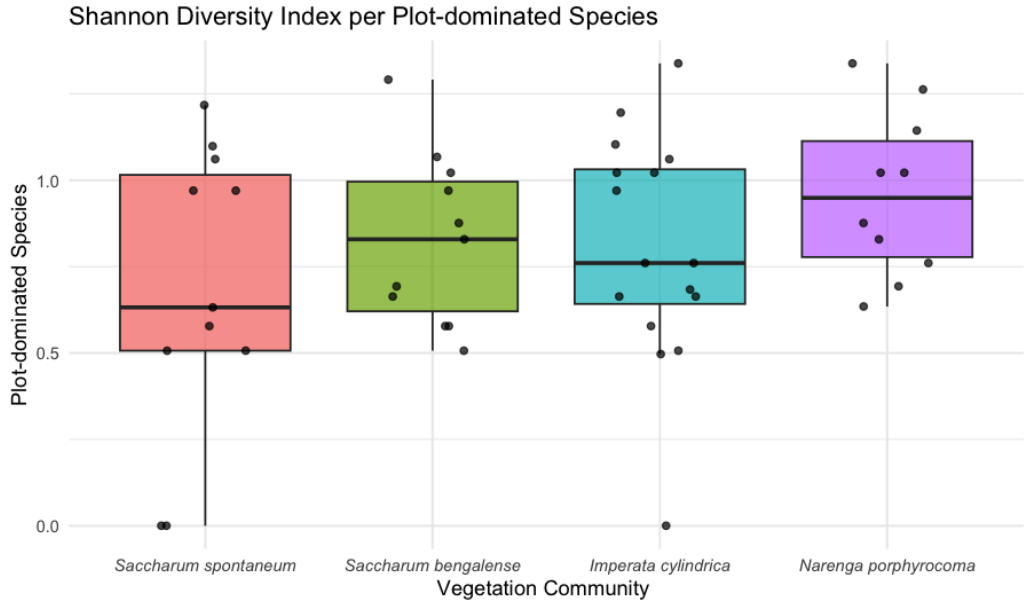

Figure 4.4.6 *Shannon Diversity Index across Plot-Dominant Species. ANOVA found no significant differences (F(3,44) = 1.267, p = 0.297), though minor visual differences are present. Full statistical analysis in Appendix E7*

Fire Frequency and Shannon per Plot-Dominant Species

A linear regression analysis was done to assess the relationship between fire frequency and species-level Shannon Diversity Index which can be seen in **figure 4.4.7**. The results revealed that *S. spontaneum* showed a statistically significant positive relationship between burn frequency and Shannon Index (R^2 = 0.38, p = 0.042). The residuals were normally distributed (p = 0.212), and the model met the assumption of homoscedasticity (p = 0.600). In contrast, no statistically significant relationships were found for *S. bengalense* (p = 0.335), *I. cylindrica* (p = 0.516), or *N. porphyrocoma* (p = 0.625), despite all models satisfying assumptions of normality and equal variance.

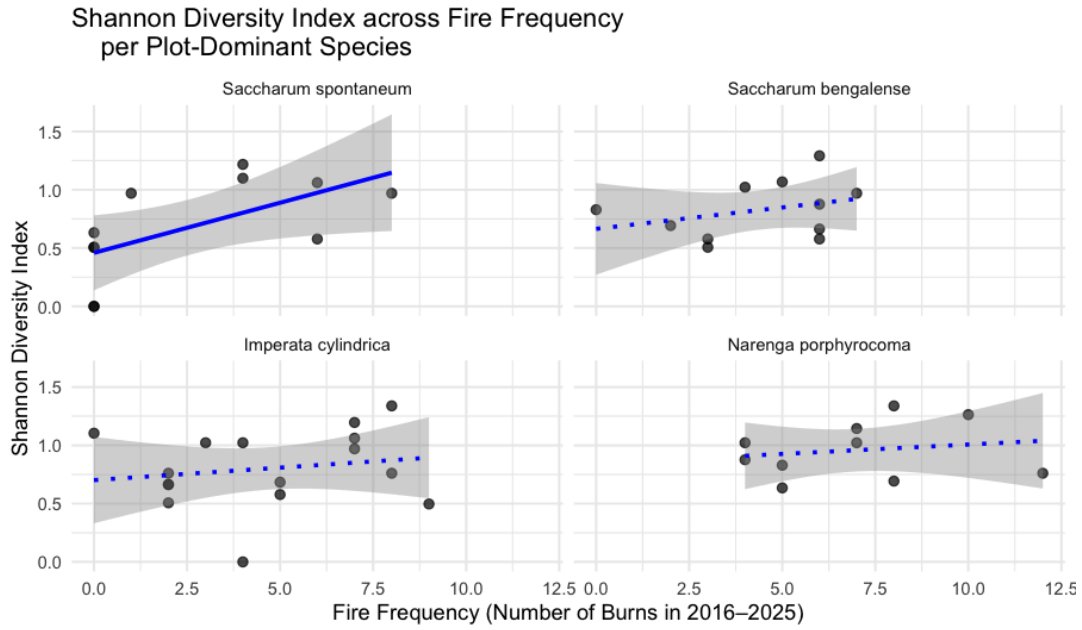

Figure 4.4.7 *Linear regression between fire frequency and Shannon Index across Plot-Dominant Species. Only S. spontaneum showed a significant response (R^2 = 0.38, p = 0.042); other species did not show significant patterns. See Appendix E8 for full results.*

Shannon across Fire Occurrence per Plot-Dominant Species

To investigate whether species-level plant diversity was influenced by recent burning, Wilcoxon rank-sum tests were conducted for each of the four dominant grass species. This has been visualised in **figure 4.4.8**. A statistically significant difference in the Shannon diversity index was found for *Saccharum spontaneum* (*W* = 22.5, *p* = 0.0399) and *Narenga porphyrocoma* (*W* = 22, *p* = 0.0422). In contrast, no significant differences were observed for *Saccharum bengalense* (*W* = 5, *p* = 1) and *Imperata cylindrica* (*W* = 35, *p* = 0.792).

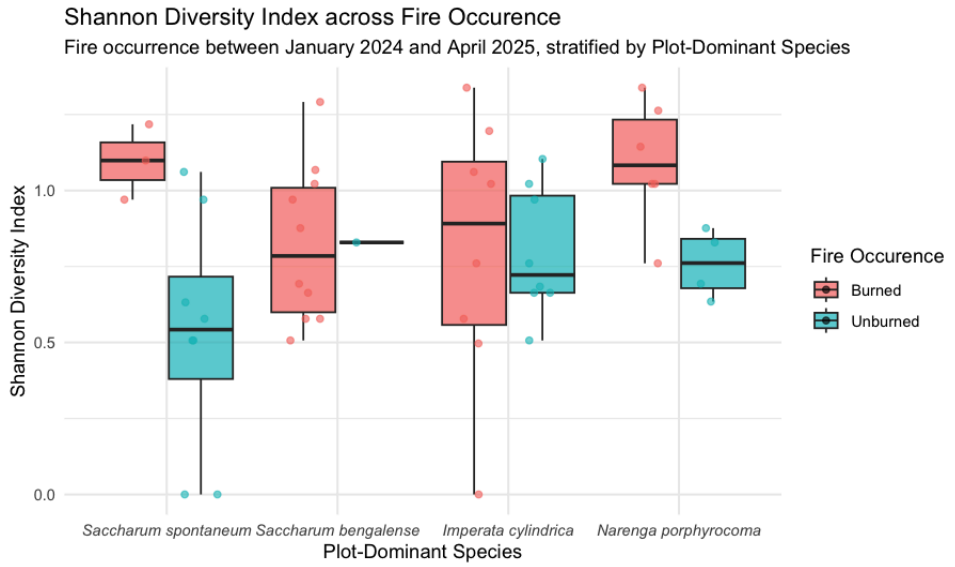

Figure 4.4.8 *Shannon Diversity Index for burned and unburned plots across dominant species. Significant differences were found for S. spontaneum (p = 0.0399) and N. porphyrocoma (p = 0.0422), with no effects observed for the other species. See Appendix E9 for full results.*

5. Discussion

5.1 Accuracy of fire model

The fire detection model demonstrated a strong performance capturing fire events during the early fire season (January - February 2025) when validated against ground truth data. It achieved a high overall accuracy of 92%, with a kappa statistic of 0.8379 indicating an 'almost perfect agreement' with the ground truth observations (Rashkovetsky et al., 2021). The model was especially effective at correctly identifying burned areas, with a recall of 0.963 and precision of 0.897. When comparing the output to satellite imagery from the same period, the spatial patterns match well with the Planet imagery. Not only at the locations with ground truth data, but also across other areas where no field validation was available. This further supports the model's accuracy. Despite its strengths, the model has a slightly reduced accuracy of the 'No Fire' class which suggested that the model is more prone to false negatives. Overall, the model performed reliably in detecting short-term fire dynamics during the early season. However, its performance in capturing fire events outside this short window remains untested and the accuracy of fire detection during the remainder of the dry season is far less certain.

While the early fire frequency model showed consistent and ecologically plausible results, detection became less reliable during the middle period (March to April). Unexpected fire activity appeared in Sal-dominated forest areas which is slightly unusual given both ecological expectations and field observations from rangers (Dinerstein, 1979b; Ghimire et al., 2014). One of the most noticeable features in the middle-season fire map is a clear vertical divide, with most of the fire activity being detected in the eastern part of the park. It is most likely that burns also occurred in the western section, but because many of these areas had already burned in February, they were included in the "before" composite, masking any subsequent spectral change.

These issues are likely a result of several methodological limitations. First, the use of median pixel composites tends to smooth out more extreme spectral values, reducing the visibility of burn scars and weakening the disturbance signal. Second, the timing of the composite images can lead to mismatches. The middle-season fire map is based on before-and-after composites covering February as the "before" and May as the "after". Fires that occur in February are already included in the "before" image which cancels out or weakens their spectral signal. Similarly, burns that happen in early March may go undetected if vegetation has recovered by the time the May image is used as the "after" composite. Since the median values average across the time window, the resulting image may reflect regrowth rather than disturbance itself.

These timing issues also affected the final fire period in May, where fires activity appeared very limited. This deviates significantly from both ranger reports and literature identifying May as a peak fire month in the grasslands, yet the model failed to capture most of this activity (Dinerstein, 1979b; Bhusal et al., 2024). Other ways of dividing the fire season were tested, but they did not align better with known fire patterns. Due to time constraints, further refinement of the seasonal classification was not possible. This has contributed to a weaker detection performance later on in the dry season.

Another limitation is that the model may not be able to clearly distinguish fire from other vegetation disturbance such as mowing and grazing. Since the classification is based on spectral changes in vegetation (dNBR and NDVI), activities such as grazing and mowing could mimic fire signals. This could lead to incorrect classification of mowed areas as burned. While the current threshold of 0.3 is meant to capture significant vegetation loss, it may still include changes unrelated to fire. Adjusting this threshold could help improve the model's ability to separate actual fire events from other forms of disturbance and make the results more accurate.

Given these limitations, the fire model cannot be considered a precise representation of seasonal fire activity, particularly for the middle and late periods. However, it still captured the deliberate management fires of January and February with high accuracy and aligned with both ground observations and ranger testimonies (Lamichhane et al., 2024). Despite the reduced reliability later in the season, the early fire detection remains robust enough to offer valuable insights into spatial fire patterns and their link with vegetation dynamics in Bardia National Park.

5.2 Fire Regime Patterns

The spatial and temporal dynamics of fire in Bardia National Park reveal a complex pattern shaped by both ecological gradients and deliberate management. The fire frequency map (Figure 4.2.1) shows a distinct mosaic across the landscape, with high fire recurrence particularly concentrated in the northeastern part of the park. This region is at higher elevations, which likely dries out quickler after the monsoon due to increased drainage and reduced water retention. This leads to the area becoming more flammable as the dry season progresses (Bhusal et al., 2024). This interpretation is further supported by the moderate positive correlation between elevation and burn frequency (figure 4.2.3). Earlier work by Ghimire et al. (2014) also identified the northeastern and northwestern part of the park as areas with very high fire risk.

This elevated fire risk can partially be explained by topographic features. Although most of Bardia is low-lying, about 30% of the park is above 500 metres (see **Appendix B3** for elevation map). Slope is an important factor in fire dynamics with Morandini et al. (2005) stating that a 10 degree increase in slope can double the rate at which fire spreads. The steep terrain also makes it harder to fight and suppress fires. Additionally, higher elevation areas in Bardia have a greater tree density and experience less seasonal flooding which allows fuel load to accumulate and leads to increased fire activity (Das et al., 2022). Field insights from rangers support this, noting that the northern grasslands often ignite later in the season when conditions are driest and harder to manage (Lamichhane et al., 2024). All these patterns suggest that natural flammability, rather than deliberate burning, plays a large role in fire recurrence in the northern part of the park.

Ghimiere et al. (2014) also identifies the southern border of BNP as an area with increased fire risk. However, the fire pattern in these southern grasslands differs from that in the north, as frequent burning here clearly reflects deliberate fire use. The area is at a lower elevation near the Karnali River which means that it retains soil moisture for longer periods due to the

monsoonal flooding which also deposits nutrient-rich silt (Peet et al., 1999). As a result, these wetter grasslands and adjacent forest edges are less likely to burn during the early and mid-dry season, due to reduced fuel flammability (Bhusal et al., 2024). If they burn, fire often stimulates rapid regrowth due to improved nutrient cycling and soil conditions (Thapa et al., 2021). The fire that occurs in those southern grasslands is mostly the result of anthropogenic management. The largest grasslands of BNP for example, Lamkauli and Baghaura, are known management sites which are easily accessible and well used by herbivores. Here, rangers conduct prescribed burns early in the dry season to reduce fuel loads, stimulate the regrowth of palatable shoots, and maintain open habitat structure (Lamichhane et al., 2024; Bhusal et al., 2024). These management burns are part of broader conservation strategies aimed at supporting habitat quality for large herbivores and their predators (Dinerstein, 1979b).

5.3 Impact on Vegetation

The results of the study shows that fire plays a complex role in the subtropical grasslands of Bardia National Park and is in turn shaped by the grasslands themselves. One of the notable results is the absence of a significant difference in dried biomass between recently burned and unburned plots. This suggests that fire, at least in the short term, does not reduce total above ground biomass. Instead, the grasslands appear to recover relatively quickly after burning, likely due to fire-adapted traits of the plants (Dinerstein, 1979b; Lehmkuhl, 1989). Even when biomass was assessed across functional groups, no consistent reduction was observed in response to fire. The results align with other research of Lamichhane et al. (2024) and Bhusal et al. (2024), who also found no significant biomass differences across fire treatments in Bardia. This supports the idea that these ecosystems have a broader ecological resilience and that fire acts as a non-destructive and more shaping force within Bardia's grassland (Lehmkuhl, 1989; Peet et al. 1999).

While dried biomass remained stable across fire categories, NDVI, used as a proxy for vegetation greenness, showed something different. A clear, statistically positive relationship was found between fire frequency and NDVI. The lowest values in plots have not burned for nine or more years. The results indicate that greenness, which is more sensitive to recent vegetative activity, increases with fire exposure. This suggests that fire may stimulate vegetative growth, particularly in grasslands where there is domination of disturbance-tolerant species which are capable of rapid post-fire regeneration.

Species composition patterns support this interpretation. *Imperata cylindrica* was more commonly found in frequently burned plots, which fits with their known ability to recover quickly after disturbance (Dinerstein, 1979a; Lehmkuhl, 1989; Lamichhane et al., 2024). At the same time, *Narenga porphyrocoma* was more often present in areas with less fires which fits with its link to later successional stages (Lehmkuhl, 1989). However, the relatively high occurrence of *Saccharum spontaneum* in long-unburned sites was unexpected. This may partly be due to sample size limitations or possible field misidentification, and should be interpreted with care. Overall, these trends suggest that fire exposure may filter species according to their regeneration strategies (Das et al. 2021; Bhusal et al., 2024). Visual inspection of relative dominance patterns further show Saccharum bengalense and Imperata cylindrica were more common at intermediate fire frequencies, likely due to their ability to regenerate quickly after fire and tolerate repeated disturbance.

Fire also had a clear effect on species diversity. The Shannon Diversity Index increased significantly with fire frequency, showing that more frequently burned plots support higher diversity (Figure 4.4.4). This pattern somewhat aligns with the Intermediate Disturbance Hypothesis, which suggests that regular disturbance can prevent competitive exclusion and allow a wider range of species to coexist (Connell, 1978). In these grasslands, repeated fire may reduce the dominance of a few aggressive species and create space for others to establish, maintaining a more diverse community over time. However, the relationship found in this research was linear rather than unimodal, meaning that diversity did not peak at intermediate fire levels. This still supports the general idea behind the IDH but does not fully reflect its typical curve.

Recently burned plots also showed significantly higher diversity than long unburned ones (Figure 4.4.5), suggesting that fire has a short-term positive effect on species richness, likely because fire opens up space and resources, allowing new or previously suppressed species to establish. However, no significant differences were found between moderately and recently burned plots, which suggests that this effect may taper off over time. These results, together with the positive relationship between fire frequency and diversity, indicate that both recent fire and repeated burning can promote species coexistence, but not uniformly across all conditions. Lamichhane et al. (2024) similarly found that in the Baghaura grassland in BNP burned plots supported taller vegetation and greater species diversity. At the species level, the results showed that these fire effects vary depending on the dominant grass community. *S. spontaneum* responded positively to both fire frequency and recent burning (Figures 4.4.7 and 4.4.8), while no significant effects were observed for *S. bengalense*, *I. cylindrica*, or *N. porphyrocoma*. This suggests that some grassland types are more responsive to fire in terms of maintaining or enhancing diversity, while others remain relatively stable regardless of fire history.

Taken together, the findings appear to somewhat support the IDH. Intermediate fire frequencies may help to maintain species coexistence and structural heterogeneity (Lehmkuhl, 1989; Das et al., 2021). However, too frequent burning risks homogenisation, favouring only the most fire-tolerant species, while fire suppression may lead to woody succession and biodiversity loss (Dinerstein, 1979a; Thapa et al., 2021; Bijlmakers et al., 2023; Ghimire et al., 2014). While the IDH remains a useful conceptual tool, it is debated due to its unclear thresholds and limited empirical consistency (Fox, 2012). In Bardia, the observed trends in diversity broadly align with IDH expectations, but conclusions should remain cautious due to limited sample size and the lack of sites with very high fire frequency.

Interpretations based on species-level patterns must also acknowledge the study's sampling limitations. With only 50 vegetation samples and highly uneven species representation (*Themeda arundinacea* only occurred in two plots and consequently was excluded for most analyses), statistical power was limited. Even among the more common species, the number of samples was limited: *S. Bengalanese (11), I. cylindrica (16), N. porphyrocoma (10)* and *S. spontaneum (11).* Several field-observed trends, such as higher SLA or increased leaf number, were not statistically significant but might have been under a larger or more balanced sampling design. In addition, identifying grasses in the field remains difficult, and misclassification can’t be ruled out. As such, some trends appear ecologically meaningful but should not be interpreted as definitive.

To maintain biodiversity in fire-prone grasslands like Bardia, it requires an integrated approach that combines different disturbance regimes to shape vegetation structure and ecological function over time. Biodiversity is not only essential for supporting habitat quality and forage availability for herbivores and their predators, but also for the long-term resilience of the ecosystem (Brockerhoff et al., 2017). More diverse plant communities are typically better able to recover after disturbance, buffer against stress, and provide critical resources across seasons (Bhusal et al., 2024). These dynamics are becoming increasingly important as climate change raises the risk of extreme fire events and prolonged dry periods across Nepal (Pokharel et al., 2023). Kirkland et al. (2024) point out that areas undergoing natural succession, such as abandoned agricultural land, are particularly vulnerable to fire under these drying trends. This has direct relevance for Bardia, where many short grasslands lie upon former agricultural lands and are now maintained through prescribed burning. In their study, Kirkland et al. (2024) show that while grazing has benefits, it is not enough to maintain ecological function on its own, highlighting the need for integrated disturbance strategies. Lamichhane (2024) similarly shows that combining controlled fire with small-scale cutting improves grazing access and promotes greater structural heterogeneity, thereby supporting more diverse and resilient grassland communities.Together, this emphasises the importance of adaptive, multi-faceted disturbance regimes for maintaining both biodiversity and ecological function in Bardia's grasslands.

Sustaining ecological function in Bardia's grasslands therefore depends not only on the application of individual tools like fire, grazing, or cutting, but on how these are combined and timed within the broader ecological and climatic context. However, without adaptive and ongoing management, the system remains vulnerable. Pressures such as fire suppression, changing rainfall regimes, and expanding land use could shift the balance toward fuel accumulation, woody encroachment, and biodiversity decline (Bijlmakers, 2023; Das et al., 2021; Ghimire, 2014). Long-term resilience will require not just ecological insight, but also flexible management and institutional support that responds to climate uncertainty and changing social dynamics

6. Conclusion

This thesis examined how fire regimes shape vegetation structure and species composition in the subtropical grasslands of Bardia National Park. By combining a decade of satellite-derived fire frequency data with fifty vegetation plots, the research investigated how different fire histories influenced biomass, greenness, species diversity, and dominant grass types across the study area.

Fires were most frequent in dry grasslands, upland zones, and key management areas, especially in the south where early-season burns are regularly applied to maintain open habitat. Some fire patterns likely reflect natural variation in flammability and drainage, but accessibility and conservation priorities also played a role. Sites near roads, such as Lamkauli and Baghaura, were among the most frequently burned, highlighting the impact of strategic management. Fires in the drier Sal forest terraces of the north were more likely to occur later in the season and were often unplanned.

Seasonally, the fire model detected most burning in January and February, when prescribed fires were commonly set and detection conditions were optimal. The accuracy of the early fire season was 92 % with a Cohen κ of 0.84 for January- February fires. However, this does not fully represent the actual fire regime. Limitations in the model, including rapid vegetation regrowth and image timing, contributed to under-detection later in the season. Despite these shortcomings, the early-season outputs aligned well with ground data and offered a reliable basis for assessing fire-vegetation interactions.

Vegetation structure showed observable trends across the fire gradient. Although canopy height and bulk density tended to decrease with more frequent burning, these differences were not statistically significant. However, NDVI increased significantly with fire frequency, while dried biomass remained stable. These results indicate that fire resets structural attributes without reducing overall productivity. Early-successional traits, especially those of pioneer tall grasses, appeared to drive this structural shift. In contrast, species composition responded less strongly. Saccharum spontaneum was more common in frequently burned areas, while Narenga porphyrocoma was associated with long-unburned sites. Still, overall species turnover was modest. Shannon diversity increased linearly with fire frequency and recent burns, offering partial support for the Intermediate Disturbance Hypothesis, though no clear peak in diversity was found at intermediate fire levels.

Effective management in the future will require fire management to further adapt to local conditions and changing climate. Managing fire in small, varied patches across the landscape can help maintain habitat diversity, prevent tree encroachment, and ensure forage availability for large herbivores and the endangered species that rely on open grasslands. As the region faces longer dry spells and more erratic monsoon rains, improved fire detection will be increasingly important. This study shows that fire is both a natural part of Bardia's grasslands and a practical tool for their management. By combining spatial fire data with field observations, it becomes possible to better understand how different fire histories shape grassland structure and composition. At the same time, the findings show the need for improved monitoring across the full dry season and more balanced sampling across fire gradients. As climate conditions become less predictable, understanding these dynamics will be key to supporting resilient and functioning grassland ecosystems.

7. Bibliography

Ahrestani, F. S., & Sankaran, M. (2016). The ecology of large herbivores in South and Southeast Asia. In *Ecological studies*. https://doi.org/10.1007/978-94-017-7570-0

Amnesty International Nepal. (2021, August 9). *NEPAL: VIOLATIONS IN THE NAME OF CONSERVATION*. https://amnestynepal.org/report/nepal-violations-in-the-name-of-conservation

Bhattarai, B. P., & Kindlmann, P. (2011). Habitat heterogeneity as the key determinant of the abundance and habitat preference of prey species of tiger in the Chitwan National Park, Nepal. *ACTA THERIOLOGICA*, *57*(1), 89–97. https://doi.org/10.1007/s13364-011-0047-8

Bhusal, N., Bhusal, B., & Pokharel, B. (2024). Effects of fire and cutting on vegetation physical properties and herbivorous foraging behavior in the grassland of Bardia National Park, Nepal. *Journal of Forest and Natural Resource Management*, *4*(1), 33–50. https://doi.org/10.3126/jfnrm.v4i1.74232

Bijlmakers, J., Griffioen, J., & Karssenberg, D. (2023). Environmental drivers of spatio-temporal dynamics in floodplain vegetation: grasslands as habitat for megafauna in Bardia National Park (Nepal). *Biogeosciences*, *20*(6), 1113–1144. https://doi.org/10.5194/bg-20-1113-2023

Blondel, J. (2003). Guilds or functional groups: does it matter? *Oikos*, *100*(2), 223–231. https://doi.org/10.1034/j.1600-0706.2003.12152.x

Brockerhoff, E. G., Barbaro, L., Castagneyrol, B., Forrester, D. I., Gardiner, B., González-Olabarria, J. R., Lyver, P. O., Meurisse, N., Oxbrough, A., Taki, H., Thompson, I. D., Van Der Plas, F., & Jactel, H. (2017). Forest biodiversity, ecosystem functioning and the provision of ecosystem services. Biodiversity and Conservation, 26(13), 3005–3035. https://doi.org/10.1007/s10531-017-1453-2

CNP. (2016). Grassland Habitat Mapping in Chitwan National Park. In *Department of National Parks and Wildlife Conservation*. Chitwan National Park Office. Retrieved November 21, 2024, from https://dnpwc.gov.np/media/publication/GRASSLAND_HABITAT_MAPPING_CNP.pdf

Connell, J. H. (1978). Diversity in Tropical Rain Forests and Coral Reefs. *Science*, *199*(4335), 1302–1310. https://doi.org/10.1126/science.199.4335.1302

Das, D., Banerjee, S., Lehmkuhl, J., Krishnaswamy, J., & John, R. (2021). The influence of abiotic and spatial variables on woody and herbaceous species abundances in a woodland–grassland system in the Eastern Terai of India. *Journal of Plant Ecology*, *15*(1), 155–167. https://doi.org/10.1093/jpe/rtab080

Dinerstein, E. (1979). An ecological survey of the royal Karnali-Bardia Wildlife Reserve, Nepal. Part I: Vegetation, modifying factors, and successional relationships. *Biological Conservation*, *15*(2), 127–150. https://doi.org/10.1016/0006-3207(79)90030-2

DNPWC. (2023). *Tiger Conservation Action Plan (2023-2032)*. Department of National Parks and Wildlife Conservation. Retrieved December 2, 2024, from https://dnpwc.gov.np/media/publication/Final_Tiger_Conservation_Action_Plan_2023.indd.pdf

Enright, N. J., Fontaine, J. B., Lamont, B. B., Miller, B. P., & Westcott, V. C. (2014). Resistance and resilience to changing climate and fire regime depend on plant functional traits. *Journal of Ecology*, *102*(6), 1572–1581. https://doi.org/10.1111/1365-2745.12306

Flory, S., Langeland, K., MacDonald, G., Ferrell, J., Enloe, S., Sellers, B., & Brecke, B. (2018, October 4). *Cogongrass (Imperata cylindrica) Biology, Ecology, and Management in Florida Grazing Lands*. Ask IFAS - Powered by EDIS. https://edis.ifas.ufl.edu/publication/WG202

Fox, J. W. (2012). The intermediate disturbance hypothesis should be abandoned. *Trends in Ecology & Evolution*, *28*(2), 86–92. https://doi.org/10.1016/j.tree.2012.08.014

Garnier, E., Shipley, B., Roumet, C., & Laurent, G. (2001). A standardized protocol for the determination of specific leaf area and leaf dry matter content. *Functional Ecology*, *15*(5), 688–695. https://doi.org/10.1046/j.0269-8463.2001.00563.x

Gautam, D. N. (2013). Assessment of wild ungulates in the Karnali flood plain of Bardia National Park, Nepal. *DOAJ (DOAJ: Directory of Open Access Journals)*. https://doaj.org/article/4db4db9eba124d4a9bc1d247e5517ce2

Gautam, K. H., & Devoe, N. N. (2005). Ecological and anthropogenic niches of sal (Shorea robusta Gaertn. f.) forest and prospects for multiple-product forest management – a review. *Forestry an International Journal of Forest Research*, *79*(1), 81–101. https://doi.org/10.1093/forestry/cpi063

Keeley, J. E., & Pausas, J. G. (2022). Evolutionary ecology of fire. *Annual Review of Ecology Evolution and Systematics*, *53*(1), 203–225. https://doi.org/10.1146/annurev-ecolsys-102320-095612

Kirkland, M., Atkinson, P. W., Aliácar, S., Saavedra, D., De Jong, M. C., Dowling, T. P. F., & Ashton-Butt, A. (2024). Protected areas, drought, and grazing regimes influence fire occurrence in a fire-prone Mediterranean region. *Fire Ecology*, *20*(1). https://doi.org/10.1186/s42408-024-00320-9

Lamichhane, B., Karki, J. B., Thapa, S. K., Bhandari, A., & Basyal, B. (2024). Effect of cutting and burning on grassland habitat in Bardia National Park, Nepal. *Ecosphere*, *15*(9). https://doi.org/10.1002/ecs2.70004

Lehmann, C. E. R., Anderson, T. M., Sankaran, M., Higgins, S. I., Archibald, S., Hoffmann, W. A., Hanan, N. P., Williams, R. J., Fensham, R. J., Felfili, J., Hutley, L. B., Ratnam, J., Jose, J. S., Montes, R., Franklin, D., Russell-Smith, J., Ryan, C. M., Durigan, G., Hiernaux, P., . . . Bond, W. J. (2014). Savanna Vegetation-Fire-Climate relationships differ among continents. *Science*, *343*(6170), 548–552. https://doi.org/10.1126/science.1247355

Lehmkuhl, J. (1989). *The ecology of South-Asian tall-grass communities* [Phd dissertation, University of Washington, Seattle, WA]. https://pdf.usaid.gov/pdf_docs/pnabi208.pdf

Lehmkuhl, J. (1994). A classification of subtropical riverine grassland and forest in Chitwan National Park, Nepal. *Plant Ecology*, *111*(1), 29–43. https://doi.org/10.1007/bf00045575

Matin, M. A., Chitale, V. S., Murthy, M. S. R., Uddin, K., Bajracharya, B., & Pradhan, S. (2017). Understanding forest fire patterns and risk in Nepal using remote sensing, geographic

information system and historical fire data. *International Journal of Wildland Fire*, *26*(4), 276. https://doi.org/10.1071/wf16056

Moi, D. A., Garcia-Rios, R., Hong, Z., Daquila, B. V., & Mormul, R. P. (2020). Intermediate Disturbance Hypothesis in Ecology: A Literature Review. *Annales Zoologici Fennici*, *57*(1/6), 67–78. https://www.jstor.org/stable/27100676.

Morandini, F., Simeoni, A., Santoni, P. A., & Balbi, J. H. (2005). A MODEL FOR THE SPREAD OF FIRE ACROSS a FUEL BED INCORPORATING THE EFFECTS OF WIND AND SLOPE. Combustion Science and Technology, 177(7), 1381–1418. https://doi.org/10.1080/00102200590950520

Odden, M., Wegge, P., & Storaas, T. (2005). Hog deer Axis porcinus need threatened tallgrass floodplains: a study of habitat selection in lowland Nepal. *Animal Conservation*, *8*(1), 99–104. https://doi.org/10.1017/s1367943004001854

Pandey, H. P., Pokhrel, N. P., Thapa, P., Paudel, N. S., & Maraseni, T. N. (2022). Status and practical implications of forest fire management in Nepal. *Journal of Forest and Livelihood*, *21*(1), 32–45. https://doi.org/10.3126/jfl.v21i1.56583

Peet, N., Watkinson, A., Bell, D., & Kattel, B. (1999). Plant diversity in the threatened sub-tropical grasslands of Nepal. *Biological Conservation*, *88*(2), 193–206. https://doi.org/10.1016/s0006-3207(98)00104-9

Pokharel, B., Sharma, S., Stuivenvolt-Allen, J., Wang, S. S., LaPlante, M., Gillies, R. R., Khanal, S., Wehner, M., Rhoades, A., Hamal, K., Hatchett, B., Liu, W., Mukherjee, S., & Aryal, D. (2023). Amplified drought trends in Nepal increase the potential for Himalayan wildfires. *Climatic Change*, *176*(2). https://doi.org/10.1007/s10584-023-03495-3

Pokheral, S. K. (1993). *Floristic composition, biomass production, and biomass harvest in the grasslands of the Royal Bardia National Park, Bardia, Nepal* [MS thesis]. Agricultural University of Norway.

Rashkovetsky, D., Mauracher, F., Langer, M., & Schmitt, M. (2021). Wildfire detection from multisensor satellite imagery using deep semantic segmentation. *IEEE Journal of Selected Topics in Applied Earth Observations and Remote Sensing*, *14*, 7001–7016. https://doi.org/10.1109/jstars.2021.3093625

Reddy, C. S., Bird, N. G., Sreelakshmi, S., Manikandan, T. M., Asra, M., Krishna, P. H., Jha, C. S., Rao, P. V. N., & Diwakar, P. G. (2019). Identification and characterization of spatio-temporal hotspots of forest fires in South Asia. *Environmental Monitoring and Assessment*, *191*(S3). https://doi.org/10.1007/s10661-019-7695-6

Sapkota, R. P., Dhital, N. B., & Rijal, K. (2023). Fire-mediated biomass loss of woody species seedlings causing demographic bottleneck in the Terai Forests of Central Nepal. *Global Ecology and Conservation*, *48*, e02705. https://doi.org/10.1016/j.gecco.2023.e02705

Schrader, J., Shi, P., Royer, D. L., Peppe, D. J., Gallagher, R. V., Li, Y., Wang, R., & Wright, I. J. (2021). Leaf size estimation based on leaf length, width and shape. *Annals of Botany*, *128*(4), 395–406. https://doi.org/10.1093/aob/mcab078

Singh, J. S., & Singh, S. P. (1992). *Forests of Himalaya: Structure, functioning, and Impact of man*. Gyanodaya Prakashan.

Stevens, C. J. (2018). Recent advances in understanding grasslands. *F1000Research*, *7*, 1363. https://doi.org/10.12688/f1000research.15050.1

Thapa, S. K. (2023). *Deer for the Tiger - Managing subtropical monsoon grasslands for preserving a flagship species* [PhD thesis, University of Wageningen]. https://doi.org/10.18174/640107

Thapa, S. K., De Jong, J. F., Subedi, N., Hof, A. R., Corradini, G., Basnet, S., & Prins, H. H. (2021). Forage quality in grazing lawns and tall grasslands in the subtropical region of Nepal and implications for wild herbivores. *Global Ecology and Conservation*, *30*, e01747. https://doi.org/10.1016/j.gecco.2021.e01747

Turner, M. G., & Seidl, R. (2023). Novel disturbance regimes and ecological responses. *Annual Review of Ecology Evolution and Systematics*, *54*(1), 63–83. https://doi.org/10.1146/annurev-ecolsys-110421-101120

Vitousek, P. M. (2015). Grassland ecology: Complexity of nutrient constraints. *Nature Plants*, *1*(7). https://doi.org/10.1038/nplants.2015.98

Webb, E. L., & Sah, R. N. (2003). Structure and diversity of natural and managed sal (Shorea robusta Gaertn.f.) forest in the Terai of Nepal. *Forest Ecology and Management*, *176*(1–3), 337–353. https://doi.org/10.1016/s0378-1127(02)00272-4

Zhang, H. (2011). *Building materials in civil engineering*. Woodhead Publishing.

8. Appendix

This chapter shows extra figures and tables and for the already mentioned figures in the text their statistical analysis if applicable.

Appendix A - Methods

A.1 Table of Braun Blaunquets conversion

Table A.1: A table showing Braun-Blaunquet values, percentage range, their description and the converted midpoint value which was used in further quantitative analysis

Braun-Blanquet	Percentage Range	Description	Converted midpoint value
i	One unique individual	Very rare	0.001
r	0-1%	Rare	0.005
+	1-5% (few individuals)	Sparse	0.01
1	1-5% (numerous individuals)	Low cover	0.05
2	5-25%	Moderate cover	0.15
3	25-50%	High cover	0.375
4	50-75%	Very high cover	0.625
5	75-100%	Dominant	0.875

Appendix B - Research Question 1

B.1 Fire Model Classification Map

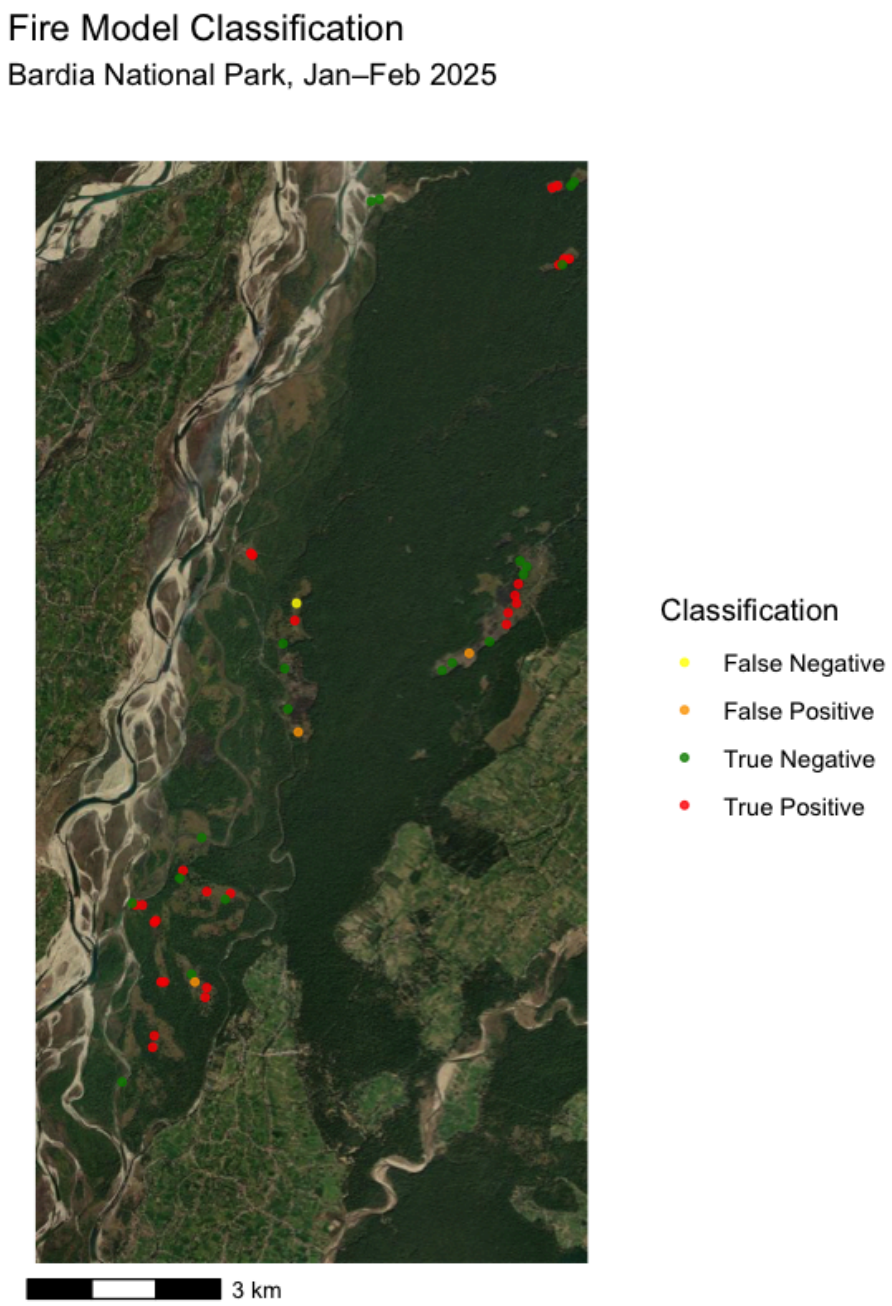

Figure B.1 *Spatial distribution of true and false classifications from the fire detection model across the study area. Yellow and orange points indicate misclassifications, while the red and green points are classified correctly.*

B.2 Land Cover Map Bardia National Park

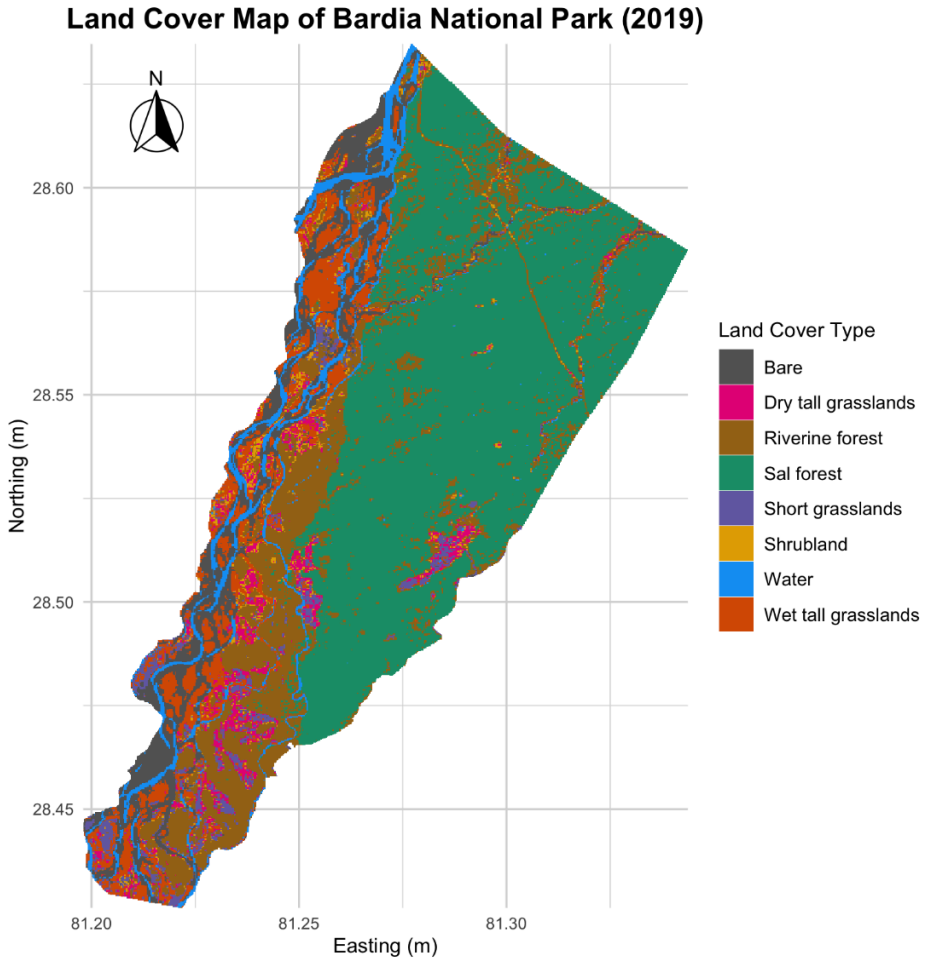

Figure B.2 *Land cover classification of Bardia NP (2019), based on Bijlmakers et al. (2019), showing different types of grasslands, forests, shrubland, bare soil and water*

B.3 Digital Elevation Model Bardia NP

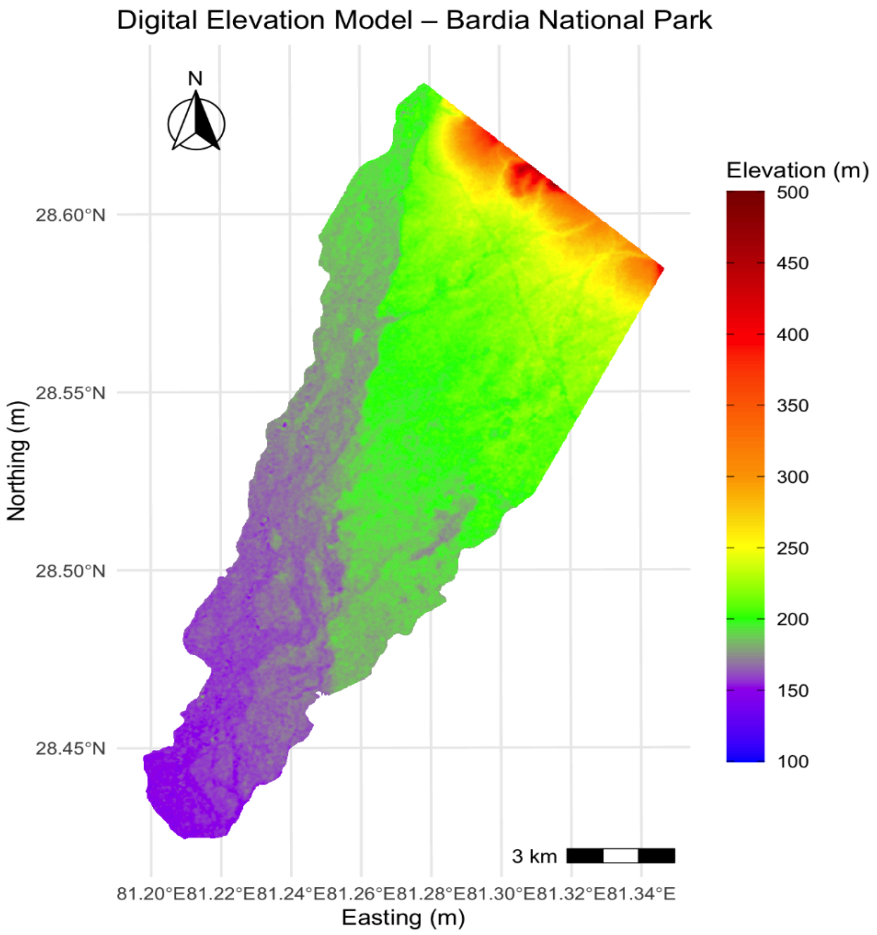

Figure B.3 Digital Elevation Model (DEM) of Bardia National Park, Nepal. Elevation values range from approximately 100 to 500 metres above sea level, based on 30-metre resolution SRTM data obtained via the 'elevatr' package in R. The map illustrates topographic variation across the park, with higher elevations concentrated in the north-eastern region.

B.4 Elevation and Burn Frequency

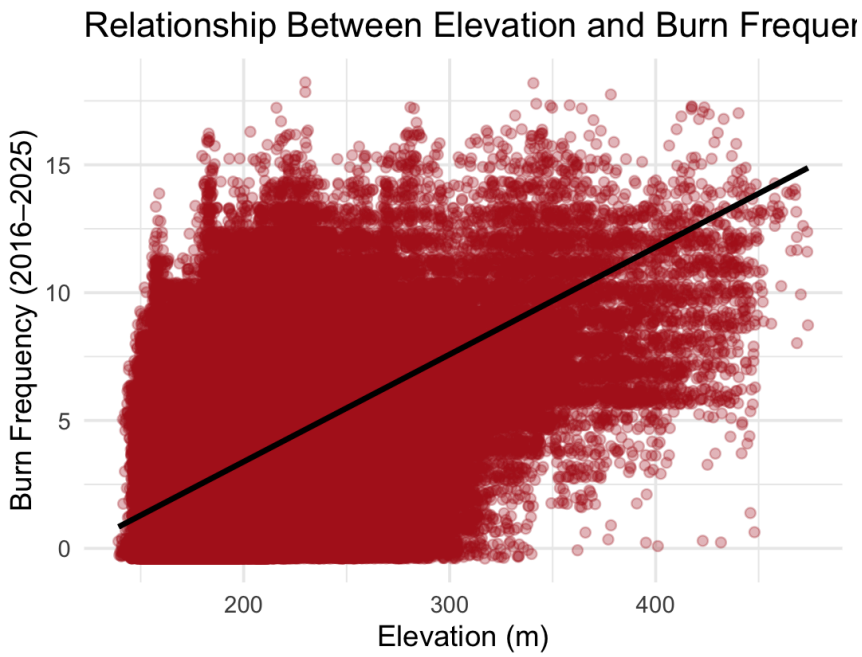

Figure B.4 Relationship between elevation and burn frequency (2016–2025) across the research area in Bardia National Park. Each point represents a pixel value from the fire frequency map plotted against corresponding elevation (in metres). A positive trend is visible, with higher burn frequencies generally occurring at higher elevations. The Spearman correlation coefficient (ρ = 0.537) indicates a moderate positive association.

Appendix C - Research Question 2

C.1 Grassland Middle Fire Frequency Map

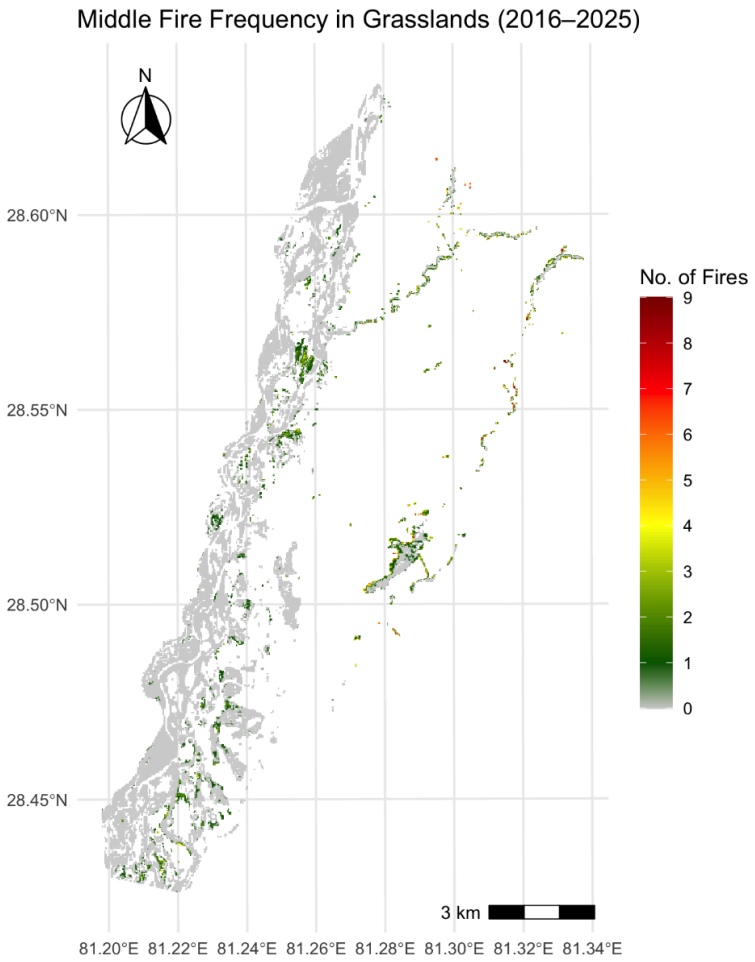

Figure C.1 Middle fire season (March and April), burn frequency of grasslands (Bijlmakers et al., 2019) map in Bardia National Park, Nepal (2016–2025) . Colours indicate the number of years each pixel was classified as burned, based on dNBR thresholding of Sentinel-2 imagery. Coordinate system: UTM Zone 44N (EPSG:32644). Data: Copernicus Sentinel-2 (harmonised)

C.2 Grasslands Late Fire Frequency

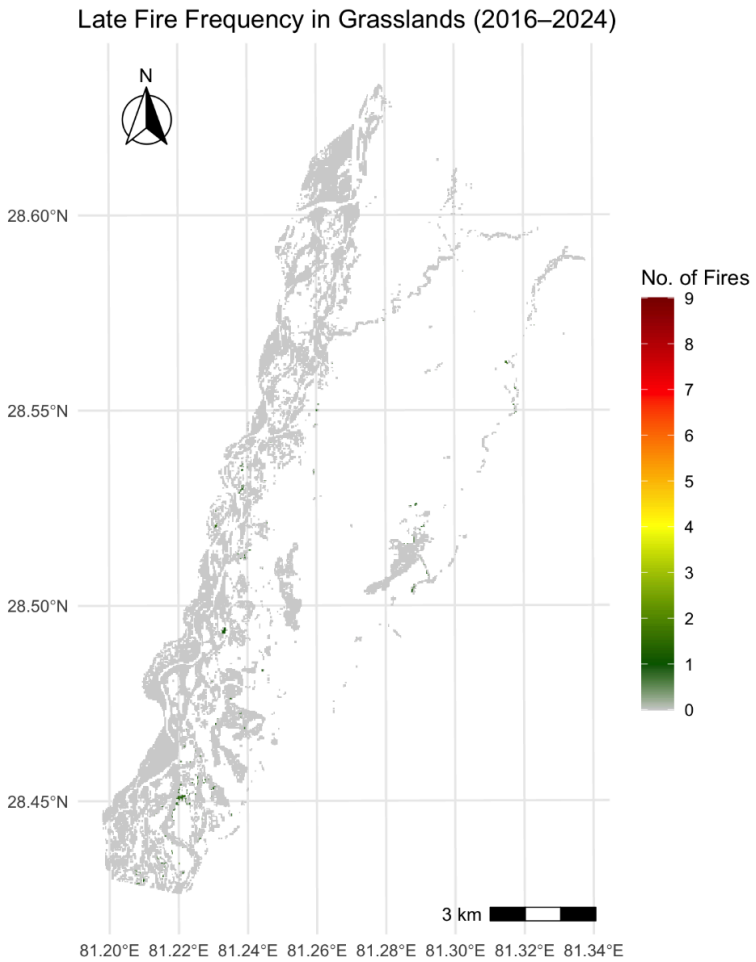

Figure C.2 Late fire season May), burn frequency of grasslands (Bijlmakers et al., 2019) map in Bardia National Park, Nepal (2016–2025) . Colours indicate the number of years each pixel was classified as burned, based on dNBR thresholding of Sentinel-2 imagery. Coordinate system: UTM Zone 44N (EPSG:32644). Data: Copernicus Sentinel-2 (harmonised)

C.3 Middle Fire Burn Frequency by Land Type

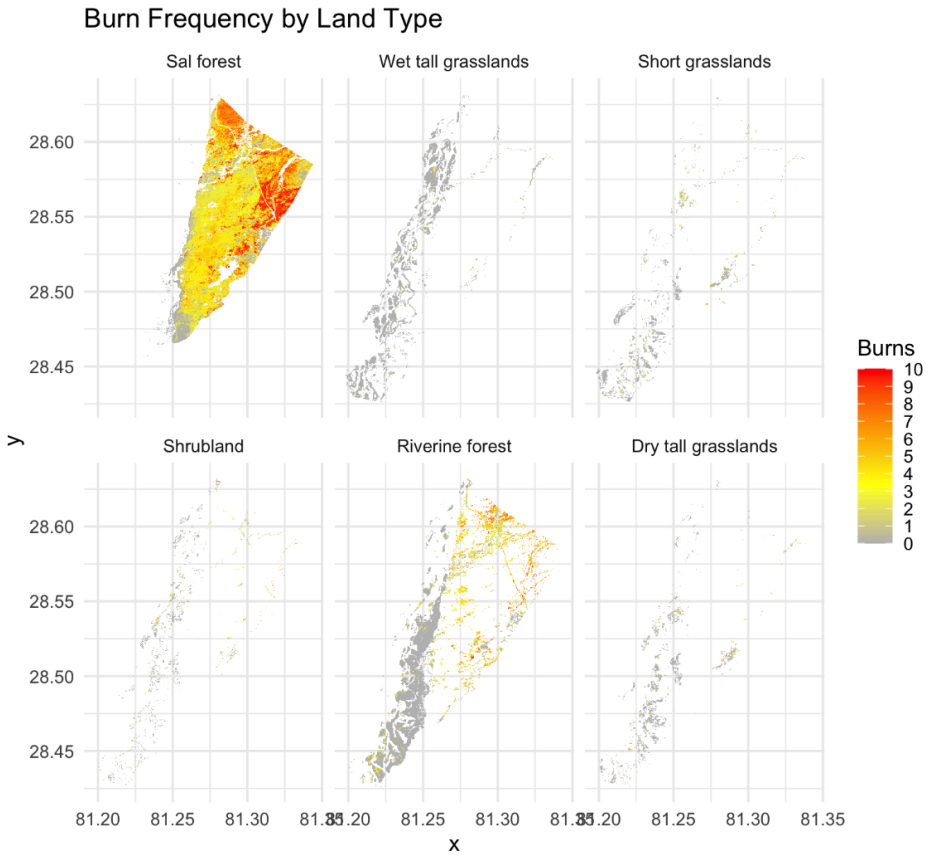

Figure C.3 *Middle fire period (March–April) burn frequency across different land cover types in Bardia National Park. The panels show spatial patterns of fire occurrence by land cover class, with the highest number of burns recorded in Sal forest and riverine forest. Burn frequencies are classified from 0 to 10 based on the number of fire events detected between 2016 and 2025*

Appendix C - Research Question 3

D.1 Biomass by Fire Occurrence

This is the statistical analysis of a figure which can be found in the text as figure 4.3.1

- Shapiro-Wilk
  - Burned: W = 0.66608, p-value = 9.784e-07
  - Unburned: W = 0.73622, p-value = 5.867e-05
- Levene's:
  - Df F value Pr(>F)
  - group 1 0.4581 0.5018
  - 48
- Wilcoxon rank-sum test
  - W = 343, p-value = 0.5001
  - alternative hypothesis: true location shift is not equal to 0

D. 2 Biomass per Fire Occurrence across Functional Groups

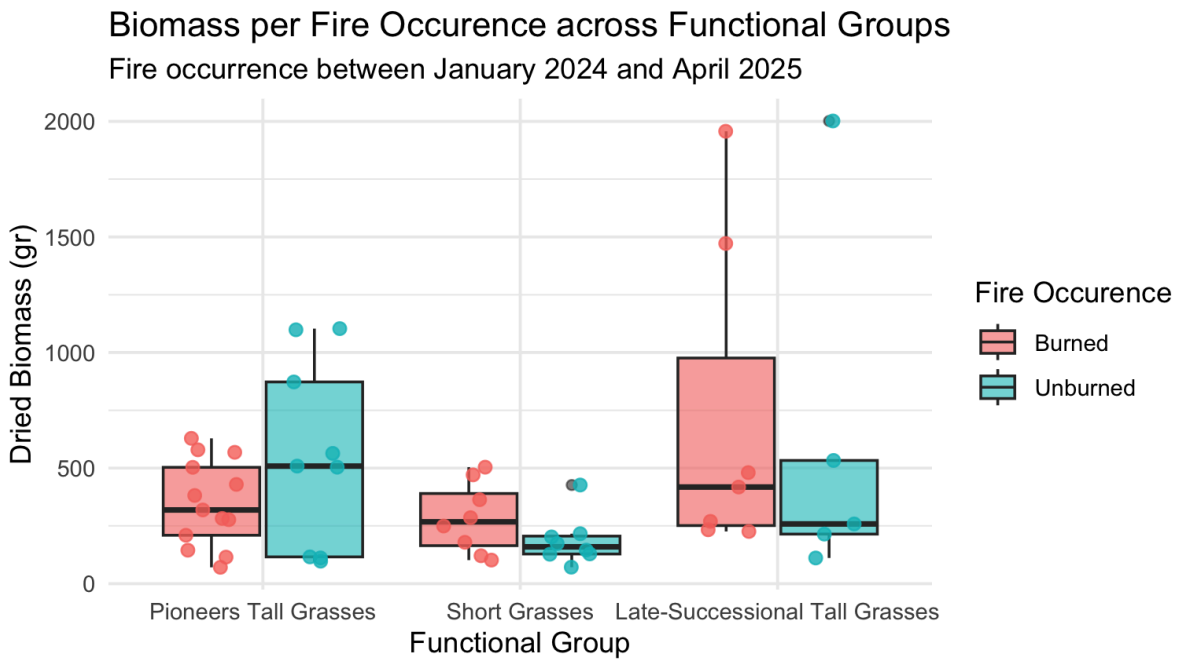

Figure D2 *Dried biomass in recently burned vs unburned classes across the functional groups*

- Shapiro-Wilk Test
  - Pioneers Tall grass:
    - Burned W = 0.951, p = 0.608
    - Unburned W = 0.877, p = 0.145
  - Short Grasses:
    - Burned W = 0.933, p = 0.544
    - Unburned W = 0.821, **p = 0.048**
  - Late-Successional Tall Grasses:
    - Burned W = 0.752, **p = 0.013**
    - Unburned **:** W = 0.720, **p = 0.015**
- Levene's:
  - Pioneers Tall grass:
    - Df F value Pr(>F)
    - group 1 4.793 0.**0406** *
    - 20
  - Short Grasses:
    - Df F value Pr(>F)
    - group 1 1.6706 0.2171
    - 14
  - Late-Successional Tall Grasses:
    - Df F value Pr(>F)
    - group 1 0.0011 0.9745
    - 10
- Wilcoxon Rank-Sum Tests by Functional Group short & late
  - Short Grasses: W = 44, p-value = 0.2345
  - Late-Successional Tall Grasses: W = 21, p-value = 0.6389
- Welch T-test for Pioneers
  - t = -1.43, df = 10.38, p = 0.182
  - Mean biomass (Burned) = 346.81
  - Mean biomass (Unburned) = 552.80
  - 95% CI: [–525.18, 113.20]

D.3 Biomass per Fire frequency

This is the statistical analysis of a figure which can be found in the text as figure 4.3.3

- Shapiro-Wilk normality test
  - data: residuals(model_31)
  - W = 0.8343, p-value = 5.968e-06
- leveneTest(biomass_dried ~ as.factor(burnfreq), data = data)
  - Levene's Test for Homogeneity of Variance (center = median)
  - Df F value Pr(>F)
  - group 11 1.2242 0.3051 38
- kruskal.test(biomass_dried ~ burnfreq, data = data)
  - Kruskal-Wallis rank sum test
  - data: biomass_dried by burnfreq
  - Kruskal-Wallis chi-squared = 7.7713, df = 11, p-value = 0.7336

D. 4 Living Green Biomass across fire frequency

This is the statistical analysis of a figure which can be found in the text as figure 4.3.4

- Shapiro-Wilk normality test
  - data: residuals(model)
  - W = 0.94963, p-value = 0.03295
- Levene's Test for Homogeneity of Variance (center = median)
  - Df F value Pr(>F)
  - group 11 1.071 0.4089
  - 38
- Kruskal-Wallis rank sum test
  - data: fresh_weight_green_leaf by as.factor(burnfreq)
  - Kruskal-Wallis chi-squared = 7.8674, df = 11, p-value = 0.7251

D. 5 NDVI across Fire Frequencies

This is the statistical analysis of a figure which can be found in the text as figure 4.3.5

- Shapiro-Wilk
  - W = 0.97753, p-value = 0.4532
- Breausch-Pagann test (linear model!)
  - BP = 10.355, df = 11, p-value = 0.4988
- Linear regression analysis
  - lm(formula = NDVI ~ burnfreq, data = data)
  - Residuals:
  - Min 1Q Median 3Q Max
  - -0.11769 -0.02391 0.00000 0.02795 0.13664
  - Coefficients:
  - Estimate Std. Error t value Pr(>|t|)
  - (Intercept) 0.24077 0.02012 11.964 1.87e-14 ***
  - burnfreq1 0.05126 0.05692 0.901 0.37350
  - burnfreq2 0.07919 0.03118 2.540 0.01530 *
  - burnfreq3 0.04977 0.03674 1.354 0.18358
  - burnfreq4 0.07760 0.02756 2.816 0.00767 **
  - burnfreq5 0.17551 0.02962 5.925 7.22e-07 ***
  - burnfreq6 0.07969 0.02962 2.690 0.01055 *
  - burnfreq7 0.14776 0.02962 4.988 1.38e-05 ***
  - burnfreq8 0.15314 0.03118 4.912 1.75e-05 ***
  - burnfreq9 0.29136 0.05692 5.119 9.16e-06 ***
  - burnfreq10 0.07122 0.05692 1.251 0.21852

- burnfreq12 0.29144 0.05692 5.120 9.12e-06 ***
- ---
- Signif. codes: 0 ‘***’ 0.001 ‘**’ 0.01 ‘*’ 0.05 ‘.’ 0.1 ‘ ’ 1
- Residual standard error: 0.05324 on 38 degrees of freedom
- Multiple R-squared: 0.6759, Adjusted R-squared: 0.5821
- F-statistic: 7.204 on 11 and 38 DF, p-value: 1.915e-06

D.6 NDVI across fire frequency in functional groups

This is the statistical analysis of a figure which can be found in the text as figure4.3.6

Pioneers Tall Grasses

- Shapiro-Wilk normality test: W = 0.906 , p = 0.04
- Levene’s Test: F = 0.8 , p = 0.611
- Adjusted R² = 0.546 | p = 0 | n = 22

Analysis for: Short Grasses

- Shapiro-Wilk normality test: W = 0.958 , p = 0.619
- Levene’s Test: F = 8.36 , p = 0.004
- Adjusted R² = 0.286 | p = 0.019 | n = 16

Late-Successional Tall Grasses

- Shapiro-Wilk normality test: W = 0.968 , p = 0.884
- Levene’s Test: F = 6.1 , p = 0.024
- Adjusted R² = 0.03 | p = 0.275 | n = 12

D.7 NDVI across Time since Last Fire

This is the statistical analysis of a figure which can be found in the text as figure 4.3.7

- Shapiro-Wilk normality test
  - W = 0.91878, p-value = 0.00213
- Levene's Test for Homogeneity of Variance (center = median)
  - Df F value Pr(>F)
  - group 2 0.832 0.4415
  - 47
- Kruskal-Wallis rank sum test
  - Kruskal-Wallis chi-squared = 14.782, df = 2, p-value = 0.0006167
- Dunn (1964) Kruskal-Wallis multiple comparison
  - p-values adjusted with the Bonferroni method.
  - Comparison
  - 1 Long unburned [9+ years] - Moderate time since burn [1-4 years ago]
  - 2 Long unburned [9+ years] - Recent burn [0 years]
  - 3 Moderate time since burn [1-4 years ago] - Recent burn [0 years]
  - Z P.unadj P.adj
  - 1 -3.39839564 0.0006778232 0.0020334695
  - 2 -3.72213005 0.0001975492 0.0005926477
  - 3 -0.05410875 0.9568485186 1.0000000000

D.8 Plant water content across fire frequencies

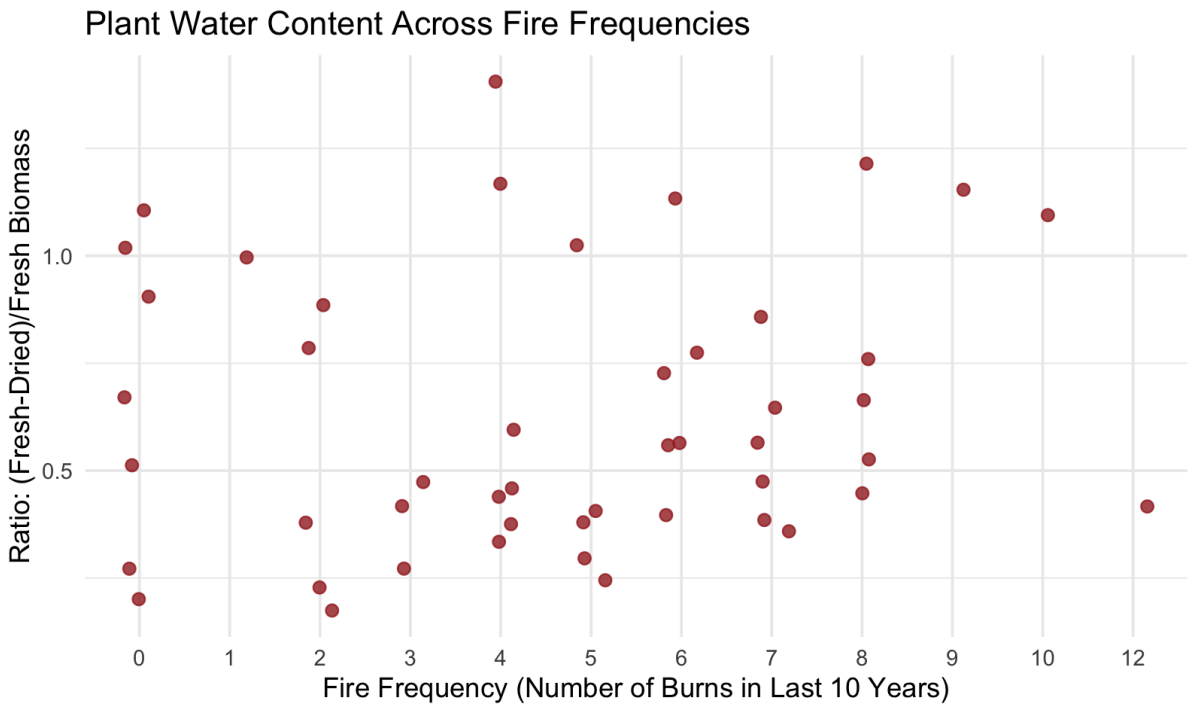

Figure 4.3.8 *Plant water content (dried-to-fresh biomass ratio) across fire frequencies. Kruskal–Wallis test showed no significant difference ($\chi^2 = 10.83$, $p = 0.457$, $n = 50$).*

- Shapiro-wilk Test
  - W = 0.93936, p-value = 0.01271
- Levene's Test for Homogeneity of Variance :
  - Levene's Test for Homogeneity of Variance (center = median)
  - Df F value Pr(>F)
  - group 11 0.6327 0.7895
  - 38
- Kruskal-wallis test
  - Kruskal-Wallis chi-squared = 10.833, df = 11, p-value = 0.4573

D.9 Water Content per Vegetation Community

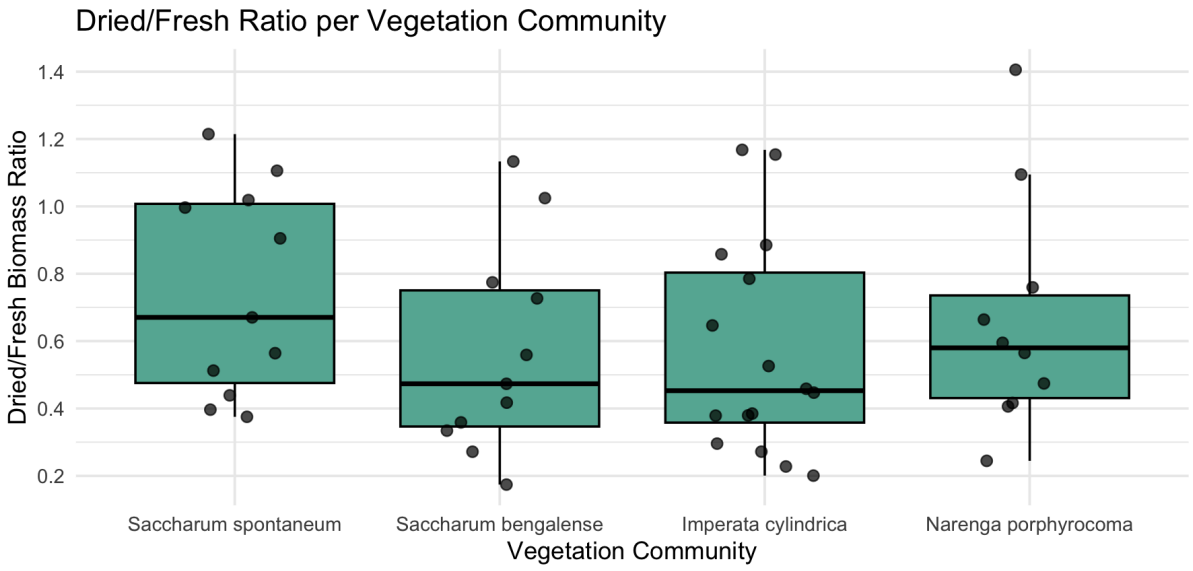

Figure D9 *Water content across vegetation communities. Kruskal–Wallis test found no significant species-level differences ($\chi^2 = 3.04$, df = 3, p = 0.385).*

- Shapiro-Wilk normality test
  - data: residuals(model_water)
  - W = 0.92271, p-value = 0.003709
- Levene's Test for Homogeneity of Variance (center = median)
  - Df F value Pr(>F)
  - group 3 0.0429 0.988
  - 44
- Kruskal-Wallis
  - chi-squared = 3.0404, df = 3, p-value = 0.3854

D.10 Stem diameter across fire occurrence per vegetation communities

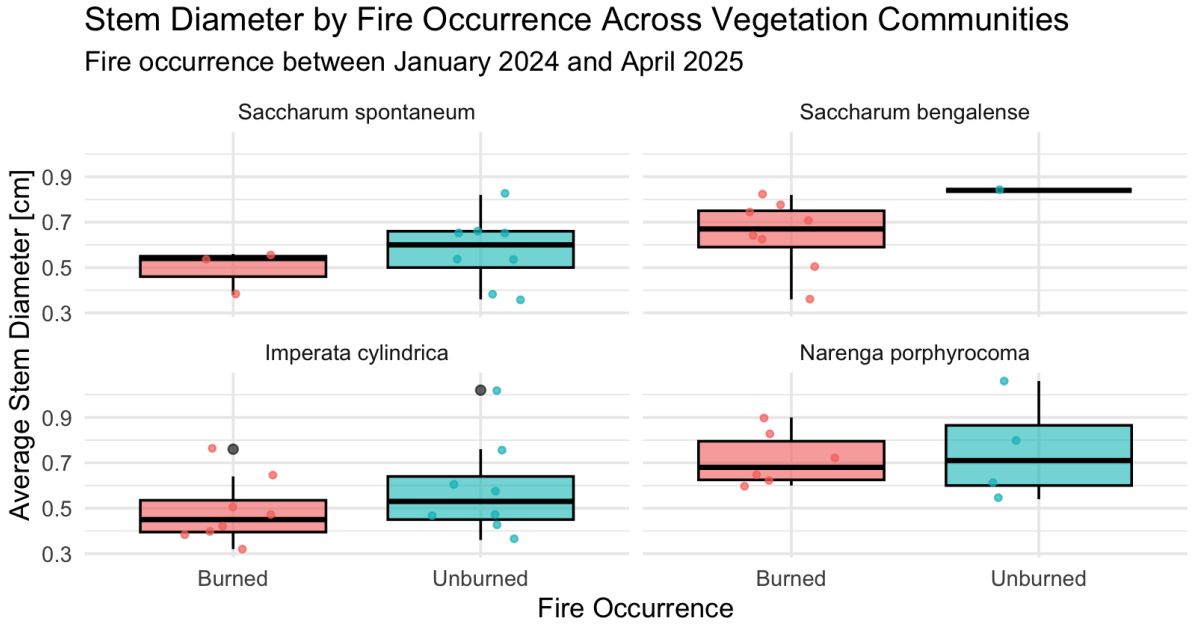

Figure D.10 Average stem diameter [cm] in burned and unburned plots across dominant vegetation communities in Bardia National Park between January 2024 and April 2025. While burned plots of Saccharum spontaneum, Imperata cylindrica, and Narenga porphyrocoma showed slightly smaller average stem diameters compared to unburned plots, these differences were not statistically significant (p > 0.3). Shapiro–Wilk tests confirmed normality for most groups (all p > 0.19), and Levene's test showed no significant variance differences between burned and unburned groups. A non-parametric Wilcoxon test was used for Saccharum bengalense due to small sample size, also indicating no significant difference (p = 0.43).

- Shapiro-wilk Test
  - data: subset(data_no_TA, scientific_names == "Saccharum spontaneum" & burned_status == "Burned")$avg_stem_diameter
    - W = 0.83219, p-value = 0.1939
  - data: subset(data_no_TA, scientific_names == "Saccharum spontaneum" & burned_status == "Unburned")$avg_stem_diameter
    - W = 0.92531, p-value = 0.4744
  - data: subset(data_no_TA, scientific_names == "Saccharum bengalense" & burned_status == "Burned")$avg_stem_diameter
    - W = 0.63194, p-value = 0.0001332
  - Error in shapiro.test(subset(data_no_TA, scientific_names == "Saccharum bengalense" & :
    - sample size must be between 3 and 5000

    - data: subset(data_no_TA, scientific_names == "Imperata cylindrica" & burned_status == "Burned")$avg_stem_diameter
        - W = 0.91228, p-value = 0.3704
    - data: subset(data_no_TA, scientific_names == "Imperata cylindrica" & burned_status == "Unburned")$avg_stem_diameter
        - W = 0.88854, p-value = 0.2268
    - data: subset(data_no_TA, scientific_names == "Narenga porphyrocoma" & burned_status == "Burned")$avg_stem_diameter
        - W = 0.89678, p-value = 0.3552
        - data: subset(data_no_TA, scientific_names == "Narenga porphyrocoma" & burned_status == "Unburned")$avg_stem_diameter
            - W = 0.94053, p-value = 0.6576
- Levene's Test for Homogeneity of Variance :
    - Saccharum spontaneum:
        - Df F value Pr(>F)
        - group 1 1.1355 0.3144
        - 9
    - Imperata cylindrica
        - Df F value Pr(>F)
        - group 1 0.5617 0.466
        - 14
    - Narenga porphyrocoma
        - Df F value Pr(>F)
        - group 1 1.6775 0.2314
        - 8
- Wilcoxon
    - Saccharum bengalense:W = 2, p-value = 0.4292
- T test (two sample)
    - Saccharum spontaneum:
        - t = -0.8606, df = 9, p-value = 0.4118
        - alternative hypothesis: true difference in means between group Burned and group Unburned is not equal to 0
        - 95 percent confidence interval:
        - -0.3054045 0.1370711
        - sample estimates:
        - mean in group Burned mean in group Unburned
        - 0.4933333 0.5775000
    - Imperata cylindrica
        - t = -1.0596, df = 14, p-value = 0.3073
        - alternative hypothesis: true difference in means between group Burned and group Unburned is not equal to 0
        - 95 percent confidence interval:
        - -0.29485493 0.09985493
        - sample estimates:
        - mean in group Burned mean in group Unburned
        - 0.4875 0.5850
    - Narenga porphyrocoma
        - t = -0.34825, df = 8, p-value = 0.7366
        - alternative hypothesis: true difference in means between group Burned and group Unburned is not equal to 0
        - 95 percent confidence interval:
        - -0.2921648 0.2154981
        - sample estimates:
        - mean in group Burned mean in group Unburned
        - 0.7166667 0.7550000

D.11 Average Leaf Size per Fire occurrence and Vegetation Community

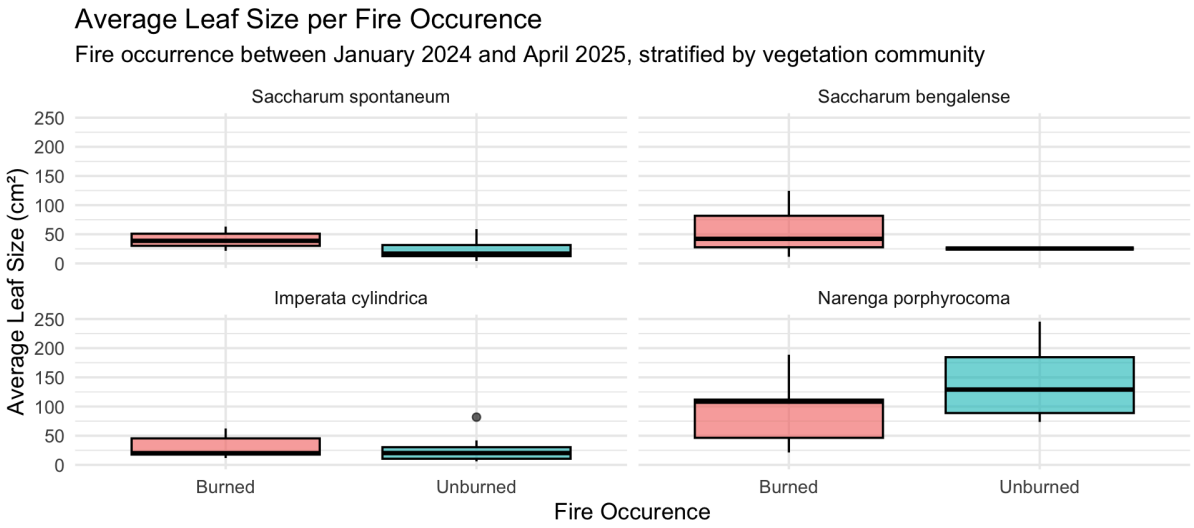

Figure D.11 Average leaf size (cm²) in burned and unburned plots across dominant vegetation communities in Bardia National Park, based on fire occurrence between January 2024 and April 2025. None of the observed differences in average leaf size were statistically significant ($p > 0.18$, Wilcoxon and t-tests). Shapiro–Wilk tests showed non-normal distributions for some unburned groups ($p < 0.05$), and Levene's test indicated no significant variance difference ($p = 0.53$) in Narenga porphyrocoma. Despite variation in means, statistical tests did not support a meaningful effect of fire occurrence on average leaf size

- Shapiro-wilk Test
    - data: subset(data_no_TA, scientific_names == "Saccharum spontaneum" & burned_status == "Burned")$avg_leaf_size
        - W = 0.98992, p-value = 0.8079
    - data: subset(data_no_TA, scientific_names == "Saccharum spontaneum" & burned_status == "Unburned")$avg_leaf_size
        - W = 0.79889, p-value = 0.02785
    - data: subset(data_no_TA, scientific_names == "Saccharum bengalense" & burned_status == "Burned")$avg_leaf_size
        - W = 0.90918, p-value = 0.2754
    - Error in shapiro.test(subset(data_no_TA, scientific_names == "Saccharum bengalense" & :
    - sample size must be between 3 and 5000
    - data: subset(data_no_TA, scientific_names == "Imperata cylindrica" & burned_status == "Burned")$avg_leaf_size
        - W = 0.84476, p-value = 0.08428
    - data: subset(data_no_TA, scientific_names == "Imperata cylindrica" & burned_status == "Unburned")$avg_leaf_size
        - W = 0.8073, p-value = 0.03425
    - data: subset(data_no_TA, scientific_names == "Narenga porphyrocoma" & burned_status == "Burned")$avg_leaf_size
        - W = 0.88841, p-value = 0.31
    - data: subset(data_no_TA, scientific_names == "Narenga porphyrocoma" & burned_status == "Unburned")$avg_leaf_size
        - W = 0.92768, p-value = 0.5808
- Wilcoxon
    - Saccharum spontaneum
        - Wilcoxon rank sum test with continuity correction
        - data: avg_leaf_size by burned_status
        - W = 19, p-value = 0.1846
        - alternative hypothesis: true location shift is not equal to 0

    - Saccharum bengalense
        - Wilcoxon rank sum test with continuity correction
        - data: avg_leaf_size by burned_status
        - W = 8, p-value = 0.4292
        - alternative hypothesis: true location shift is not equal to 0
    - Imperata cylindrica
        - Wilcoxon rank sum test with continuity correction
        - data: avg_leaf_size by burned_status
        - W = 39, p-value = 0.4948
        - alternative hypothesis: true location shift is not equal to 0
    - Narenga porphyrocoma
        - Levene's Test for Homogeneity of Variance (center = median)
        - Df F value Pr(>F)
        - group 1 0.4296 0.5306
        - 8
- T-test
    - Narenga porphyrocoma
        - Two Sample t-test
        - t = -1.1278, df = 8, p-value = 0.2921
        - alternative hypothesis: true difference in means between group Burned and group Unburned is not equal to 0
        - 95 percent confidence interval:
        - -152.45285 52.31035
        - sample estimates:
        - mean in group Burned mean in group Unburned
        - 94.1950 144.2663

D.12 Grass height across fire occurrence

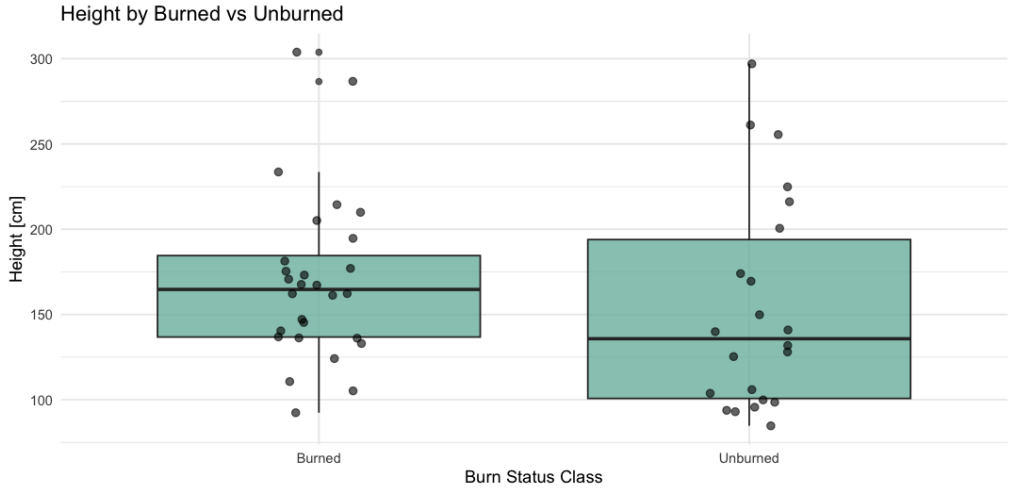

Figure D.12 Plant height comparison between burned and unburned plots. Although the median height in burned plots appears higher, this difference was not statistically significant (p = 0.15, Wilcoxon rank-sum test). Shapiro–Wilk tests indicated a deviation from normality in both groups (p < 0.05), while Levene's test confirmed homogeneity of variance (p = 0.17). Despite visible spread differences, the analysis does not support a significant effect of burn status on plant height.

- Shapiro-Wilk normality test
    - Burned
        - W = 0.92, p-value = 0.03468
    - Unburned
        - W = 0.88482, p-value = 0.01495

- Homoscedasticity (Levene's test)
    - Df F value Pr(>F)
    - group 1 1.9208 0.1724
    - 46
- Wilcoxon rank-sum test
    - W = 353, p-value = 0.1516
    - alternative hypothesis: true location shift is not equal to 0

D.13 Grass height across fire frequency by vegetation communities

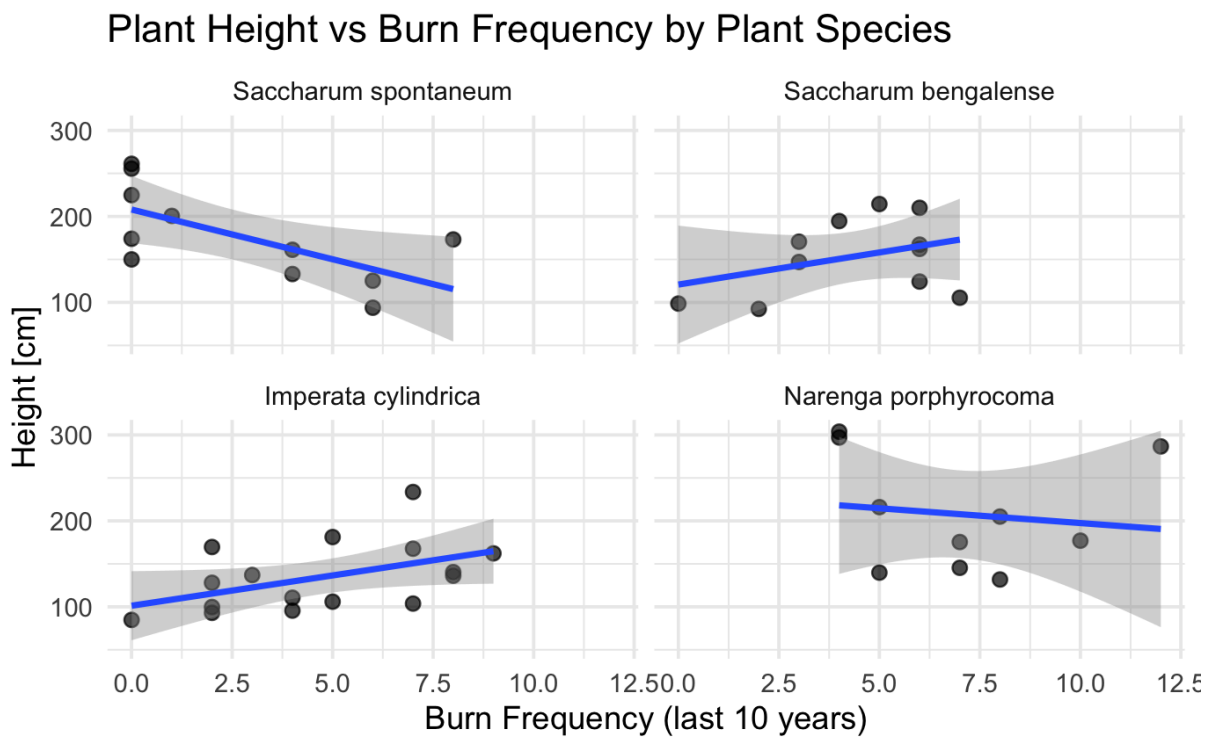

Figure D.13 Relationships between plant height and fire frequency over the past 10 years across dominant grass species. Regression analysis revealed differing trends per species. Saccharum spontaneum showed a significant decline in height with increasing burn frequency ($p = 0.026$), while Narenga porphyrocoma exhibited a similar pattern with multiple significant negative coefficients ($p < 0.05$). In contrast, Imperata cylindrica and Saccharum bengalense showed no statistically significant trends ($p > 0.1$). Residuals conformed to normality (Shapiro–Wilk $p > 0.3$) and heteroscedasticity tests (Breusch–Pagan $p > 0.07$), except for S. bengalense, which showed slight deviation from normality ($p = 0.016$).

- Linear regression
    - Imperata cylindrica
        - Residuals:
        - Min 1Q Median 3Q Max
        - -64.533 -11.325 0.000 5.925 65.267
        - Coefficients:
        - Estimate Std. Error t value Pr(>|t|)
        - (Intercept) 84.80 43.31 1.958 0.0859 .
        - burnfreq2 37.80 48.42 0.781 0.4575
        - burnfreq3 52.20 61.25 0.852 0.4189
        - burnfreq4 18.30 53.05 0.345 0.7390
        - burnfreq5 58.80 53.05 1.108 0.2999
        - burnfreq7 83.53 50.01 1.670 0.1334
        - burnfreq8 53.50 53.05 1.009 0.3427
        - burnfreq9 77.40 61.25 1.264 0.2419

        - Signif. codes: 0 ‘***’ 0.001 ‘**’ 0.01 ‘*’ 0.05 ‘.’ 0.1 ‘ ’ 1
        - Residual standard error: 43.31 on 8 degrees of freedom
        - Multiple R-squared: 0.3854, Adjusted R-squared: -0.1524
        - F-statistic: 0.7166 on 7 and 8 DF, p-value: 0.6632
    - Narenga porphyrocoma
        - Residuals:
        - 3 6 9 13 15 17
        - -1.500e+01 -3.810e+01 1.500e+01 3.660e+01 -3.400e+00 -3.660e+01
        - 19 47 48 49
        - -1.776e-15 3.400e+00 3.810e+01 5.329e-15
        - Coefficients:
        - Estimate Std. Error t value Pr(>|t|)
        - (Intercept) 300.40 27.51 10.919 0.0004 ***
        - burnfreq5 -122.50 38.91 -3.148 0.0346 *
        - burnfreq7 -140.00 38.91 -3.598 0.0228 *
        - burnfreq8 -132.00 38.91 -3.393 0.0275 *
        - burnfreq10 -123.40 47.65 -2.590 0.0607 .
        - burnfreq12 -13.80 47.65 -0.290 0.7865
        - Signif. codes: 0 ‘***’ 0.001 ‘**’ 0.01 ‘*’ 0.05 ‘.’ 0.1 ‘ ’ 1
        - Residual standard error: 38.91 on 4 degrees of freedom
        - Multiple R-squared: 0.8477, Adjusted R-squared: 0.6572
        - F-statistic: 4.451 on 5 and 4 DF, p-value: 0.08652
    - Saccharum bengalense
        - Residuals:
        - 1 8 25 26 27 28
        - 8.604e-15 -1.199e-15 2.488e-16 -3.700e+00 2.970e-16 -4.170e+01
        - 29 31 38 43 44
        - 4.410e+01 -1.180e+01 -1.137e-14 1.180e+01 1.300e+00
        - Coefficients:
        - Estimate Std. Error t value Pr(>|t|)
        - (Intercept) 98.60 31.53 3.127 0.0353 *
        - burnfreq2 -6.20 44.60 -0.139 0.8961
        - burnfreq3 60.20 38.62 1.559 0.1941
        - burnfreq4 96.00 44.60 2.153 0.0977 .
        - burnfreq5 115.80 44.60 2.597 0.0603 .
        - burnfreq6 67.30 35.26 1.909 0.1289
        - burnfreq7 6.80 44.60 0.152 0.8862
        - Signif. codes: 0 ‘***’ 0.001 ‘**’ 0.01 ‘*’ 0.05 ‘.’ 0.1 ‘ ’ 1
        - Residual standard error: 31.53 on 4 degrees of freedom
        - Multiple R-squared: 0.7918, Adjusted R-squared: 0.4796
        - F-statistic: 2.536 on 6 and 4 DF, p-value: 0.1935
    - Saccharum spontaneum
        - Residuals:
        - Min 1Q Median 3Q Max
        - -63.12 -14.90 0.00 14.90 48.08
        - Coefficients:
        - Estimate Std. Error t value Pr(>|t|)
        - (Intercept) 213.12 18.85 11.307 2.86e-05 ***
        - burnfreq1 -12.52 46.17 -0.271 0.795
        - burnfreq4 -66.02 35.26 -1.872 0.110
        - burnfreq6 -103.62 35.26 -2.939 0.026 *
        - burnfreq8 -39.92 46.17 -0.865 0.420
        - Signif. codes: 0 ‘***’ 0.001 ‘**’ 0.01 ‘*’ 0.05 ‘.’ 0.1 ‘ ’ 1
        - Residual standard error: 42.15 on 6 degrees of freedom
        - Multiple R-squared: 0.628, Adjusted R-squared: 0.38
        - F-statistic: 2.532 on 4 and 6 DF, p-value: 0.1485
- Shapiro-Wilk normality test
    - data: residuals(model_ic)

        - W = 0.93729, p-value = 0.3172
    - data: residuals(model_np)
        - W = 0.93048, p-value = 0.4526
    - data: residuals(model_sb)
        - W = 0.81694, p-value = 0.01572
    - data: residuals(model_ss)
        - W = 0.96241, p-value = 0.8013
- Breusch-Pagan
    - data: model_ic
        - BP = 8.6233, df = 7, p-value = 0.2808
    - data: model_np
        - BP = 10, df = 5, p-value = 0.07524
    - data: model_sb
        - BP = 4.1124, df = 6, p-value = 0.6615
    - data: model_ss
        - BP = 5.8947, df = 4, p-value = 0.2071

D.14 Bulk density across fire frequency

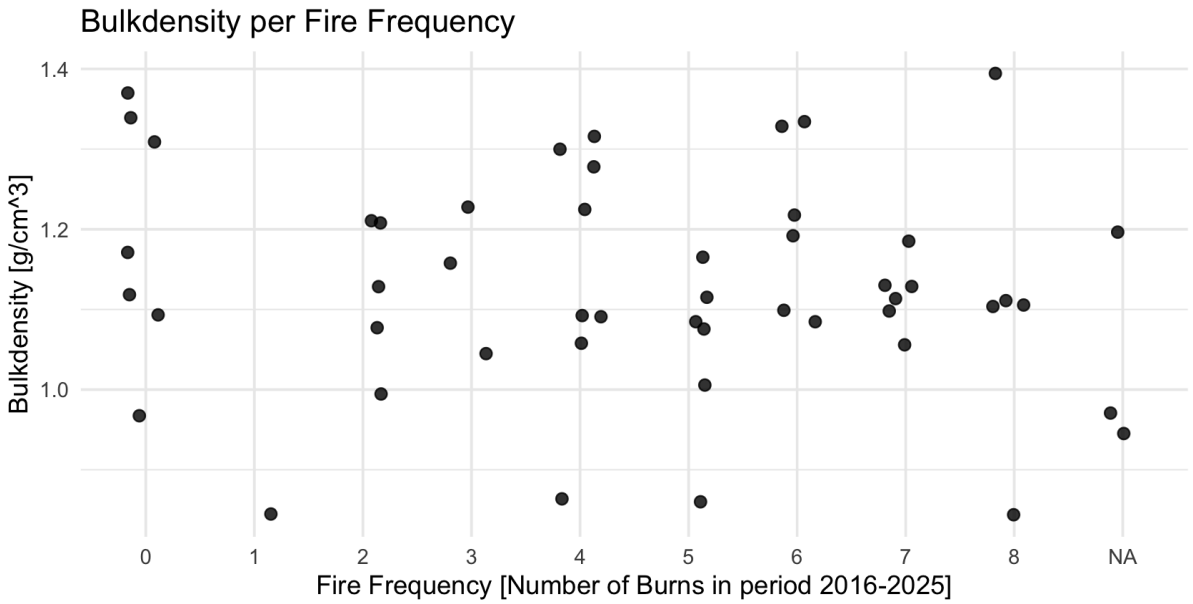

Figure D.14 Bulk density across different fire frequencies between 2016 and 2025. No significant relationship was detected between fire frequency and bulk density ($F_{11,38}$ = 1.42, p = 0.206). Assumptions of normality (Shapiro–Wilk p = 0.354) and homogeneity of variances (Levene's p = 0.368) were met.

- Shapiro-wilk Test
    - p-value = 0.354
- Levene's Test for Homogeneity of Variance :
    - p-value = 0.3684
- One-way ANOVA
    - > summary(model_bulkburn)
    - Df Sum Sq Mean Sq F value Pr(>F)
    - as.factor(burnfreq) 11 0.2577 0.02343 1.416 0.206
    - Residuals 38 0.6287 0.01655

D. 15 Volumetric moisture Content

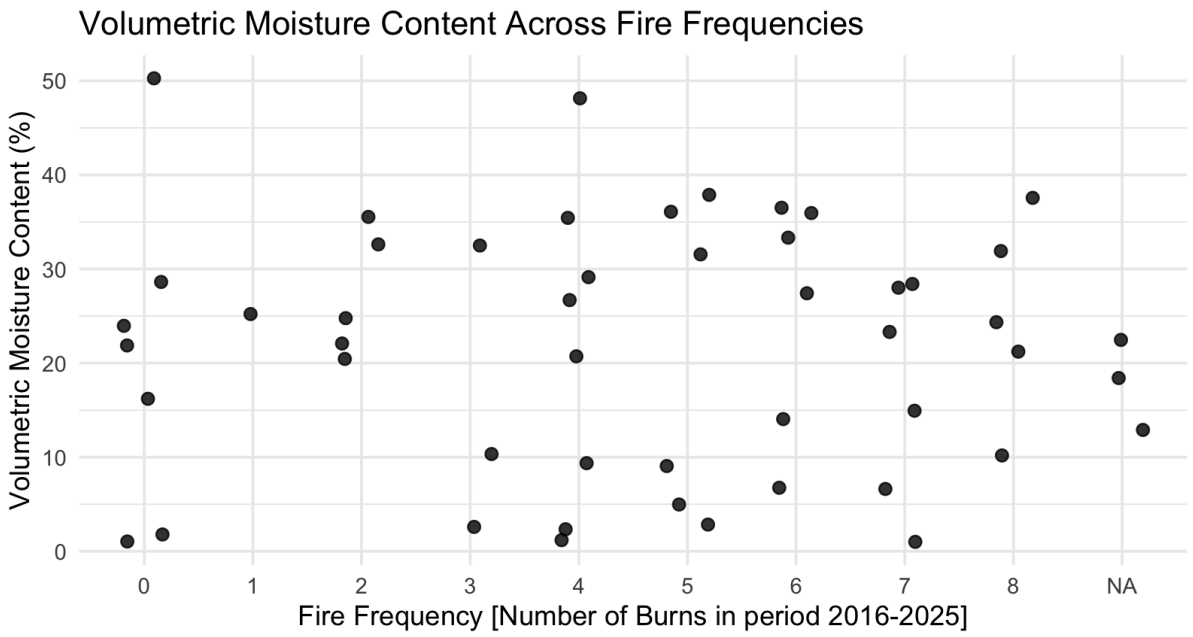

Figure D.15 Volumetric soil moisture content across different fire frequencies (2016–2025). No statistically significant differences in moisture content were found among fire frequency classes ($F_{11,38}$ = 0.31, p = 0.979). Assumptions of normality (Shapiro–Wilk p = 0.226) and equal variances (Levene's p = 0.323) were satisfied

- Shapiro-wilk Test
  - W = 0.96974, p-value = 0.2258
- Levene's Test for Homogeneity of Variance :
  - Df F value Pr(>F)
  - group 11 1.1958 0.3226
  - 38
- One-way ANOVA
  - Df Sum Sq Mean Sq F value Pr(>F)
  - as.factor(burnfreq) 11 675 61.37 0.31 0.979
  - Residuals 38 7516 197.80

Appendix D - Research Question 4

E.1 Fire Frequencies across Vegetation Communities

This is the statistical analysis of a figure which can be found in the text as figure 4.4.1

- Shapiro-wilk Test
  - W = 0.95403, p-value = 0.05794
- Levene's Test for Homogeneity of Variance :
  - Df F value Pr(>F)
  - group 3 0.5399 0.6574
  - 44
- One way anova
  - summary(model_ta)
  - Df Sum Sq Mean Sq F value Pr(>F)
  - as.factor(dominant_species) 3 100.7 33.57 4.727 0.00606 **
  - Residuals 44 312.5 7.10
  -
- Tukey HSD Post Hoc Test
  - $`as.factor(scientific_names)`

- diff lwr upr
- Saccharum bengalense-Saccharum spontaneum 1.7272727 -1.3069625 4.761508
- Imperata cylindrica-Saccharum spontaneum 2.0511364 -0.7359867 4.838259
- Narenga porphyrocoma-Saccharum spontaneum 4.3636364 1.2544704 7.472802
- Imperata cylindrica-Saccharum bengalense 0.3238636 -2.4632594 3.110987
- Narenga porphyrocoma-Saccharum bengalense 2.6363636 -0.4728023 5.745530
- Narenga porphyrocoma-Imperata cylindrica 2.3125000 -0.5560160 5.181016
- p adj
- Saccharum bengalense-Saccharum spontaneum 0.4345399
- Imperata cylindrica-Saccharum spontaneum 0.2167826
- Narenga porphyrocoma-Saccharum spontaneum 0.0028106
- Imperata cylindrica-Saccharum bengalense 0.9895023
- Narenga porphyrocoma-Saccharum bengalense 0.1223004
- Narenga porphyrocoma-Imperata cylindrica 0.1527969

E.2 Average Leaf Size across fire freq

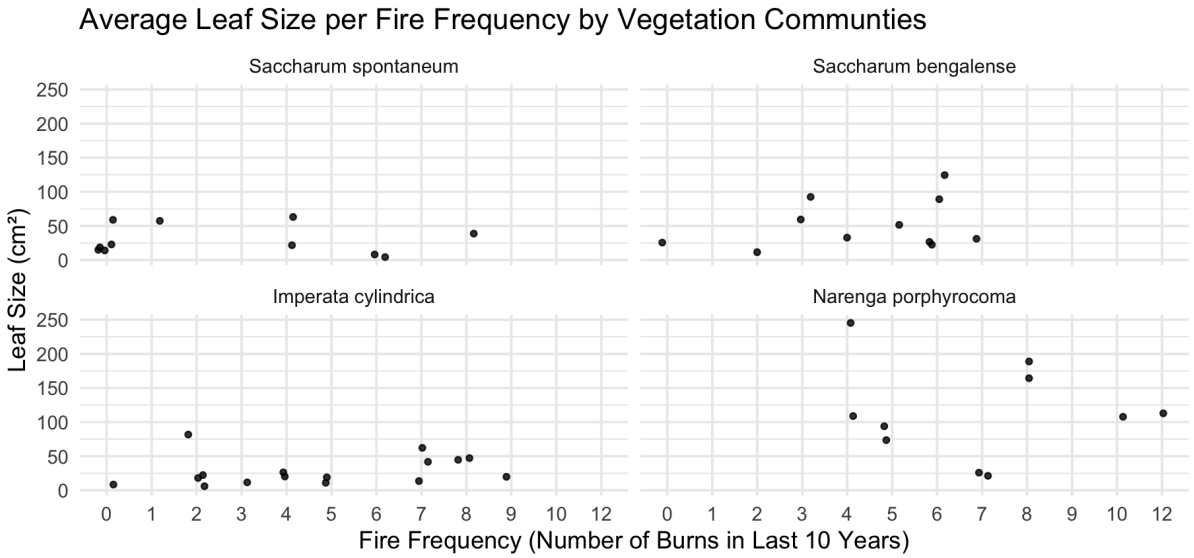

Figure E.2 Leaf size across fire frequencies for four dominant grass species. No significant relationships were found (all p > 0.3), and model assumptions were only violated in N. porphyrocoma (variance) and I. cylindrica, S. spontaneum (normality).

Saccharum bengalense

- Shapiro-Wilk normality test: W = 0.889 p = 0.136
- Levene's Test: F = 2.85 p = 0.165
- Adjusted R^2 = -0.047 | p = 0.476

Imperata cylindrica

- Shapiro-Wilk normality test: W = 0.824 p = 0.006
- Levene's Test: F = 0.45 p = 0.842
- Adjusted R^2 = 0.007 | p = 0.312

Narenga porphyrocoma

- Shapiro-Wilk normality test: W = 0.965 p = 0.842
- Levene's Test: F = 2.487109e+30 p = 0
- Adjusted R^2 = -0.115 | p = 0.793

Saccharum spontaneum

- Shapiro-Wilk normality test: W = 0.844 p = 0.035
- Levene's Test: F = 0.75 p = 0.594
- Adjusted R^2 = -0.098 | p = 0.755

E.3 Amount of Leaves across fire freq

This is the statistical analysis of a figure which can be found in the text as figure 4.4.3

- Shapiro-Wilk normality test
  - data: residuals(model_labf)
  - W = 0.84574, p-value = 1.189e-05
- Levene's Test for Homogeneity of Variance (center = median)
  - Df F value Pr(>F)
  - group 11 2.2111 0.03466 *
  - 38
  - ---
  - Signif. codes: 0 ‘***’ 0.001 ‘**’ 0.01 ‘*’ 0.05 ‘.’ 0.1 ‘ ’ 1
- Kruskal-Wallis rank sum test
  - data: avg_leaf by burnfreq
  - Kruskal-Wallis chi-squared = 22.143, df = 11, p-value = 0.02329
- Post hoc Dunn’s test with Bonferroni correction
  - > dunnTest(avg_leaf ~ burnfreq, data = data, method = "bonferroni")
  - Dunn (1964) Kruskal-Wallis multiple comparison
  - p-values adjusted with the Bonferroni method.

E.4 Specific Leaf Area during fire occurrence

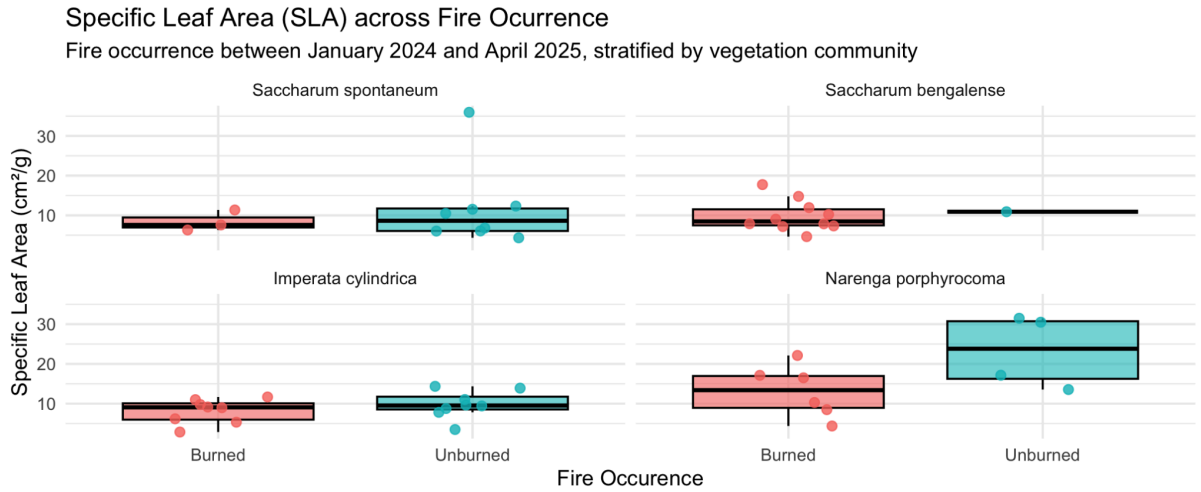

Figure E.4 Specific Leaf Area (SLA) by fire occurrence across four grass species. No significant differences were detected between burned and unburned samples (p > 0.1 for all species; Wilcoxon tests). Model assumptions were largely met, except normality violations in S. spontaneum (unburned group).

Saccharum spontaneum

- Shapiro-Wilk normality test
  - data: subset(species_data, burned_status == "Burned")$specific_leaf_area
  - W = 0.92308, p-value = 0.4633
  - data: subset(species_data, burned_status == "Unburned")$specific_leaf_area
  - W = 0.67807, p-value = 0.001269
- Levene's Test for Homogeneity of Variance (center = median)
  - Df F value Pr(>F)
  - group 1 0.6443 0.4428

- 9
- Wilcoxon rank sum test with continuity correction
    - data: specific_leaf_area by burned_status
    - W = 12, p-value = 1
    - alternative hypothesis: true location shift is not equal to 0

Imperata Cylindrica

- Shapiro-Wilk normality test
    - data: subset(species_data, burned_status == "Burned")$specific_leaf_area
    - W = 0.93216, p-value = 0.536
    - data: subset(species_data, burned_status == "Unburned")$specific_leaf_area
    - W = 0.9435, p-value = 0.6458
- Levene's Test for Homogeneity of Variance (center = median)
    - Df F value Pr(>F)
    - group 1 0.0183 0.8945
    - 14
- Wilcoxon rank sum test with continuity correction
    - data: specific_leaf_area by burned_status
    - W = 24, p-value = 0.4309
    - alternative hypothesis: true location shift is not equal to 0

Narenga porphyrocoma

- Shapiro-Wilk normality test
    - data: subset(species_data, burned_status == "*Burned*")$specific_leaf_area
    - W = 0.96464, p-value = 0.8547
    - data: subset(species_data, burned_status == "*Unburned*")$specific_leaf_area
    - W = 0.84122, p-value = 0.199
- > leveneTest(specific_leaf_area ~ burned_status, data = species_data)
- Levene's Test for Homogeneity of Variance (center = median)
    - Df F value Pr(>F)
    - group 1 2.3693 0.1623
    - 8
- > wilcox.test(specific_leaf_area ~ burned_status, data = species_data, exact = FALSE)
- Wilcoxon rank sum test with continuity correction
    - data: specific_leaf_area by burned_status
    - W = 4, p-value = 0.1098
    - alternative hypothesis: true location shift is not equal to 0

Saccharum bengalense

- Shapiro-Wilk normality test
    - data: subset(species_data, burned_status == "Burned")$specific_leaf_area
    - W = 0.91787, p-value = 0.3396
- Levene's Test for Homogeneity of Variance (center = median)
    - Df F value Pr(>F)
    - group 1 0.8855 0.3713
    - 9
- Wilcoxon rank sum test with continuity correction
    - data: specific_leaf_area by burned_status
    - W = 3, p-value = 0.6353
    - alternative hypothesis: true location shift is not equal to 0

E.5 Shannon across Fire Frequency

This is the statistical analysis of a figure which can be found in the text as figure 4.4.4

- Linear Model
    - Min 1Q Median 3Q Max
    - -0.77841 -0.20408 0.02674 0.24292 0.51553
    - Coefficients:

- Estimate Std. Error t value Pr(>|t|)
- (Intercept) 0.58816 0.08098 7.263 2.91e-09 ***
- burnfreq 0.04756 0.01488 3.196 0.00246 **
- Signif. codes: 0 ‘***’ 0.001 ‘**’ 0.01 ‘*’ 0.05 ‘.’ 0.1 ‘ ’ 1
- Residual standard error: 0.3027 on 48 degrees of freedom
- Multiple R-squared: 0.1755, Adjusted R-squared: 0.1583
- F-statistic: 10.22 on 1 and 48 DF, p-value: 0.002462

- Shapiro-Wilk normality test
  - data: residuals(model_shannon)
  - W = 0.96431, p-value = 0.1347
- Breusch-Pagan test
  - data: model_shannon
  - BP = 0.35715, df = 1, p-value = 0.5501

E.6 Shannon across Time Since Last Fire

This is the statistical analysis of a figure which can be found in the text as figure 4.4.5

- Shapiro-Wilk normality test
  - data: residuals(model)
  - W = 0.97007, p-value = 0.2329
- Levene's Test for Homogeneity of Variance (center = median)
  - Df F value Pr(>F)
  - group 2 1.054 0.3566
  - 47
- > summary(anova_model)
  - Df Sum Sq Mean Sq F value Pr(>F)
  - fire_recency 2 1.001 0.5007 5.432 0.00754 **
  - Residuals 47 4.332 0.0922
  - Signif. codes: 0 ‘***’ 0.001 ‘**’ 0.01 ‘*’ 0.05 ‘.’ 0.1 ‘ ’ 1
- Tukey multiple comparisons of means
  - 95% family-wise confidence level
  - Fit: aov(formula = shannon_index ~ fire_recency, data = data)
  - $fire_recency
  - diff lwr upr
  - Moderate time since burn [1-4 years ago]-Long unburned [9+ years] 0.2338883 -0.10244519 0.5702217
  - Recent burn [0 years] -Long unburned [9+ years] 0.4046157 0.09411730 0.7151141
  - Recent burn [0 years] -Moderate time since burn [1-4 years ago] 0.1707274 -0.06437816 0.4058330
  - p adj
  - Moderate time since burn [1-4 years ago]-Long unburned [9+ years] 0.2223247
  - Recent burn [0 years] -Long unburned [9+ years] 0.0077656
  - Recent burn [0 years] -Moderate time since burn [1-4 years ago] 0.1950967

E.7 Shannon Diversity Index per Vegetation Community

This is the statistical analysis of a figure which can be found in the text as figure 4.4.6

summarise(p_value = shapiro.test(shannon_index)$p.value)

scientific_names	p_value
<fct>	<dbl>
1 Saccharum spontaneum	0.194
2 Saccharum bengalense	0.652
3 Imperata cylindrica	0.531
4 Narenga porphyrocoma	0.726

- Levene's Test for Homogeneity of Variance (center = median)
  - Df F value Pr(>F)

- group 3 1.4147 0.2512
- 44

- > summary(anova_model)
  - Df Sum Sq Mean Sq F value Pr(>F)
  - scientific_names 3 0.393 0.1311   1.267 0.297
  - Residuals 44 4.553 0.1035

E.8 Fire Frequency and Shannon per Vegetation Community

This is the statistical analysis of a figure which can be found in the text as figure 4.4.7

- Shapiro-Wilk normality test
  - data: residuals(model_spont)
  - W = 0.90488, p-value = 0.2118
- studentized Breusch-Pagan test
  - data: model_spont
  - BP = 0.2753, df = 1, p-value = 0.5998

Bengalense

- Linear Model S
  - Residuals:
  - Min 1Q Median 3Q Max
  - -0.30711 -0.20929 -0.00884 0.18723 0.40620
  - Coefficients:
  - Estimate Std. Error t value Pr(>|t|)
  - (Intercept) 0.6648 0.1737 3.828 0.00404 **
  - burnfreq 0.0367 0.0360 1.019 0.33459
  - ---
  - Signif. codes: 0 ‘***’ 0.001 ‘**’ 0.01 ‘*’ 0.05 ‘.’ 0.1 ‘ ’ 1
  - Residual standard error: 0.2456 on 9 degrees of freedom
  - Multiple R-squared: 0.1035, Adjusted R-squared: 0.003919
  - F-statistic: 1.039 on 1 and 9 DF, p-value: 0.3346
- Shapiro-Wilk normality test
  - W = 0.94685, p-value = 0.604
- studentized Breusch-Pagan test
  - BP = 0.63939, df = 1, p-value = 0.4239

Imperata cylindrica

- Linear Model
- Residuals:
  - Min 1Q Median 3Q Max
  - -0.78690 -0.15090 -0.03229 0.24024 0.46590
  - Coefficients:
  - Estimate Std. Error t value Pr(>|t|)
  - (Intercept) 0.70151 0.17251 4.067 0.00116 **
  - burnfreq 0.02135 0.03207 0.666 0.51645
  - ---
  - Signif. codes: 0 ‘***’ 0.001 ‘**’ 0.01 ‘*’ 0.05 ‘.’ 0.1 ‘ ’ 1
  - Residual standard error: 0.3385 on 14 degrees of freedom
  - Multiple R-squared: 0.03068, Adjusted R-squared: -0.03856
  - F-statistic: 0.4431 on 1 and 14 DF, p-value: 0.5164
- Shapiro-Wilk normality test
  - W = 0.95167, p-value = 0.5166
- studentized Breusch-Pagan test
  - BP = 0.05039, df = 1, p-value = 0.8224

Narenga porphyrocoma

- Linear Model
  - Residuals:
  - Min 1Q Median 3Q Max
  - -0.2914 -0.2331 0.0150 0.1673 0.3639
  - Coefficients:
  - Estimate Std. Error t value Pr(>|t|)
  - (Intercept) 0.84525 0.23616 3.579 0.0072 **
  - burnfreq 0.01614 0.03179 0.508 0.6254
  - ---
  - Signif. codes: 0 ‘***’ 0.001 ‘**’ 0.01 ‘*’ 0.05 ‘.’ 0.1 ‘ ’ 1
  - Residual standard error: 0.2503 on 8 degrees of freedom
  - Multiple R-squared: 0.0312, Adjusted R-squared: -0.0899

    - F-statistic: 0.2577 on 1 and 8 DF, p-value: 0.6254
- Shapiro-Wilk normality test
    - W = 0.92742, p-value = 0.423
- studentized Breusch-Pagan test
    - BP = 2.9347, df = 1, p-value = 0.0867

E.9 Shannon across Fire Occurrence per Vegetation Community

This is the statistical analysis of a figure which can be found in the text as figure 4.4.8

Saccharum spontaneum

- Shapiro-Wilk normality test
    - W = 0.90178, p-value = 0.1943
- leveneTest(shannon_index ~ burned_status, data = spontaneum_data)
    - Df F value Pr(>F)
    - group 1 1.7044 0.2241
    - 9
- Wilcoxon rank sum test with continuity correction
    - data: shannon_index by burned_status
    - W = 22.5, p-value = 0.03985
    - alternative hypothesis: true location shift is not equal to 0

Saccharum bengalense

- Shapiro-Wilk normality test
    - W = 0.95062, p-value = 0.6519
- leveneTest(shannon_index ~ burned_status, data = bengalense_data)
    - Df F value Pr(>F)
    - group 1 2.9746 0.1187
    - 9
- Wilcoxon rank sum test with continuity correction
    - data: shannon_index by burned_status
    - W = 5, p-value = 1
    - alternative hypothesis: true location shift is not equal to 0

Imperata cylindrica

- Shapiro-Wilk normality test
    - W = 0.95254, p-value = 0.531
- leveneTest(shannon_index ~ burned_status, data = imperata_data)
    - Df F value Pr(>F)
    - group 1 3.2243 0.09416 .
    - 14
    - Signif. codes: 0 ‘***’ 0.001 ‘**’ 0.01 ‘*’ 0.05 ‘.’ 0.1 ‘ ’ 1
- Wilcoxon rank sum test with continuity correction
    - data: shannon_index by burned_status
    - W = 35, p-value = 0.7924
    - alternative hypothesis: true location shift is not equal to 0

Narenga porphyrocoma

- Shapiro-Wilk normality test
    - W = 0.95484, p-value = 0.7258
- leveneTest(shannon_index ~ burned_status, data = narenga_data)
    - Df F value Pr(>F)
    - group 1 1.0995 0.325
    - 8
- Wilcoxon rank sum test with continuity correction
    - data: shannon_index by burned_status
    - W = 22, p-value = 0.0422
    - alternative hypothesis: true location shift is not equal to 0